Quarterly Research Performance Progress Report

Federal Agency and Organization Element to Which Report is Submitted	U.S. Department of Energy Office of Fossil Energy
FOA Name	Advanced Technology Solutions for Unconventional Oil & Gas Development
FOA Number	DE-FOA-0001722
Nature of the Report	Research Performance Progress Report (RPPR)
Award Number	DE-FE0031606
Award Type	Cooperative Agreement
Name, Title, Email Address, and Phone Number for the Prime Recipient	**Technical Contact (Principal Investigator):** Abhijit Dandekar, Professor, adandekar@alaska.edu 907-474-6427 **Business Contact:** Rosemary Madnick Executive Director UAF Office of Grants and Contracts Administration rmadnick@alaska.edu, 907-474-6446
Name of Submitting Official, Title, Email Address, and Phone Number	Same as PI
Prime Recipient Name and Address	University of Alaska Fairbanks Grants and Contracts Administration PO Box 757880, Fairbanks AK 99775
Prime Recipient Type	Not for profit organization
Project Title	**FIRST EVER FIELD PILOT ON ALASKA'S NORTH SLOPE TO VALIDATE THE USE OF POLYMER FLOODS FOR HEAVY OIL EOR a.k.a ALASKA NORTH SLOPE FIELD LABORATORY (ANSFL)**

University of Alaska Fairbanks

Principal Investigator(s)	**PI:** Abhijit Dandekar, *University of Alaska Fairbanks* **Co-PIs:** Yin Zhang, *University of Alaska Fairbanks* John Barnes and Samson Ning, Hilcorp Alaska LLC Randy Seright, *New Mexico Institute* *of Mining & Technology* Baojun Bai, *Missouri University of Science and Technology* Dongmei Wang, *University of North Dakota*
Prime Recipient's DUNS number	615245164
Date of the Report	June 30, 2019
Period Covered by the Report	March 1, 2019 – May 31, 2019
Reporting Frequency	Quarterly
Signature of Principal Investigator:	Abhijit Dandekar

University of Alaska Fairbanks

TABLE OF CONTENTS

LIST OF FIGURES

LIST OF TABLES

NOMENCLATURE

A	Reservoir Area (acres); Equation 1
ANS	Alaska North Slope
B_o	Oil Formation Volume Factor (reservoir bbl/STB); Equation 1
BS&W	Basic Sediment and Water
bpd	Barrel Per Day
BHP	Bottomhole Pressure
CMG	Computer Modeling Group
C_o	Oil Concentration (Equation 2)
cP	Centipoise
DMP	Data Management Plan
EB	Emulsion Breaker
EOR	Enhanced Oil Recovery
Fr	Resistance Factor
Frr	Residual Resistance Factor
f_w	Fractional Flow of Water
ϕ	Porosity (fraction); Equation 1
h	Reservoir Thickness (Equation 1)
HPAM	Hydrolyzed Polyacrylamide
HM	History Matching
HSPF	High Salinity Polymerflood
HSWF	High Salinity Waterflood
ICD	Inflow Control Device
IPROF	Injection Profile

JBN	Johnson-Bossler-Neumann (method abbreviation for relative permeability calculations)
KI	Potassium Iodide
k or K	Permeability (generally absolute)
Kro	Relative Permeability to Oil
Krw	Relative Permeability to Water
LSWF	Low Salinity Waterflood
LSPF	Low salinity Polymerflood
md or mD	MilliDarcy
nm	Nanometer
N	STOOIP (Stock Tank Original Oil in Place); Equation 1
No	Corey Exponent for Oil
Nw	Corey Exponent for Water
OOIP	Original Oil in Place
PF	Polymerflood
PFO	Pressure Falloff
PMP	Project Management Plan
PPB	Parts Per Billion
PPM	Parts Per Million
PSU	Polymer Skid Unit
PV	Pore Volume
RPM	Rotation Per Minute
SC	Standard Conditions
SCTR	Abbreviation of Sector as used in CMG
S_{or}	Residual Oil Saturation
SPE	Society of Petroleum Engineers
STB	Stock Tank Barrel
STOOIP	Stock Tank Original Oil in Place
S_{wc} or S_{wi}	Connate/Irreducible Water Saturation
T_o	Oil Content in the Water Sample (Equation 2)
TPV	Total Pore Volume
μ	Viscosity
μg	Microgram
ULSPF	Ultra Low Salinity Polymerflood
URTeC	Unconventional Resources Technology
USBM	United State Bureau of Mines
UV	Ultraviolet
VRR	Voidage Replacement Ratio
WF	Waterflood
XRD	X-ray Diffraction
XRF	X-ray Fluorescence

University of Alaska Fairbanks

1. ACCOMPLISHMENTS

a. Project Goals

The overall objective of this project is to perform a research field experiment to validate the use of polymer floods for heavy oil Enhanced Oil Recovery (EOR) on Alaska North Slope.

The main scientific/technical objectives of the proposed project are:
1. Determine the synergy effect of the integrated EOR technology of polymer, low salinity water, horizontal wells, and conformance treatments (e.g., gels), and its potential to economically enhance heavy oil recovery.
2. Assess polymer injectivity into the Schrader Bluff formations for various polymers at various concentrations.
3. Assess and improve injection conformance along horizontal wellbore and reservoir sweep between horizontal injectors and producers.
4. Evaluate the water salinity effect on the performance of polymer flooding and gel treatments.
5. Optimize pump schedule of low-salinity water and polymer.
6. Establish timing of polymer breakthrough in Schrader Bluff N-sands.
7. Screen an optimized method to control the conformance of polymer flooding at the various stages of the polymer flooding project.
8. Estimate polymer retention from field data and compare with laboratory and simulation results.
9. Assess incremental oil recovery vs. polymer injected.
10. Assess effect of polymer production on surface facilities and remediation methods.

The technical tasks proposed in these studies focus on the following: (1) optimization of injected polymer viscosity/concentration and quantification of polymer retention via laboratory scale experiments; (2) optimization of injection water salinity and identification of contingencies for premature polymer breakthrough via laboratory scale experiments and numerical analyses; (3) reservoir simulation studies for optimization of polymer injection strategy; (4) design and implementation of a field pilot test at Milne Point on ANS; (5) identification of effective ways to treat produced water that contains polymer (including polymer fouling of heater tubes), and finally (6) the feasibility of commercial application of the piloted method in ANS heavy oil reservoirs. The project milestones, and current milestone status are shown toward the end in **Table 8**.

b. Accomplishments

The primary focus of the research program, since the start of the polymer injection in August 2018, has been monitoring the performance of the pilot in the injection wells J-23A and J-24A, and production wells J-27 and J-28 respectively. In order to complement the polymer injection, focus of other supporting tasks has been advancing reservoir simulation, tackling flow assurance challenges and laboratory corefloods. The accomplishments to date are summarized in the following bullet points:

- SPE-195257 was successfully presented at the 2019 SPE Western Regional meeting.
- Completed final manuscript for the URTeC conference paper has been submitted, and is expected to be cataloged in www.onepetro.org soon. The paper is scheduled for presentation by Dr. Samson Ning and Reid Edwards from Hilcorp LLC., at URTeC in July 2019. Full citation can be found in Section 2 Products.
- Budget Period 2 (BP2) continuation application and a WebEx was successfully conducted on April 15th, 2019, and consequently, funding for BP2 has now been approved.
- Field pilot has demonstrated that polymer can be handled and hydrated effectively on Alaska North Slope and injected at reasonable concentration and injection rate into the Schrader Bluff heavy oil reservoir via horizontal injectors.
- No polymer production or breakthrough observed 9 months after start of polymer injection, which has been confirmed with both the clay flocculation and water composition tests.
- Reservoir simulation task has advanced quite well with a robust waterflood and polymer flood history matched model that has been employed for polymer flood prediction.

Since the official project start date of June 1, 2018, the entire project team has continued the practice of working meetings every other Friday for two hours to discuss the various tasks and the project as a whole. A summary of these bi-weekly meetings is provided to the project manager. Additionally, separate meetings, as needed, between the sub-groups also take place. In the last such meeting that was on May 31st, 2019 the team also discussed pilot operational questions on (1) should we change polymer injection rate and pressure targets? (2) should we change polymer concentration? The discussion concluded that at this time it is too early to make any changes in the polymer concentration since the oil rate in both producers is showing stability and the VRR is near unity, which needs to be given sufficient time to evaluate the benefits and/or making changes in the polymer concentration.

The following summarizes the team's progress to date in relation to the various tasks and sub-tasks outlined in the Project Management Plan (PMP):

- Task 1.0 - Project Management and Planning

Following the continuation application and WebEx for BP2, both the PMP and DMP were revised on April 30th 2019. These were emailed to Mr. Cercone and the DMP was also emailed to FITS@netl.doe.gov, in order to be compliant with the reporting requirements.

- Task 2.0 - Laboratory Experiments for Optimization of Injected Polymer Viscosity/Concentration and Quantification of Polymer Retention

Polymer Retention. During the previous quarters, polymer retention studies in 6-11-Darcy Schrader Bluff NB sandpacks first revealed polymer retention values that were very high (290 µg polymer retained per gram of rock) if the sand contained old weathered oil and was not cleaned. Second, we also found high retention values (153-170 µg/g) if the sand was cleaned (with toluene and methanol) but not re-saturated with fresh oil. Third, we observed relatively low polymer retention values (28-45 µg/g) if the

sand was cleaned and then re-saturated with fresh Milne Point oil. During the present quarter, our efforts were focused on determining polymer retention in cores and sandpacks with permeabilities that are more representative of the field (i.e., 200-700 md). In our first attempt, several 1—1.5-inch-diameter cores were drilled in a 4.5-inch-diameter NB core. These cores were extensively flooded with toluene to extract the resident oil. Unfortunately, we found the permeability was very low—just a few micro-Darcy's. It was suggested that this core material was from the caprock section of the formation—accounting for the very low permeability. At any rate, the permeability was too low for polymer flow and therefore unusable.

Since this was the only remaining Milne core material in our possession, we disaggregated this sand, cleaned it (by extraction with toluene and methanol), and then prepared sandpacks using a tri-axial core holder. Normal biaxial (Hassler) core holders apply an overburden pressure radially inward through a rubber sleeve on sand or a core. For sand, there is a risk of deforming the sand in the middle of the pack to a much greater extent than at the ends—thus making a smaller flow area in the middle of the pack than on the ends. A tri-axial core holder eliminates this problem by applying the same stress throughout the sandpack (by applying the stress both radially and axially). Unfortunately, the tri-axial core holder is much more challenging to work with. A significant effort was expended this quarter getting this device to work properly. However, we eventually accomplished that. With a 1000-psi overburden pressure applied, the absolute permeability (to water) of the 14.9-cm-long, 3.8-cm-diameter core was 548 md. At residual oil (fresh) saturation, the permeability to water was 50.3 md. We injected 11.5 pore volumes of 1750-ppm HPAM in synthetic Milne Point Injection water into this core, while monitoring (1) pressure drop across the core, (2) effluent concentration of potassium iodide (KI) tracer, (3) effluent viscosity (at 7.3 s^{-1}, 25°C), (4) effluent carbon concentration, and (5) effluent nitrogen concentration. **Figure 1** plots these values, while **Figure 2** plots the same values normalized. Using this data, polymer retention was found to be 240 µg/g using nitrogen fluorescence analysis of the core effluent (green data in Figures 1 and 2). This value translates to a 108% delay in propagation of the polymer bank (meaning that the polymer bank needs to be over twice as large as if no polymer was adsorbed). The effluent viscosity (red curves in Figures 1 and 2) never rose above 88% of the injected viscosity—yielding a polymer retention value over 931 µg/g. However, oxidative degradation probably caused the viscosity loss—thus artificially inflating the retention value. If the final effluent viscosity was treated at the injected value, re-calculated retention would be 372 µg/g. As with most of our studies, retention values from the nitrogen fluorescence analysis is considered most reliable (240 µg/g in this case). All of these values are unacceptably high for a polymer flood. It was suggested that the mineralogy of this NB sand (possibly caprock material) was not representative of the flooded sand in the field project. Therefore, future polymer retention tests will focus on OA sands.
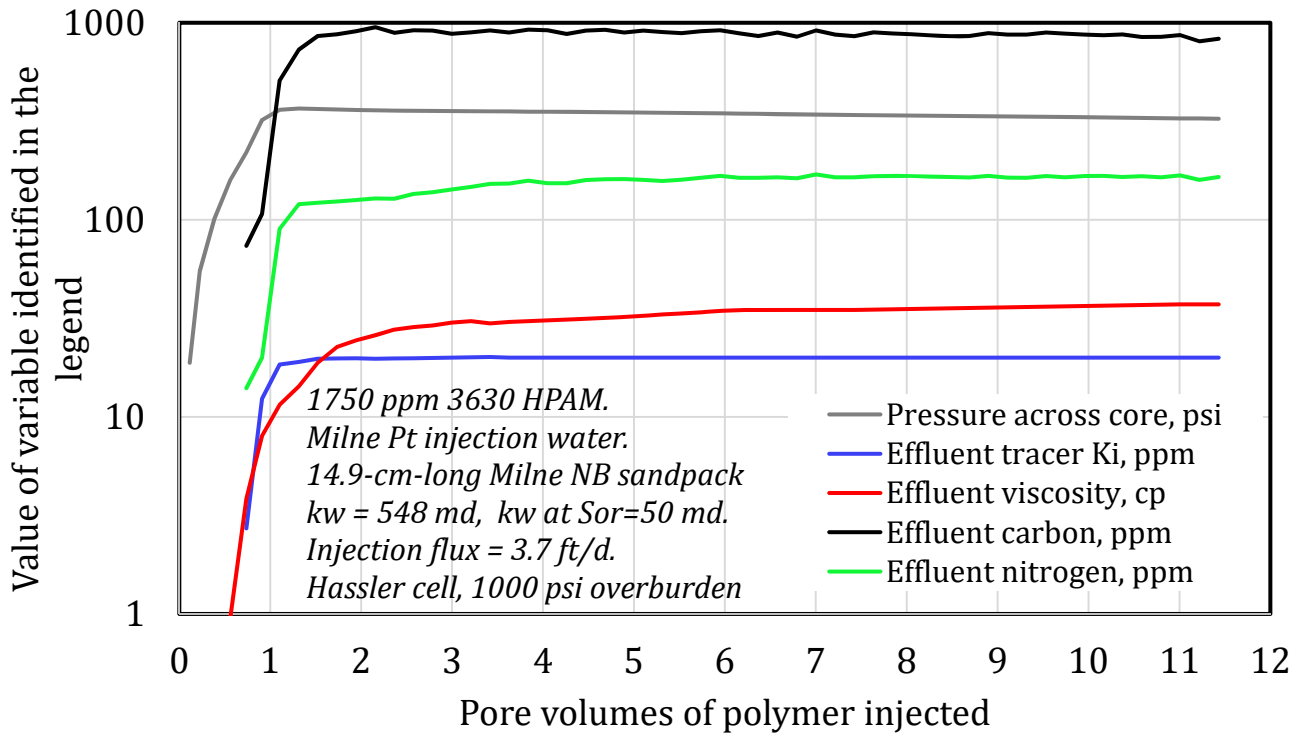
Figure 1: Parameters associated with injection into 528-md NB sandpack.
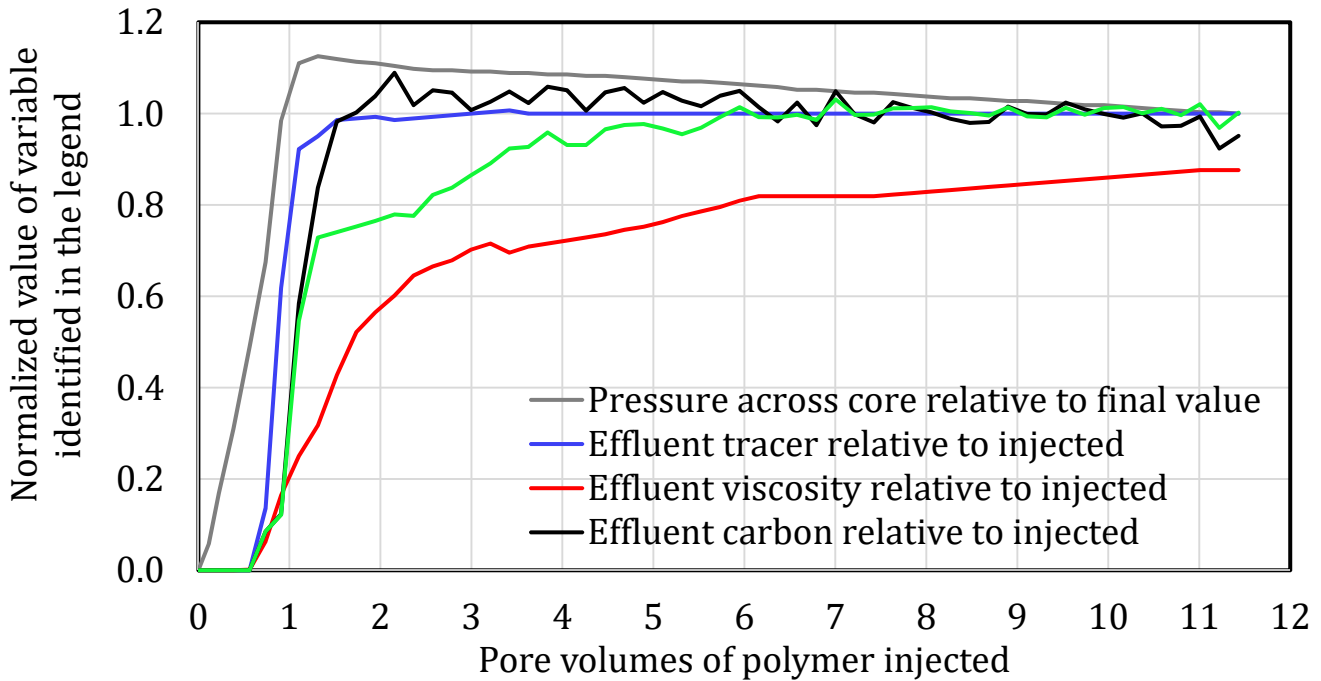
Figure 2: Normalized parameters associated with injection into 528-md NB sandpack.

Activity is ongoing.

● Task 3.0 - Laboratory Experiments for Optimization of Injection Water Salinity and Identification of Contingencies in Premature Polymer Breakthrough in the Field

In the last quarter report, we presented the coreflooding results using formation core plugs. However, the quantity of the core plugs is very limited, and the core plugs are not intact. After running a coreflooding experiment with a formation core plug (3-7#), formation sand was used and re-assembled to prepare sandpack. The sand was from the target NB formation at the Milne Point Unit provided by Hilcorp. The original sand was coated with crude oil. The content of the original oil coated on the sand was measured using Toluene with standard USBM Soxhlet Extraction method, as shown in **Figure 3(a)**. The sand before and after the extraction process is shown in **Figure 3(b) and Figure 3(c).** The original oil content was 10.5g/100g (~20 vol%). Three sandpack coreflooding experiments were carried out during this quarter. The basic parameters of the sandpacks are shown in **Table 1**. The results are encouraging. Low salinity water (LSW) and low salinity polymer (LSP) have remarkably better performance over normal salinity water or polymer. The EOR performance of LSWF and LSPF was confirmed from the experiments.

(a) Soxhlet extraction system

(b) NB sand before extraction

(c) NB sand after extraction

Figure 3: Soxhlet extraction system and the NB sand before and after extraction.

Table 1: Basic parameters of the NB sandpacks.

Sandpack	D, cm	L, cm	PV, cm^3	ϕ, fraction	K, mD	S_{wi}, fraction
1	2.54	20.40	46.82	0.450	16k	0.186
2	2.54	20.40	43.08	0.417	1,500	0.164
3 (clean sand)	2.54	20.40	24.35	0.236	248	0.261

Sandpack 1 Experiment

Objective & Procedure. This was the first sandpack prepared with NB formation sand. The main purpose was to verify the beneficial oil recovery improvement by LSWF and LSPF, as observed from our previous coreflooding experiments using commercial sand and Berea sandstone cores. Also, the effect of flooding sequence of the HSW and LSW was investigated. The objective was to test whether the oil recovery performance is better when directly starting with LSWF compared with "LSWF after HSWF". Three polymer flood processes were carried out with reduced salinity. Flow rate was set at 0.1 mL/min in all the flooding processes. The procedure is summarized as below.
1. Pack the NB sand into tube to prepare sandpack
2. Saturate the core with oil (MPU, B-28, use as received)
3. Flood process
    a) 1st flood process: HSWF (synthetic MPU formation water, salinity = 26700 ppm, filtrated with 0.8 μm filter paper)
    b) 2nd flood process: LSWF (MPU injection source water, salinity = 2498 ppm, filtrated with 0.8 μm filter paper)
    c) Re-saturate with oil (same as Step 2)
    d) 3rd flood process: LSWF (same as the 2nd flood process)
    e) 4th flood process: HSWF (same as the 1st flood process)
    f) 5th flood process: HSPF (40.1 cp, prep. with HSW, filtered)
    g) 6th flood process: LSPF (39.6 cp, prep. with LSW, filtered)
    h) 7th flood process: ULSPF (40.7 cp, prep. with 10-times-diluted LSW, filtered)

Results. The overall performance of the different flooding processes is shown in **Figures 4–7**.

The effect of flooding sequence. As shown in **Figure 6 and 7**, the oil recovery factor is significantly higher when starting directly with LSWF compared with HSWF (60.82% OOIP vs. 57.33% OOIP). The endpoint oil recovery efficiency is slightly better during the secondary flood mode, i.e. LSWF and then HSWF (61.33% OOIP vs. 60.58% OOIP).

5th flood process: Normal salinity polymer flood (HSPF). Oil production was continuous at early stage. Non-continuous oil production was observed at later stage. No emulsion was detected.

6th flood process: LSPF. Much more incremental oil was achieved at early stage than from HSPF. Oil production was continuous at early stage. Non-continuous was observed at later stage. No emulsion was detected.

7th flood process: ULSPF. The incremental oil recovery was much less significant as achieved during HSPF and LSPF. Interestingly, emulsion was observed in this flooding process.

Resistance factor and residual resistance factor. The resistance factor and residual resistance factor of the three polymer flood processes are shown in **Figure 8** and **Figure 9** respectively. The resistance factor increased as the salinity was reduced. The residual resistance factor is close to one, indicating that there is little or no permeability reduction during the polymer flooding process.
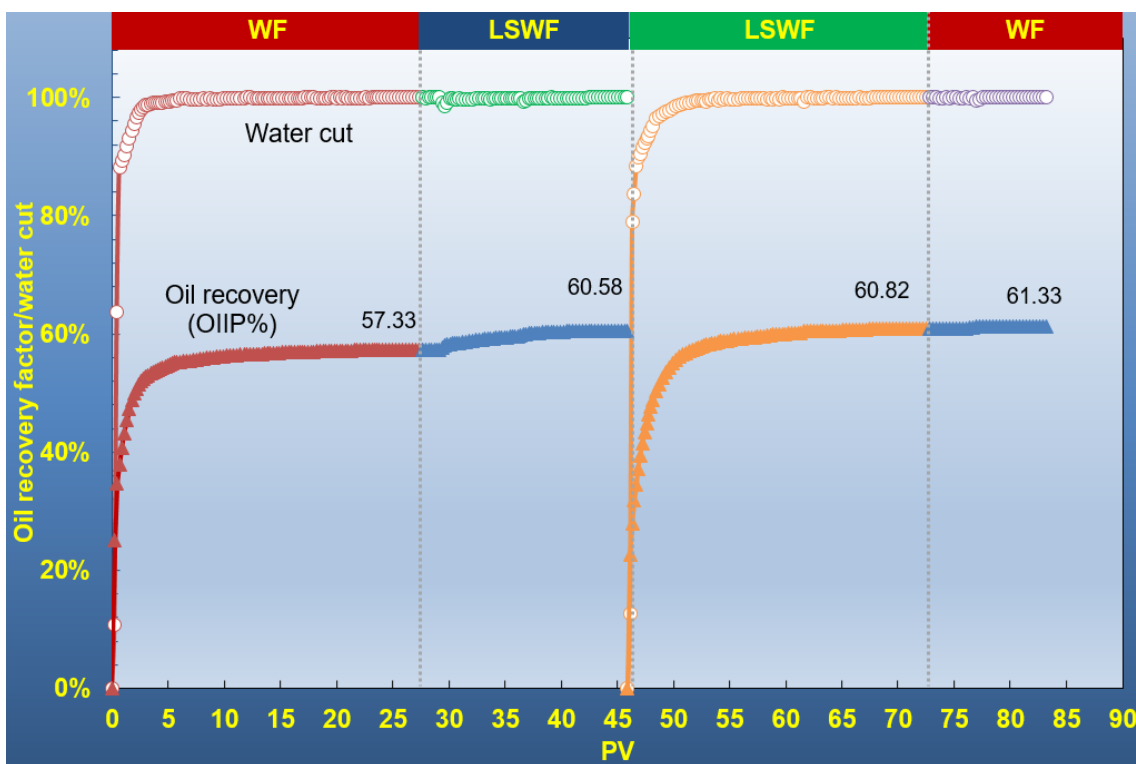
Figure 4: Oil recovery and water cut as a function of different flooding sequence for Sandpack 1.
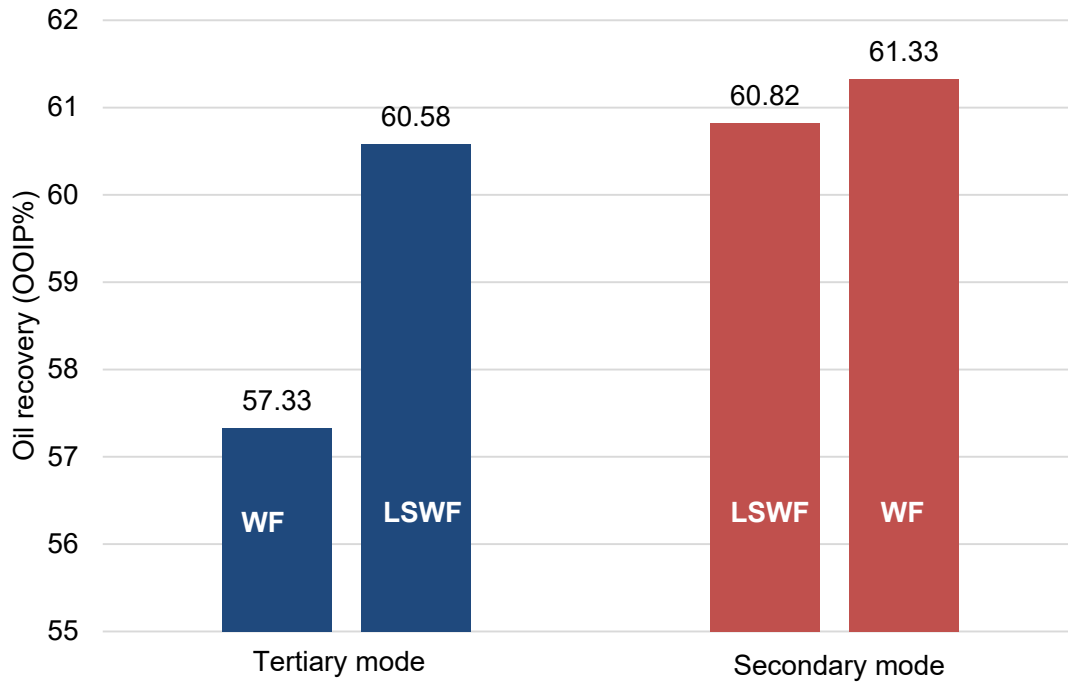
Figure 5: Impact of flooding sequence on oil recovery performance for Sandpack 1.
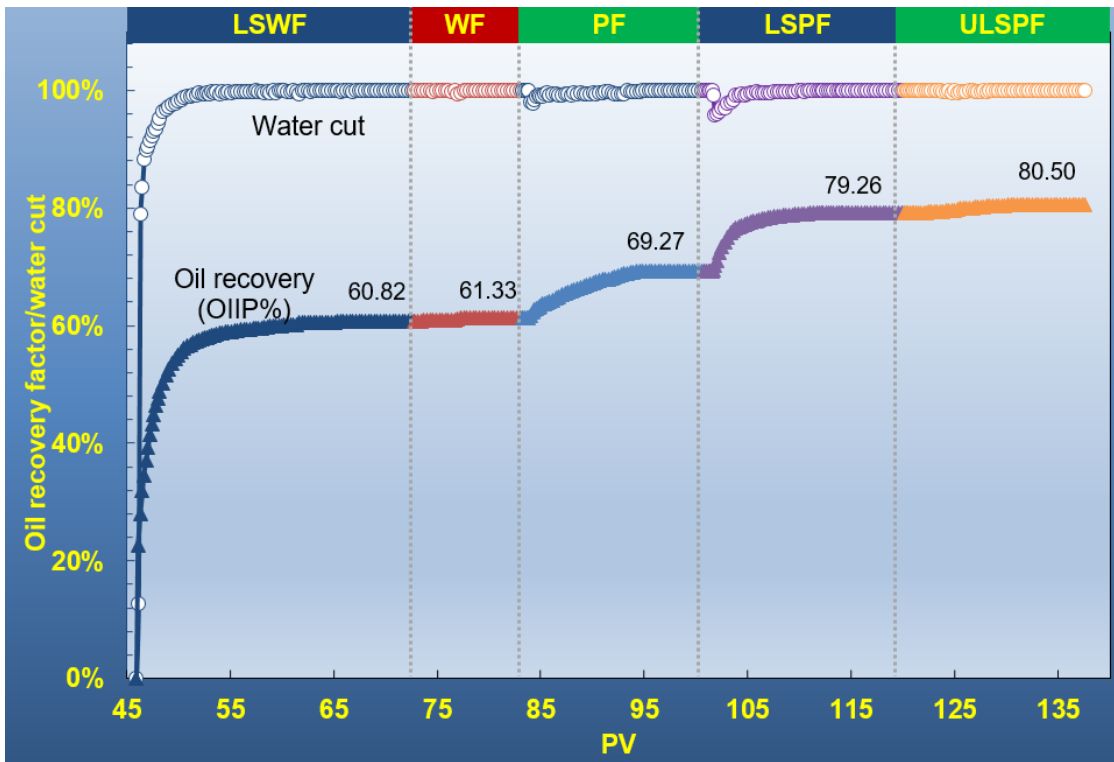
Figure 6: Oil recovery and water cut results starting with LSWF for Sandpack 1.
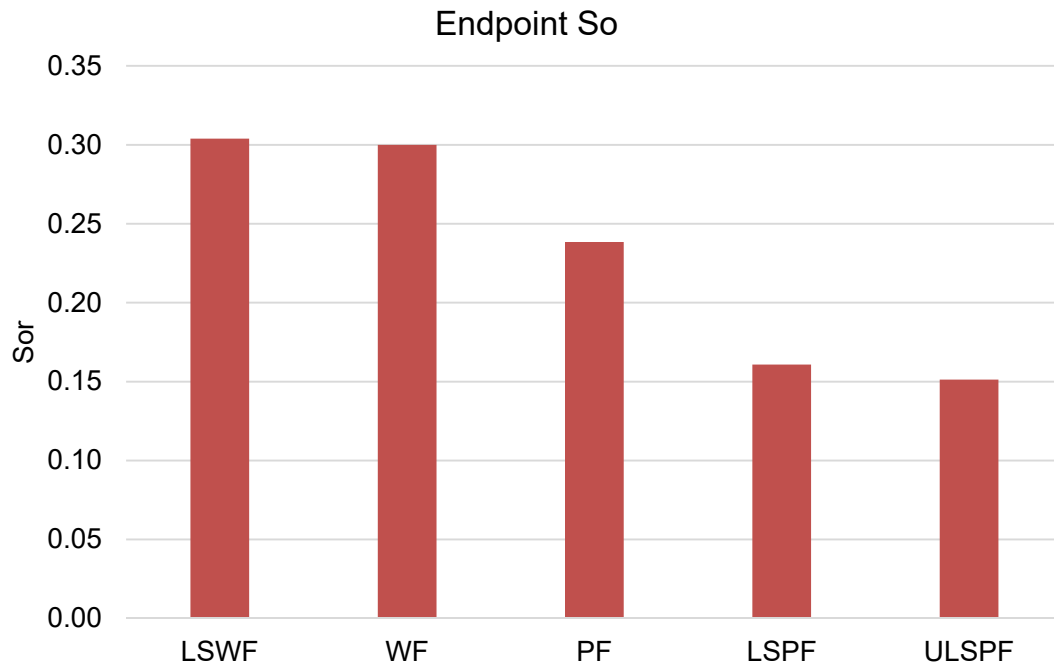
Figure 7: The endpoint oil saturation at the end of each flood process corresponding to Figure 6 for sandpack 1.
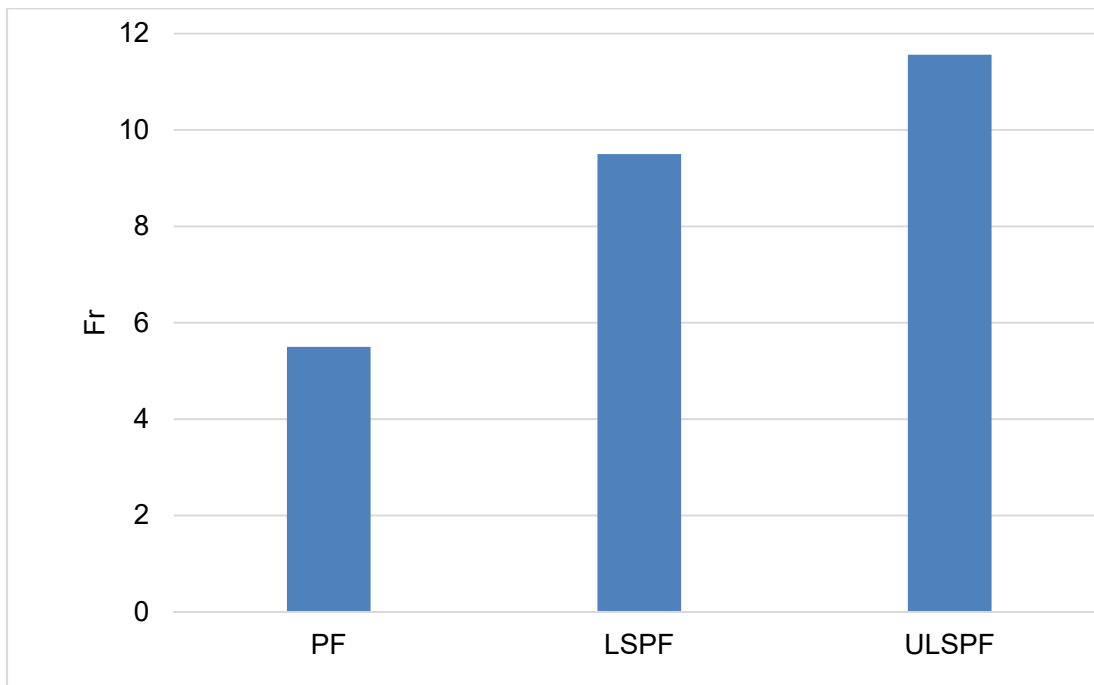
Figure 8: The resistance factor of different polymer flood processes for sandpack 1.
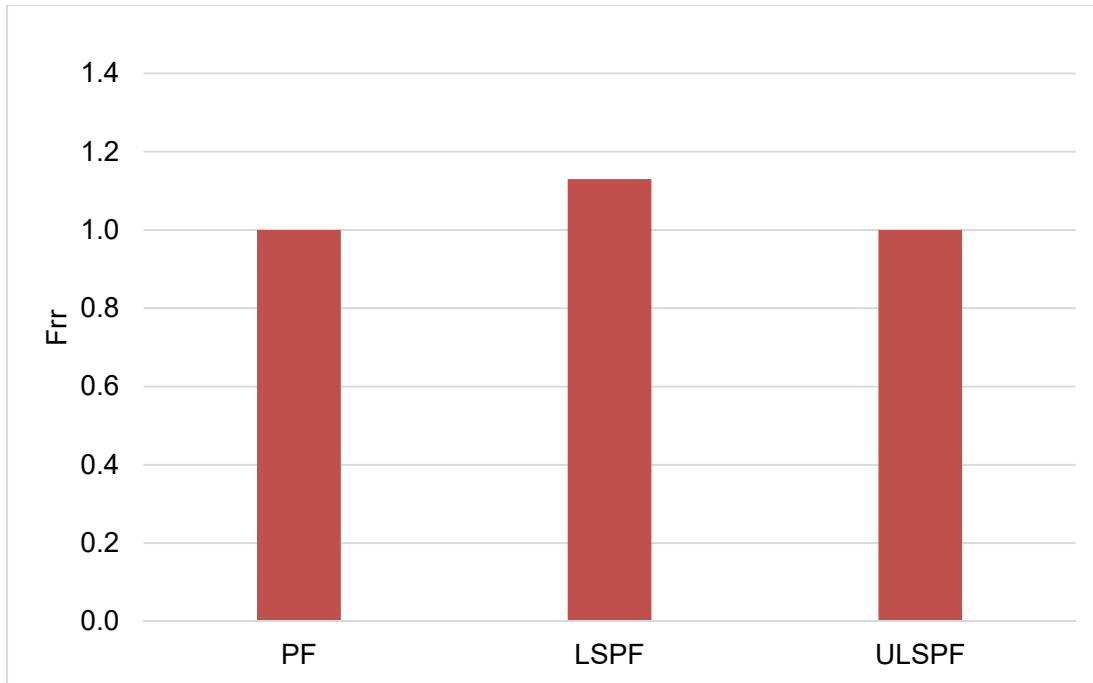
Figure 9: The residual resistance factor of different polymer flood processes for sandpack 1.

Sandpack 2 Experiment

Objectives & Procedure. Sandpack 1 experiment demonstrated that, even after extensive normal salinity polymer flooding, we could still get remarkable incremental oil by lowering the salinity and keeping viscosity almost the same. However, the permeability was 16 Darcy, which was a little too high. The 2nd sandpack was prepared with a permeability of 1.5 Darcy, which was quite representative of the target reservoir. The sandpack preparation procedure was the same as the Sandpack 1. The flooding process was slightly modified. The water flooding process was simplified. The effect of the injection sequence of HSW and LSW was tested. We focused more on polymer flooding. Similar to the 1st experiment, there were three polymer flood processes with different salinities, including HSP, LSP, and ULSP. After ULSPF, HSPF was carried out to test whether high salinity polymer after LSP can increase the oil recovery. Flow rate was set at 0.1 mL/min.

1. Pack the NB sand into tube to prepare sandpack
2. Saturate the core with oil (MPU, B-28, use as received)
   a) 1st flood: HSWF (synthetic MPU formation water, salinity = 26700 ppm, filtrated with 0.8 μm filter paper)
   b) 2nd flood: LSWF (MPU injection source water, salinity = 2498 ppm, filtrated with 0.8 μm filter paper)
   c) 3rd flood: HSPF (46.74 cp, prep. with HSW, filtered)
   d) 4th flood: LSPF (40.31 cp, prep. with LSW, filtered)
   e) 5th flood: ULSPF (44.86 cp, prep. with 10-times-diluted LSW, filtered)
   f) 6th flood: HSPF (Same as Step 5)

Results. The overall performance of the different flooding processes is shown in **Figure 10**. The endpoint oil saturation at the end of each flooding process and the pressure behavior is shown in **Figure 11** and **12** respectively.

3rd flood (HSPF). The results show that polymer flooding can still significantly increase the recovery efficiency even after extensive water flooding and low salinity water flooding, as observed in sandpack 1 experiment. Switching from LSWF to PF shows quite a rapid response. Total incremental recovery = 7.37% OOIP and 3.1% OOIP during 2 PVs of PF after response. Mobility/sweep improvement is likely the main contribution, especially at early stage. No obvious mechanical degradation was observed by monitoring the aqueous effluent viscosity

4th flood (LSPF). Low salinity polymer flooding can remarkably increase the recovery efficiency even after extensive WF, LSWF and PF sequence. Response was observed after 1 PV. A total ~8% OOIP achieved after extensive WF and PF. 4.72% OOIP recovered in 3 PVs after response. LSPF shows quite a late response (after 1 PV). Likely LS effect rather than sweep improvement since mobility/sweep improvement tend to show a rapid response.

There is fluctuation in oil production especially during PF and LSPF. The tracer test result shows quite good homogeneity of the sandpack core. HSPF after LSPF could not recover more oil.
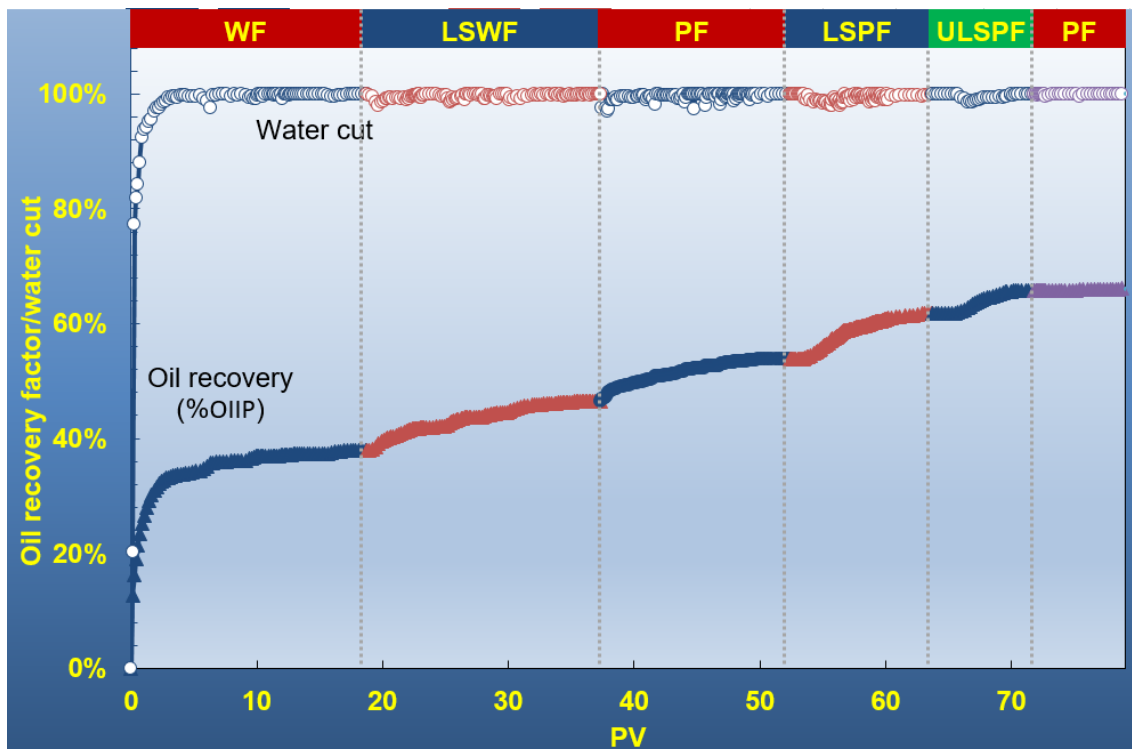
Figure 10: Oil recovery factor and water cut for sandpack 2.
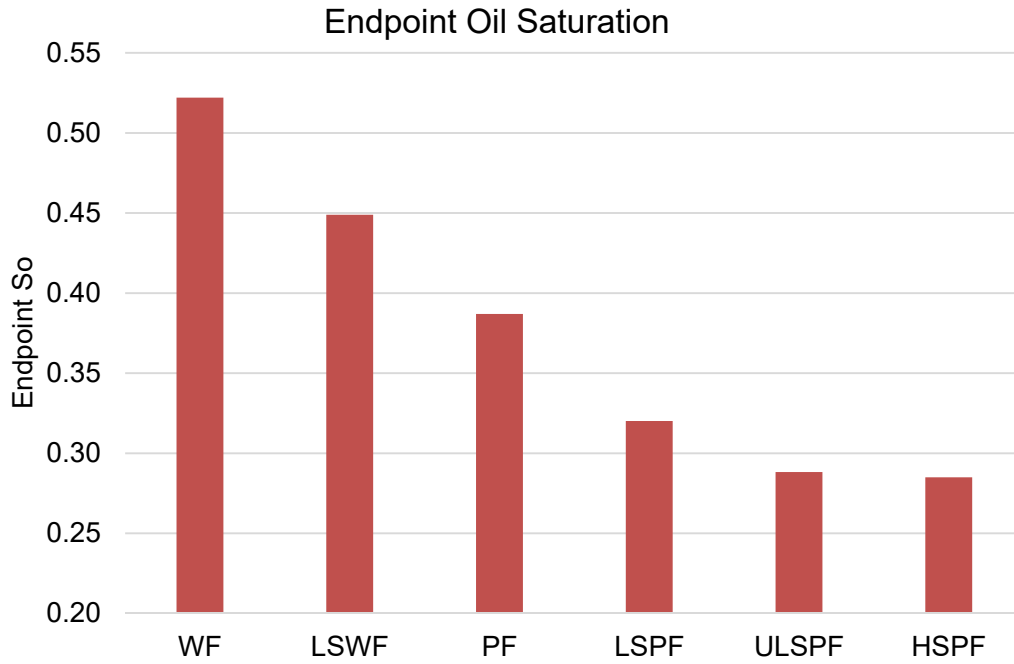
Figure 11: The endpoint oil saturation at the end of each flood process for sandpack 2.

Figure 12: Pressure behavior in different floods for sandpack 2.

Sandpack 3 Experiment

Objectives & Procedure. The purpose of this sandpack core flooding experiment was to test whether directly starting with polymer flooding rather than water flooding could achieve better oil recovery performance. The flow rate was set at 0.1 mL/min. The procedure is summarized as below.
1. Clean the NB formation sand with toluene and acetone;
2. Dry in 80 °C oven for two days;
3. Pack the NB sand into tube to prepare sandpack
4. Saturate the core with oil (MPU, B-28, use as received)
   a) HSPF (~45 cp, prep. with HSW, filtered)
   b) LSPF (~45 cp, prep. with LSW, filtered)

Results. As shown in **Figure 13**, directly starting with polymer flooding is much better than with WF as in sandpack 1 (77% vs. 62%). LSPF can achieve remarkable incremental oil even after extensive PF (~20 PV). Emulsions were produced during LSPF as shown in **Figure 14**.
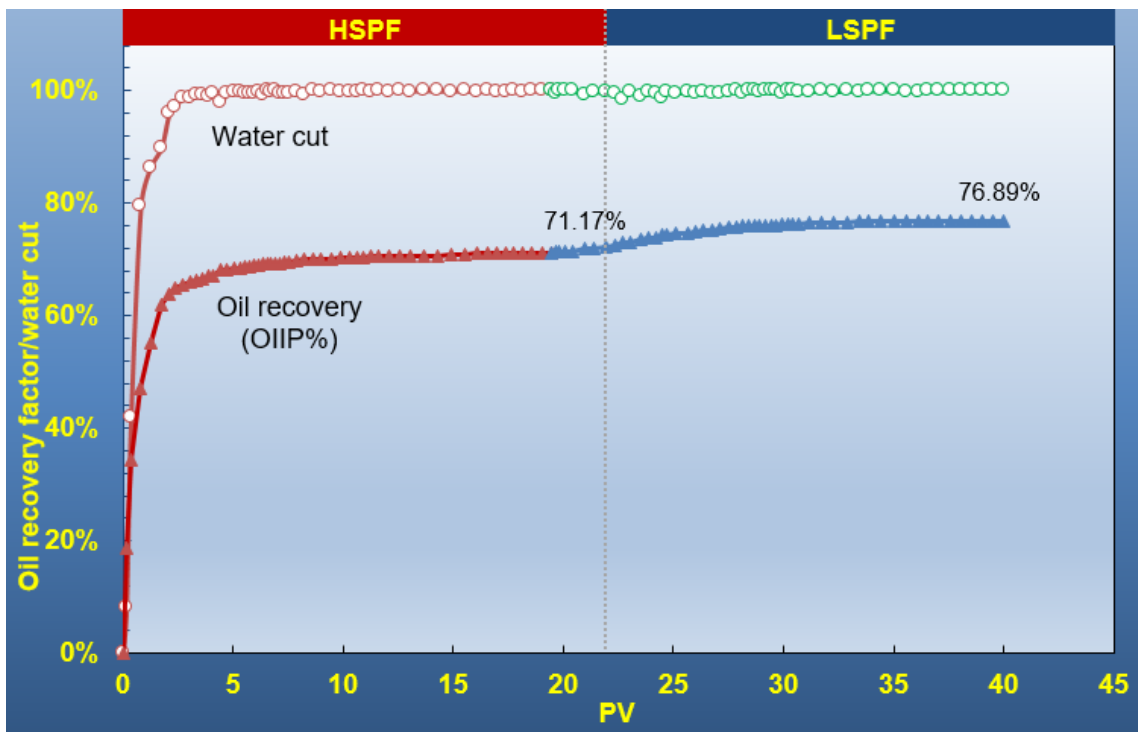
Figure 13: Oil recovery factor and water cut for sandpack 3.
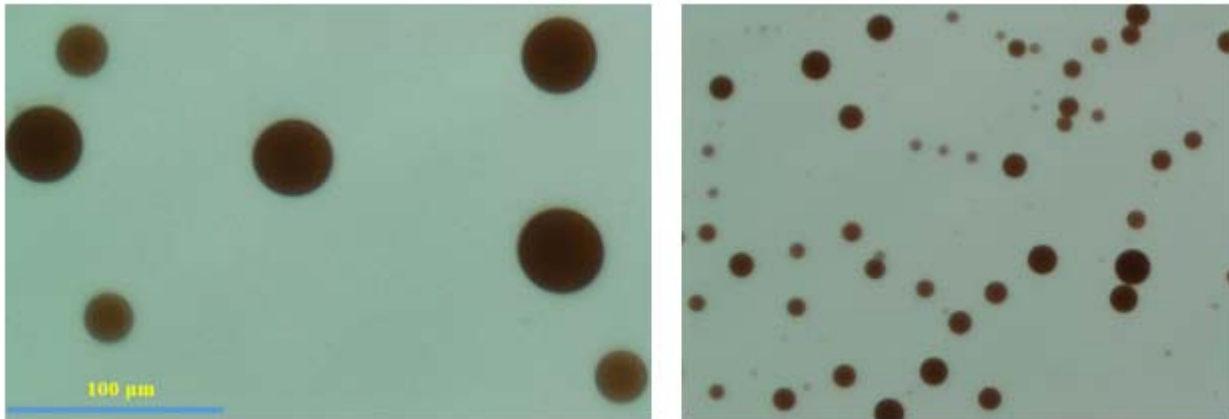
Figure 14: Emulsions produced during LSPF for sandpack 3.

History matching of the experimental data

Core-scale Simulation for Relative Permeability Curve fitting and analysis

A simulation study was established to history match sandpack 2 coreflooding experiment. In this experiment, oil production was not continuous because of the heterogeneous aged core. The traditional JBN (Johnson et. al., 1959) relative permeability curve fitting method could not produce a reasonable curve. So, we derived a direct method to fit fractional flow to get Kr coefficients with lab water cut profile instead of fitting (dp/dt vs 1/dt) in JBN method. The algorithm is listed below:

Step 1: Fitting fractional flow to get coefficient a, b: (**Figure 15**)
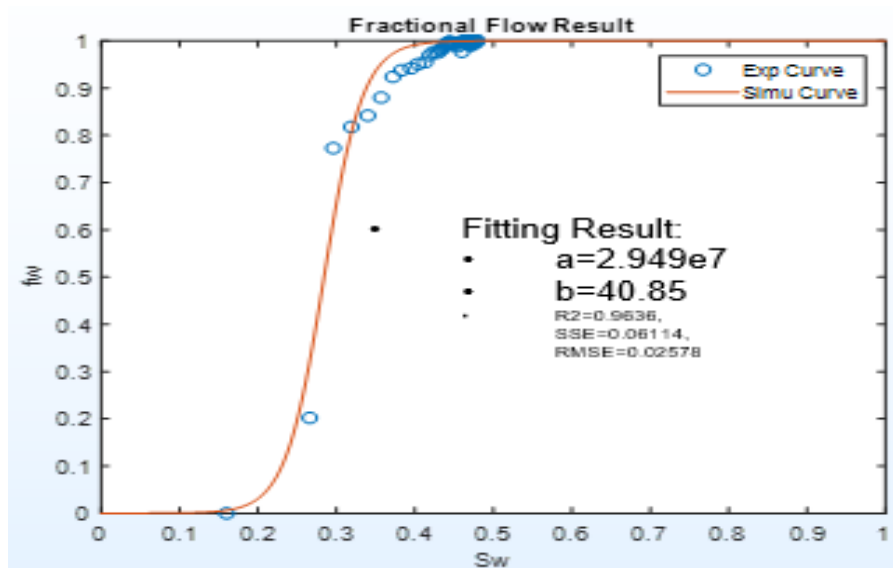
Figure 15: Fractional flow fitting result.

Step 2: Combining fractional flow equation with Corey's law

$$\frac{krw}{kro} = \frac{1}{a*\exp(-b*Sw)} = \frac{Krwiro*\left(\frac{Sw-Swc}{1-Swc-Sor}\right)^{Nw}}{Krocw*\left(\frac{So-Sor}{1-Swc-Sor}\right)^{No}} \Rightarrow \frac{Krocw/Krwiro}{a*\exp(-b*Sw)} = \frac{\left(\frac{Sw-Swc}{1-Swc-Sor}\right)^{Nw}}{\left(\frac{So-Sor}{1-Swc-Sor}\right)^{No}}$$

$$\xRightarrow{both\ side\ log} \ln\left(\frac{\frac{Krocw}{Krwiro}}{a*\exp(-b*Sw)}\right) = Nw*\ln\left(\frac{Sw-Swc}{1-Swc-Sor}\right) - No*\ln\left(\frac{So-Sor}{1-Swc-Sor}\right)$$

Step 3: Simplify and achieve Nw, No in Corey's Law

If we assume $Y=\ln\left(\frac{\frac{Krocw}{Krwiro}}{a*\exp(-b*Sw)}\right)$, $A=\ln\left(\frac{Sw-Swc}{1-Swc-Sor}\right)$, $B=ln\left(\frac{So-Sor}{1-Swc-Sor}\right)$

Then we have $Y = Nw*A - No*B = \begin{bmatrix} A & -B \end{bmatrix} * \begin{bmatrix} Nw \\ No \end{bmatrix}$

Then we have $\begin{bmatrix} Nw \\ No \end{bmatrix} = \begin{bmatrix} A & B \end{bmatrix}\backslash Y$

The theoretical result calculated by this direct method is shown in **Figure 16**.
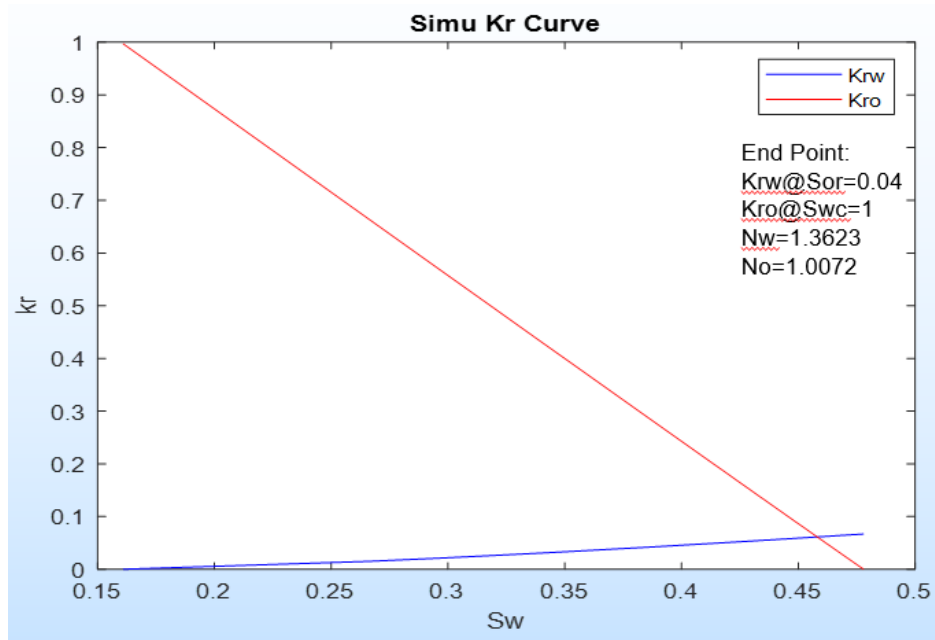
Figure 16: Theoretical relative permeability fitted by direct method for sandpack 2.

To validate the result, we used this set of relative permeability curve in CMG STARS to simulate the coreflooding process. Results are shown in **Figure 17 and 18** respectively.

21
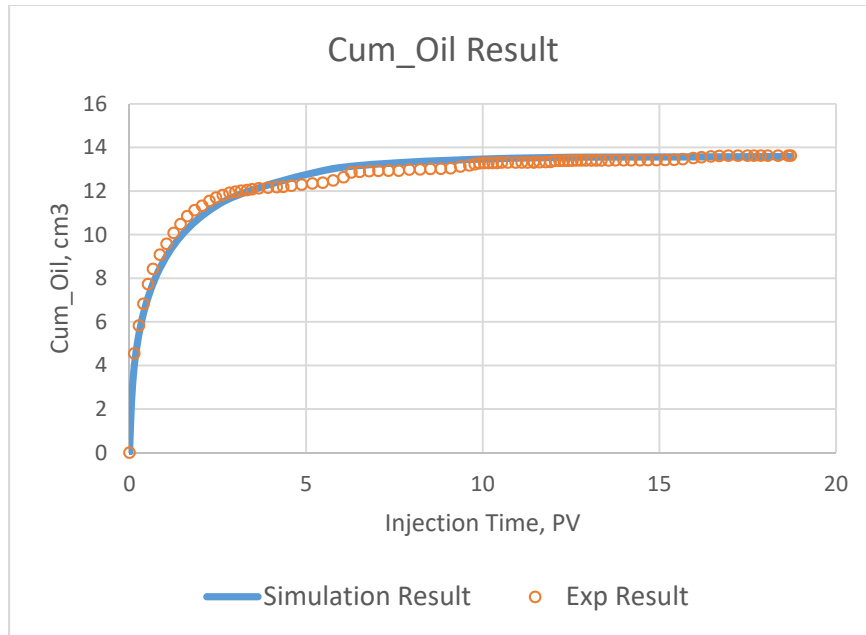
Figure 17: Cumulative oil history matching result using theoretical Kr curve (see Figure 16).
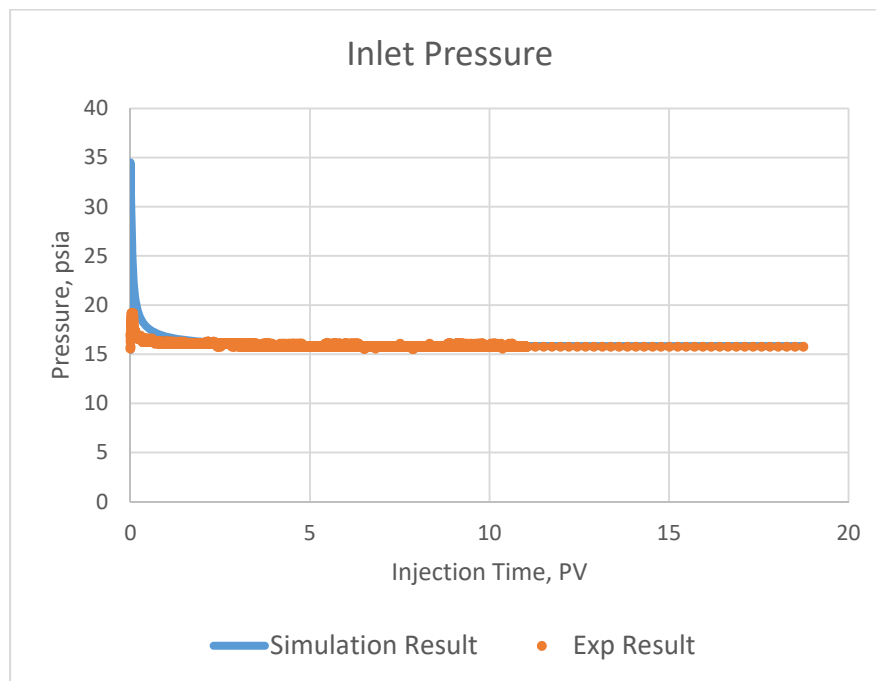
Figure 18: Inlet pressure history matching result using theoretical Kr curve (see Figure 16).

The fitting result for both oil production and pressure can be considered as acceptable. Based on this result, a CMOST design of experiment model was used to fit LSW injection period, for which the result is shown in **Figure 19 and 20** respectively.
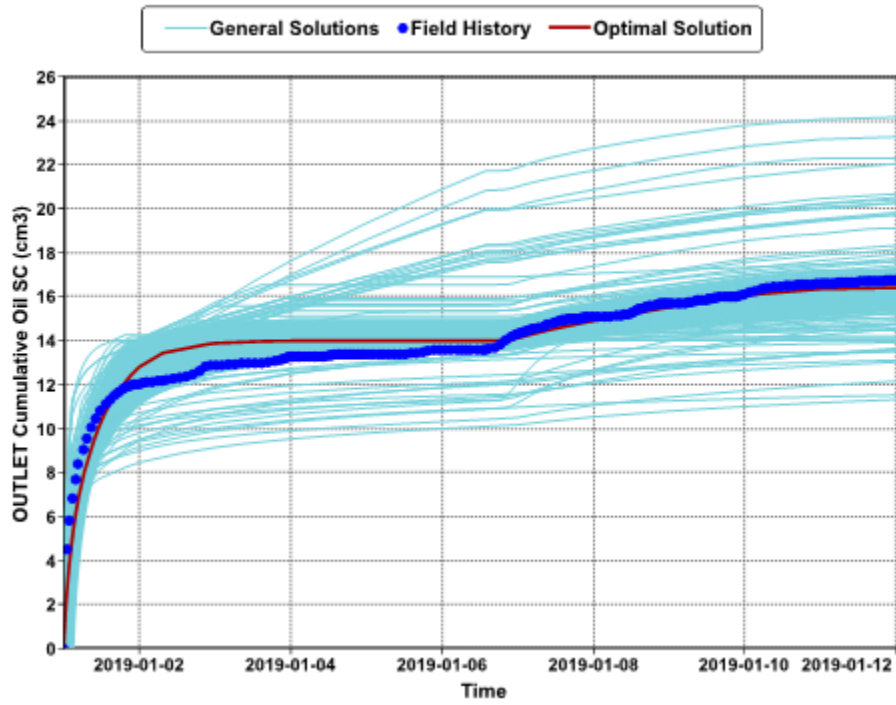
Figure 19: CMOST core-scale history matching result for oil recovery.
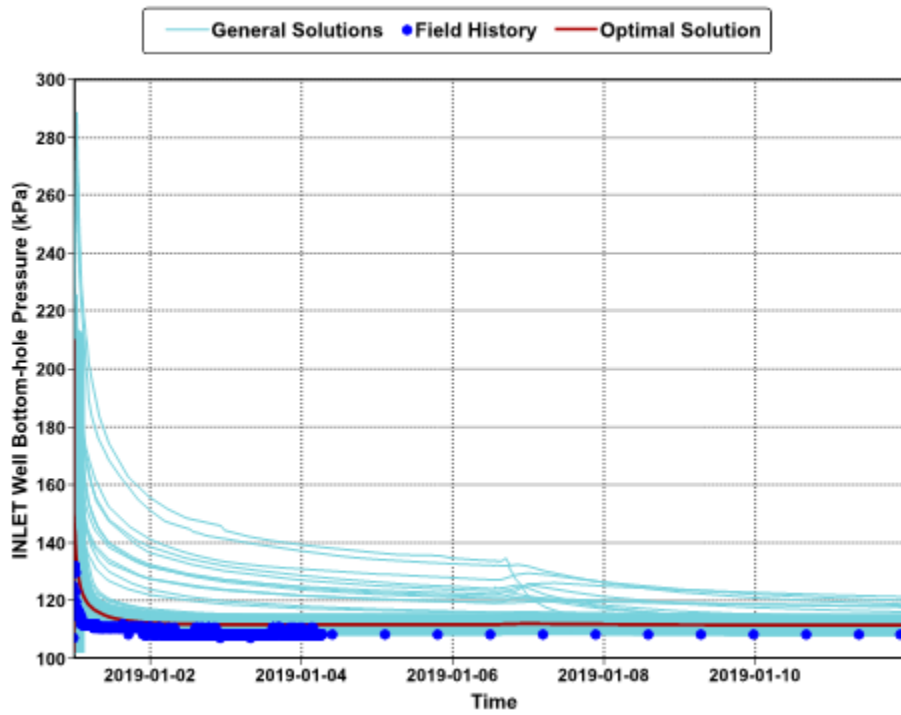
Figure 20: CMOST core-scale history matching result for inlet BHP.

The corresponding relative permeability coefficients are: Nw = 0.8, No = 1.22 for HSW, and Nw = 4.03, No = 0.82 for LSW. On the other hand, we used heterogeneous model to fit experimental result. However, the result shows similar Nw, No for both HSW and LSW period. Moreover, the history matching error was not eliminated.

Core-scale Tracer Test History Matching using Simulation Method

Based on our sandpack experiments history matching results, sandpack condition was unclear since some of the history matching was acceptable with homogeneous model however the others need heterogeneous model to achieve a perfect match. As a result, we did a tracer test before and after core flooding to test if channel existed in the sandpack and if flooding process created channels.

Diffusion and Dispersion:

Firstly, a history matching was done for tracer test before core flooding to investigate the diffusion and dispersion coefficient. The sensitivity test result is shown in **Figure 21** (the unit of the legend or the diffusion and dispersion coefficient is cm^2/s).
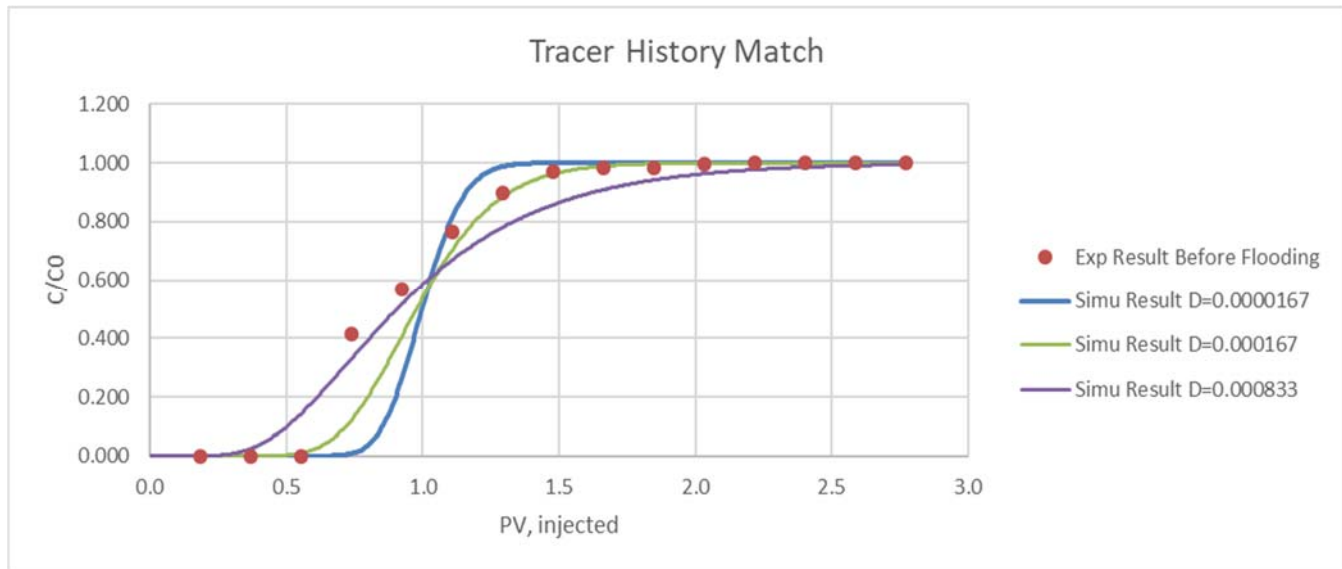
Figure 21: Sensitivity investigation on diffusion and dispersion coefficient.

Based on the results shown in **Figure 21**, we decided to use 1.67 e^{-8} cm^2/s, which fits best shown as green line.

Homogeneous Model Compared with Heterogeneous Model:

This time, we directly compared homogeneous model with heterogeneous model and tried to consider flooding process fitting result together with tracer test process. Simulation was based on CMOST design

of experiments method. Parameter ranges are listed in **Table 2**.

Table 2: CMOST parameters setting for history matching for comparing homogeneous and heterogeneous models.

Homogeneous	Lower Limit	Upper Limit
K	24.8	2480
No	0.8	5
Nw	0.8	5

Heterogeneous	Lower Limit	Upper Limit
H1, H2	0.1	1.125
K1, K2	24.8	2480
No	0.8	5
Nw	0.8	5

The matching results are shown in **Figure 22 and 23** respectively.
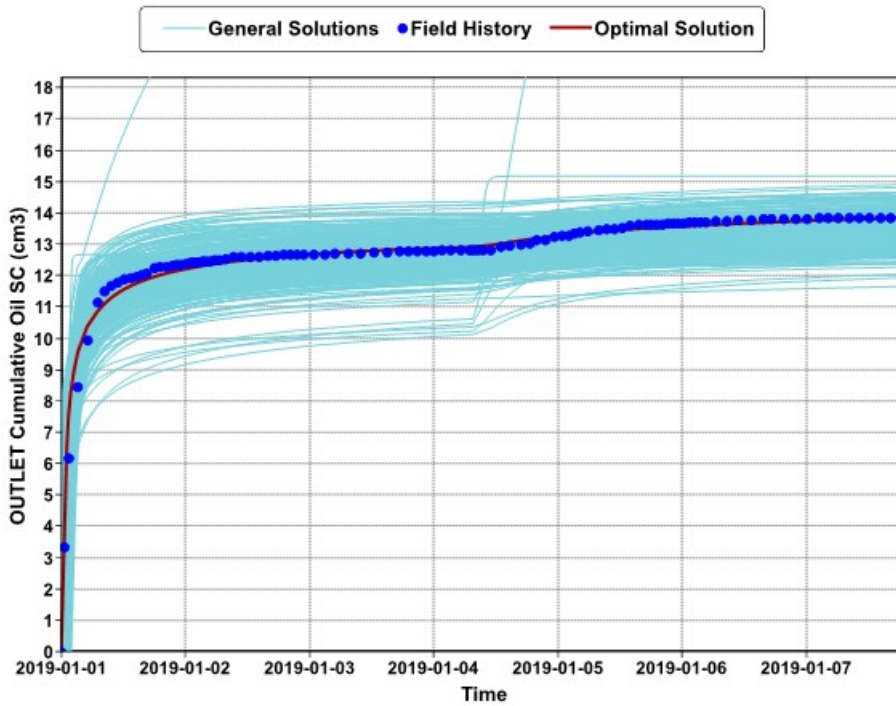
Figure 22: Cumulative oil production history matching result for homogeneous model.

25
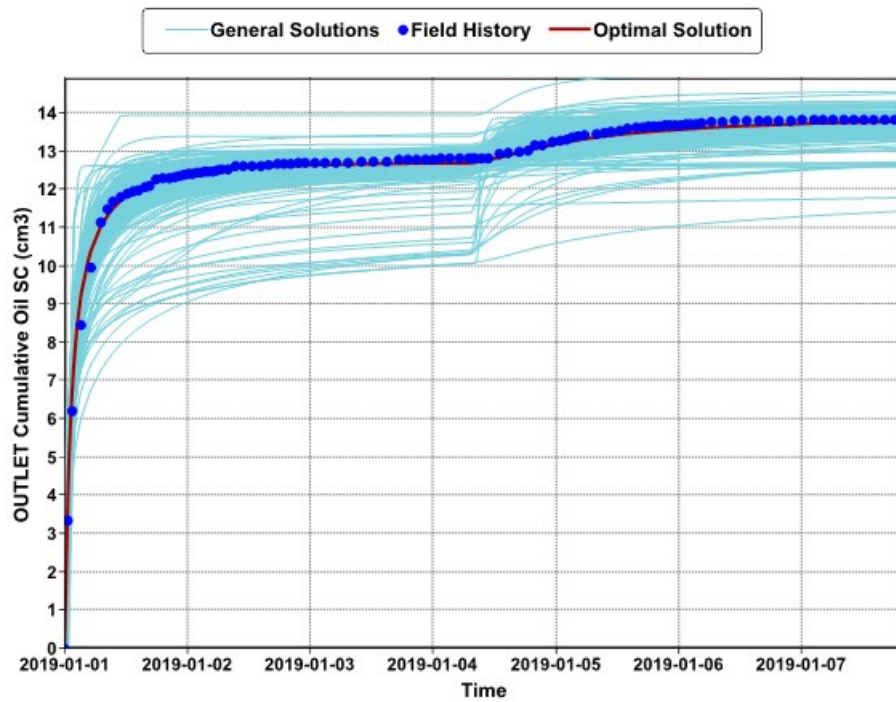
Figure 23: Cumulative oil production history matching result for heterogeneous model.

From oil recovery result, it is difficult to conclude which model fits better. As a result, we must compare fitting result of tracer test after flooding as well, which is shown in **Figure 24 and 25** respectively.
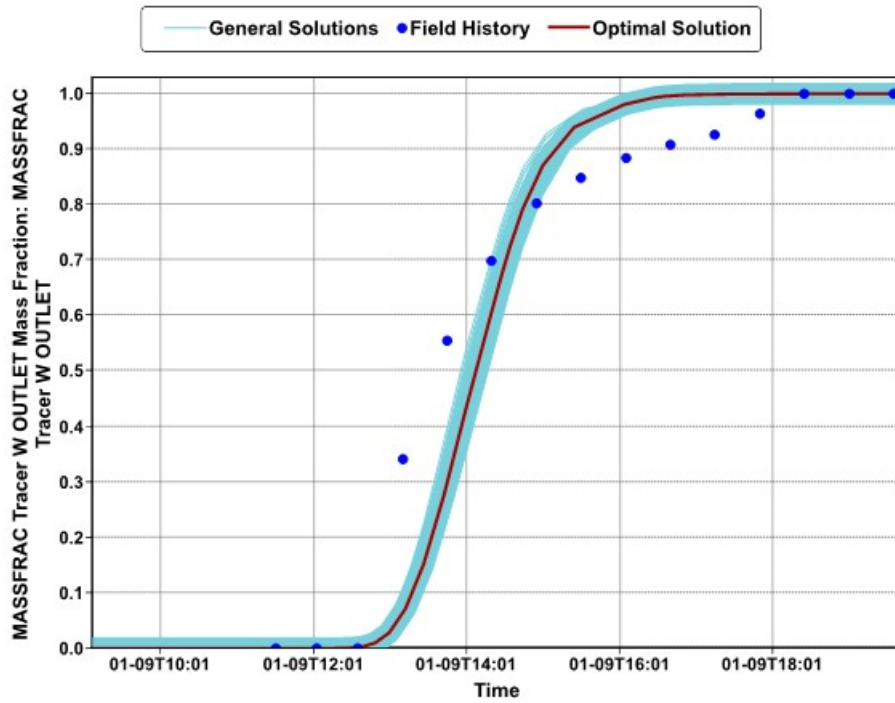
Figure 24: Tracer concentration history matching result for tracer test for homogeneous model.
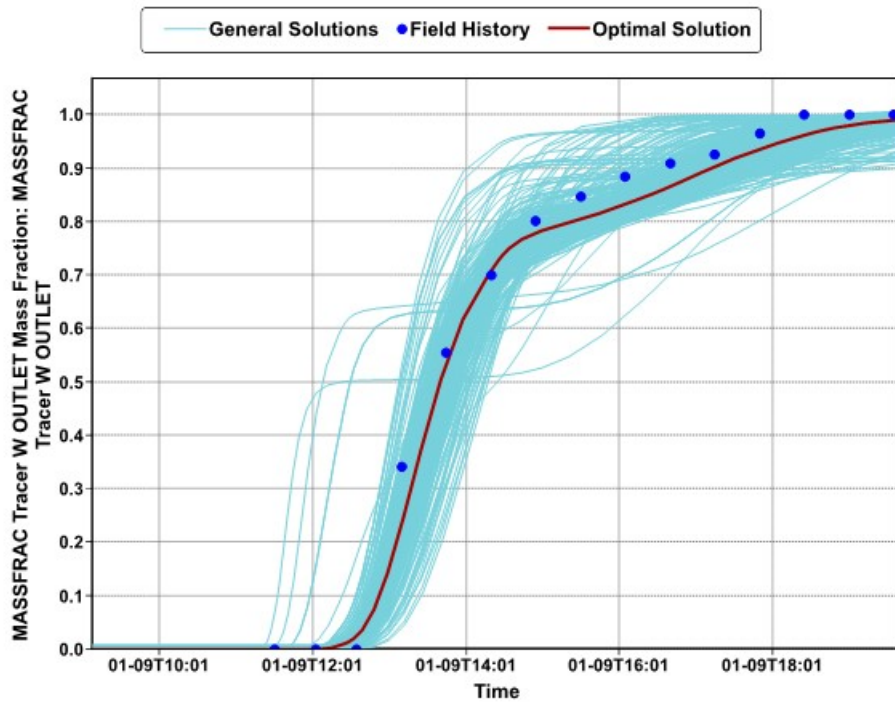
Figure 25: Tracer concentration history matching result for tracer test for heterogeneous model.

Given the fitting result of tracer test, it is clear to state that heterogeneous model can result in a better fitting than homogeneous model. Data analysis for the optimal cases was implemented to further analyze the fitting error comparing both models. Results showed that after flooding, fitting error was pronounced for both models, but homogeneous model fitting error was increased 2.5 times higher than heterogeneous.

Summary. Encouraging results were obtained from several NB formation sandpack core flooding experiments. Low salinity water (LSW) and low salinity polymer (LSP) have remarkably better performance over normal salinity water or polymer. The results confirm that LSWF and LSPF can still improve the oil recovery efficiency even after extensive water flooding and normal salinity polymer flooding. No noticeable incremental oil recovery was observed during HSPF after LSPF or ULSPF. Based on the history matching comparison and data analysis, it is suggested that homogeneous model can acceptably fit the tracer test history before flooding, but heterogeneous model can better fit the core flooding combined with tracer test history after flooding. This conclusion states that channeling may occur during the flooding process. Further experiments are needed to understand the flooding process and whether channeling occurred during LSW or polymer flooding.

Activity is ongoing.

- Task 4.0 - Reservoir Simulation Studies for Coreflooding Experiments and Optimization of Field Pilot Test Injection Strategy

Activities during this quarter completed by UND include:
- Studying ion exchange capacity and clay effect on polymer retention using a 1D homogenous model on the laboratory sandpack experiment.
- Continuing to study polymer retention effect on polymer effectiveness simulations using a 1D homogenous model on the laboratory core flooding experiments.
- History matching on production index using a field-scale model through the functions of transmissibility and dispersion, while incorporating core flooding or sandpack experimental data.

Lab-scale Models on Polymer Retention

1D homogeneous simulation models for the new polymer retention experiments

Two additional polymer retention simulations were similar to previous models as discussed in the third quarterly report (which were used for the first five polymer retention simulations). In this current report, the first model was established to study ion exchange and clay effect on polymer retention based on the actual laboratory sandpack conditions (a plastic sandpack tube), and the second model was based on the actual laboratory core plug conditions (triaxial core holder). For the plastic tube of sandpack, a 15" (1.25 ft.) in length and a 1.50 cm in effectiveness diameter were used. A 14.9 ft/day of injection flux was used for the sandpack model with variable injection pressures. The total maximum volume of the injection slug was 6.5 PV. For the core plug model, a 15" (1.25 ft.) in length and a 2.54 cm in effectiveness diameter were used. A 3.73 ft/day of injection flux was used for the core plug model with an overburden pressure of 1,000 psi and variable injection pressures. The total maximum volume of the injection slug was 11.4 PV. **Figure 26** illustrates the 1D model for the sandpack and core plug that were used for simulations.

Table 3 shows the parameters used in the two cases. All parameters are consistent with the laboratory experimental data.

Figure 26: 1D simulation model illustration for case studies.

Table 3: Parameters used for polymer retention simulation

Reservoir Parameter	Case 1	Case 2
	Oil sand	Oil core
Source formation	NB	NB
Contact material	Plastic	Triaxial core holder
Size of X– direction, foot	1.25 (15")	1.25 (15")
Size of Y– direction, cm	1.50	2.54
Injection Pore Volume, PV	6.8	11.4
Injection water salinity, ppm	2,600	2,600
Porosity, fraction	0.370	0.250
Permeability, md	10,900	548
K_{rw} at S_{or}	0.20 (NB sand at 4186.6 ft)	0.10 (Core test by NMT)
Overburden pressure, psi	0	1,000
Polymer molecular weight, Daltons	18×10^6	18×10^6
Polymer concentration, ppm	1,750	1,750
Polymer viscosity, cP	40.73	40.73

Resistance factor, fraction	1	1
Inaccessible pore volume, ft^3	0	0
Initial water saturation, fraction	0.2	0.2

Discussion of results

Clay composition determination and ion exchange effect on polymer retention

Based on two X-Ray Diffraction (XRD) analyses by New Mexico Institute of Mining & Technology (NMT), three clay minerals were found in NB sand. They were 1% chlorite, 1% kaolinite, and 1% illite, respectively (**Figures 27** and **28**). Because toluene and methanol were used for sand cleaning in the second XRD measurement, kaolinite could not be detected (**Figure 28**). Based on chemical formulas of clay mineral groups (**Table 5**), combined with X-Ray Fluorescence (XRF) analysis of NB sand (**Table 4**), the major metals in the clays were *Al*, *Fe*, *Mg*, *K*. Therefore, the three clays indeed existed in the target formation. Consequently, the simulation models need to include ion exchange between clays and injected aqueous solutions. In the simulation model, the values of ion exchange capacities were assumed based on technical manual of CMG STARS (**Table 6**).

Generally, ion exchange is a very important clay property. Calcium and sodium in the tetrahedral montmorillonite sheet are weakly held and can be exchanged for other cations that may be brought into contact with the clay.

Ion exchange has no direct relationship with oil recovery, but it could affect oil recovery by wettability and relative permeability alterations. It could also change the ionic content of the brine, which in turn, could affect polymer viscosity. It could also accentuate polymer retention, which affects polymer propagation and oil recovery.

Figure 29 illustrates the solid volume change in polymer adsorption with and without ion exchange functions incorporated in the simulation models. Based on **Figure 29**, we believe that polymer was adsorbed or entrapped shortly after polymer injection when ions from the injection water contact with clays in the sand.
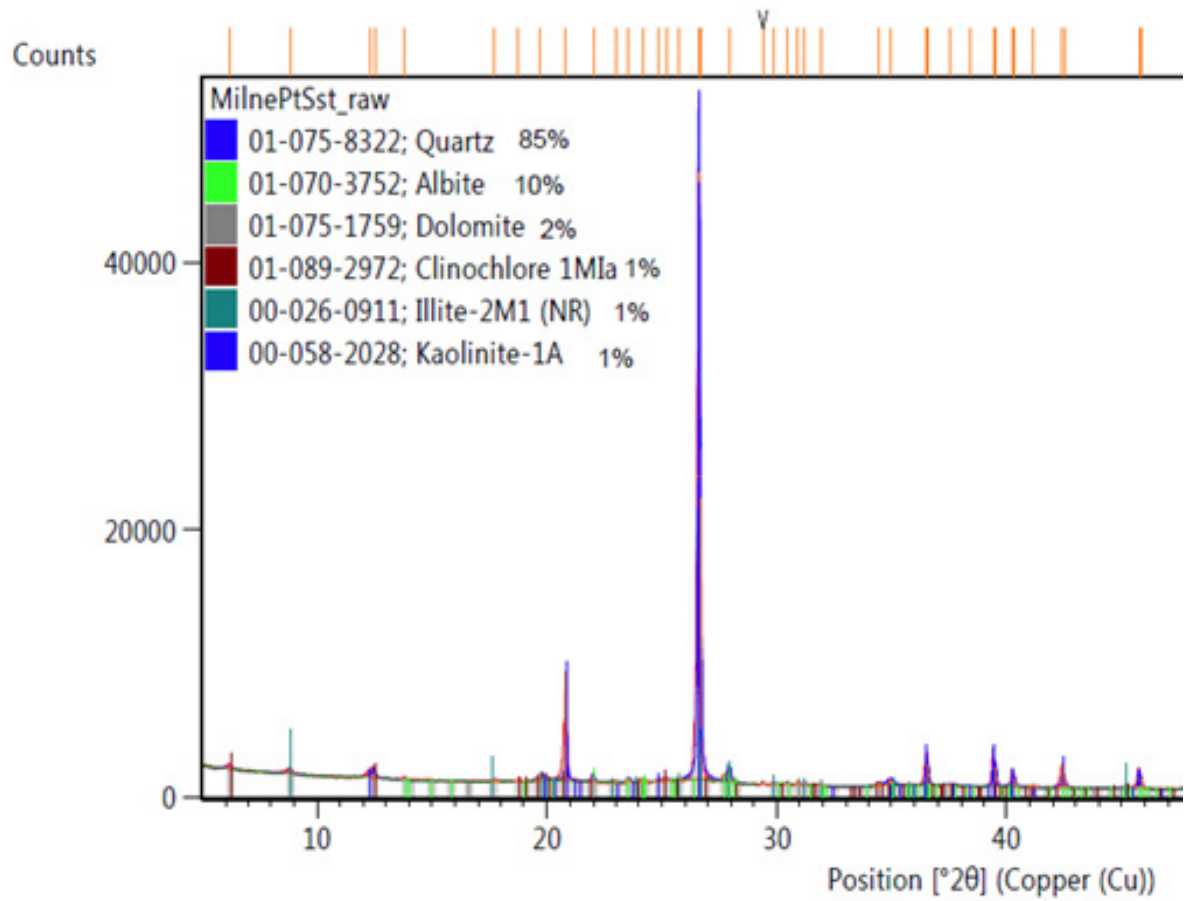
Figure 27: XRD analysis of NB sand (performed at NMT).
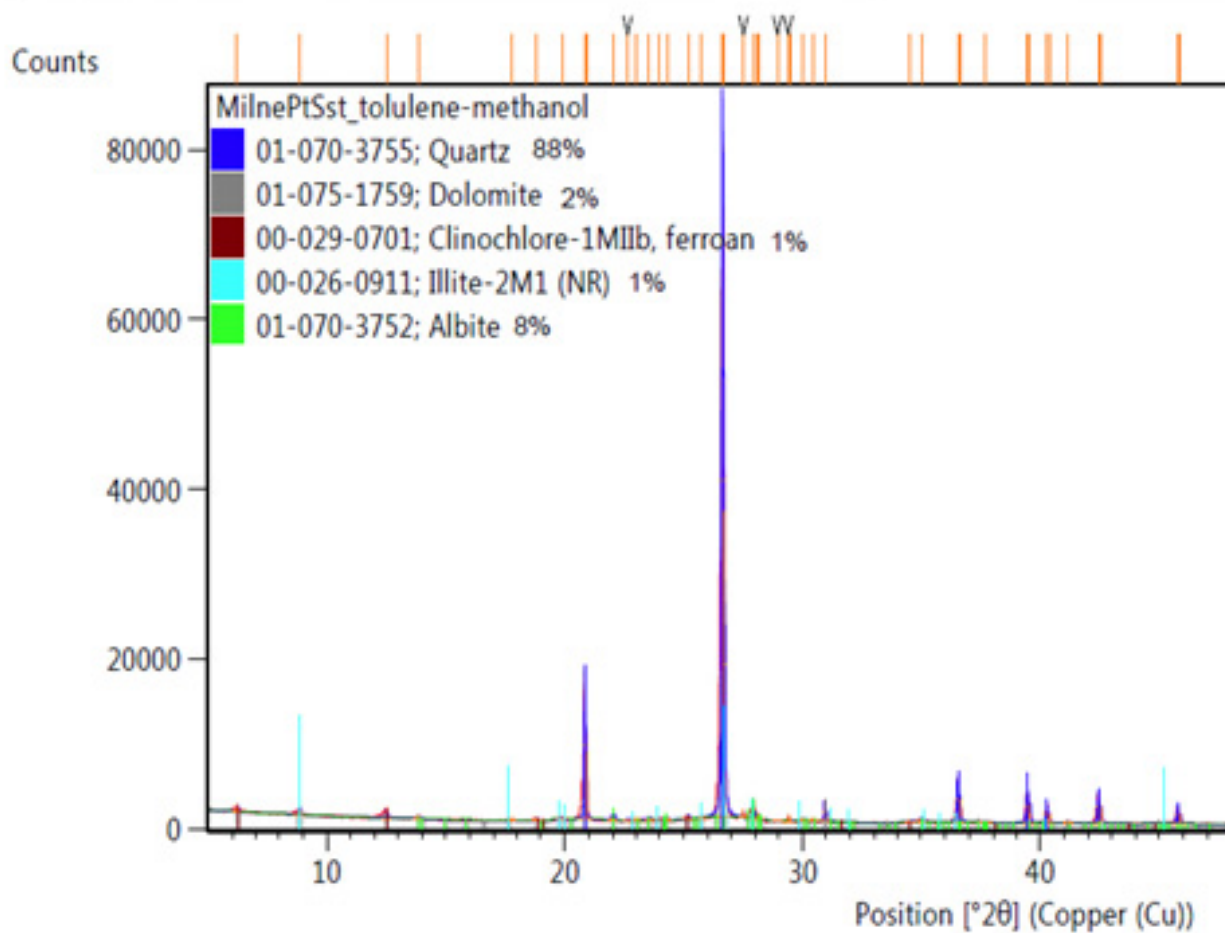
Figure 28: XRD analysis of NB sand cleaned by toluene and methanol (performed at NMT).
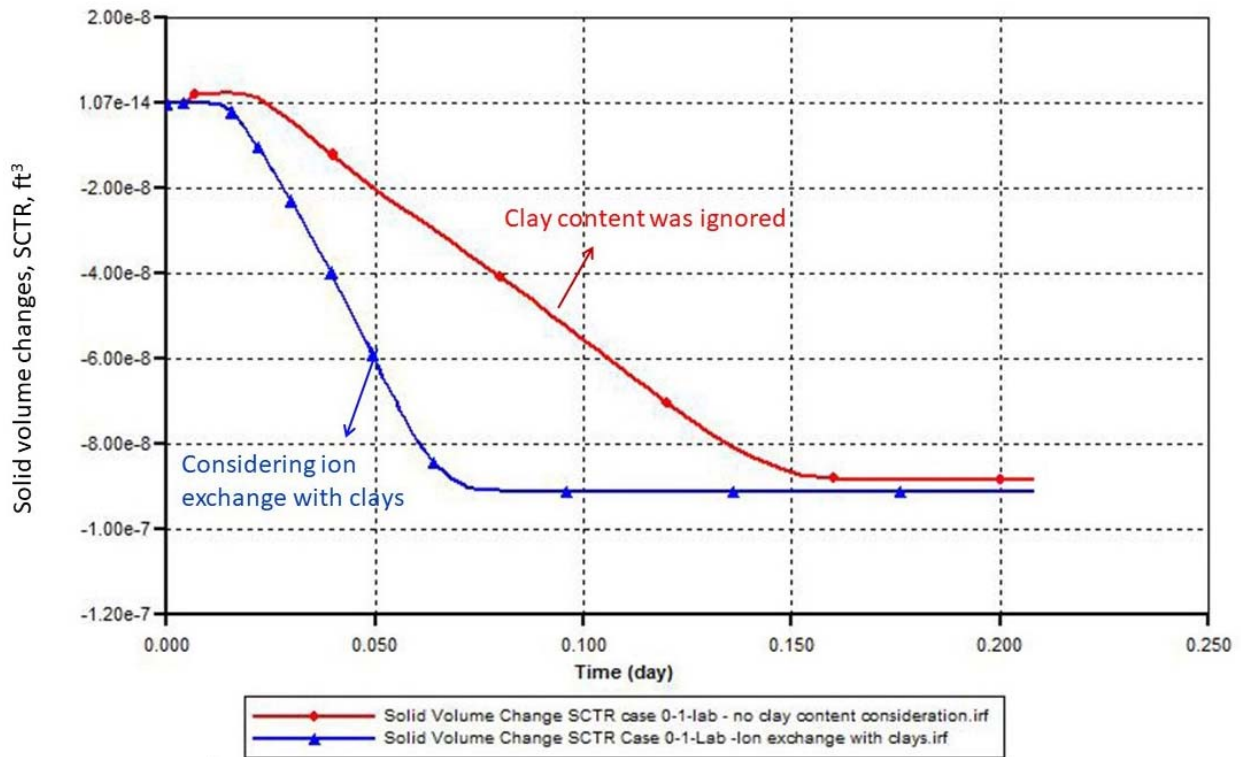
Figure 29: Solid volume changes with and without clay considerations.

Table 4: XRF analysis results.

Element	Content, %	Error
Si	30.0000	0.1897
Fe	2.3683	0.0385
Al	1.7162	0.0873
K	0.7851	0.0244
Na	0.3788	0.1122
Ti	0.2837	0.0120
Ca	0.2769	0.0156
Mg	0.2312	0.0447
S	0.1377	0.0104
Ba	0.0904	0.0265
Zr	0.0416	0.0052

P	0.0359	0.0094
Zn	0.0317	0.0068
Sr	0.0307	0.0047
Rb	0.0208	0.0047
Mn	0.0182	0.0073
V	0.0182	0.0078
Cu	0.0135	0.0099
Y	0.0083	0.0047
Ni	0.0078	0.0057

Table 5: Clay mineral group and their chemical formulation.

Clay Mineral Group	Chemical Formulations
Kaolinite	$Al_2Si_2O_5(OH)_4$
Smectite	$\sim Ca_{0,17}(Al,Mg,Fe)_2(Si,Al)_4O_{10}(OH)_2 \cdot nH_2O$
Illite	$\sim K_{0,8}\,Al_2(Al_{0,8}Si_{3,2})O_{10}(OH)_2$
Chlorite	$(Mg,Fe^{2+})_5Al_2Si_3O_{10}(OH)_8$
Vermiculite	$\sim(Mg,Ca)_{0,3}(Mg,Fe^{2+},Fe^{3+},Al)_3(Si,Al)_4O_{10}(OH)_2$

https://dnr.mo.gov/geology/geosrv/geores/indmin/clayandshale.htm

Table 6: Ion exchange capacity of clays used in the simulation model

Clay	Ion exchange capacity, meq/l
Kaolinite	0.035
Illite	0.150
Chlorite	0.05

Core plug simulation of polymer retention behavior

Figure 30 shows the solid volume changes associated with the new core flooding simulation compared to results of polymer retention in sandpack. During the simulation, the applied overburden pressures and the relative permeability curves were varied (**Figure 31**). In **Figure 31**, the *Krws* at S$_{or}$ were 0.2 (blue line with solid triangles) for sandpack simulation and 0.096 (blue lines with open triangles) for the core plug simulation. The *Krw* used for the core plug simulation was estimated based on the NMT laboratory

test of absolute permeability of 548 md and effective permeability of 53 md at S_{or}. The Krw used for the sandpack simulation was adopted from the NB sand at 4186.6 ft (water-oil table) which was provided by Hilcorp.

Since the solid volume change represents polymer adsorption in the model, the solid line with red circles indicate high polymer adsorption during the core floods with 1000 psi overburden pressure applied. In contrast, polymer adsorption was less for sandpack tests without overburden pressure. The more compacted sand exhibited higher polymer retention. In **Figure 30**, the polymer retention values were 45 µg/g for the sandpack test and 240 µg/g for the core plug test.

Sand pack retention test, K = 10,900 md, 8 PV injection, overburden pressure = 0 psi

Core retention test, K = 589 md, 12 PV injection, overburden pressure = 1,000 psi
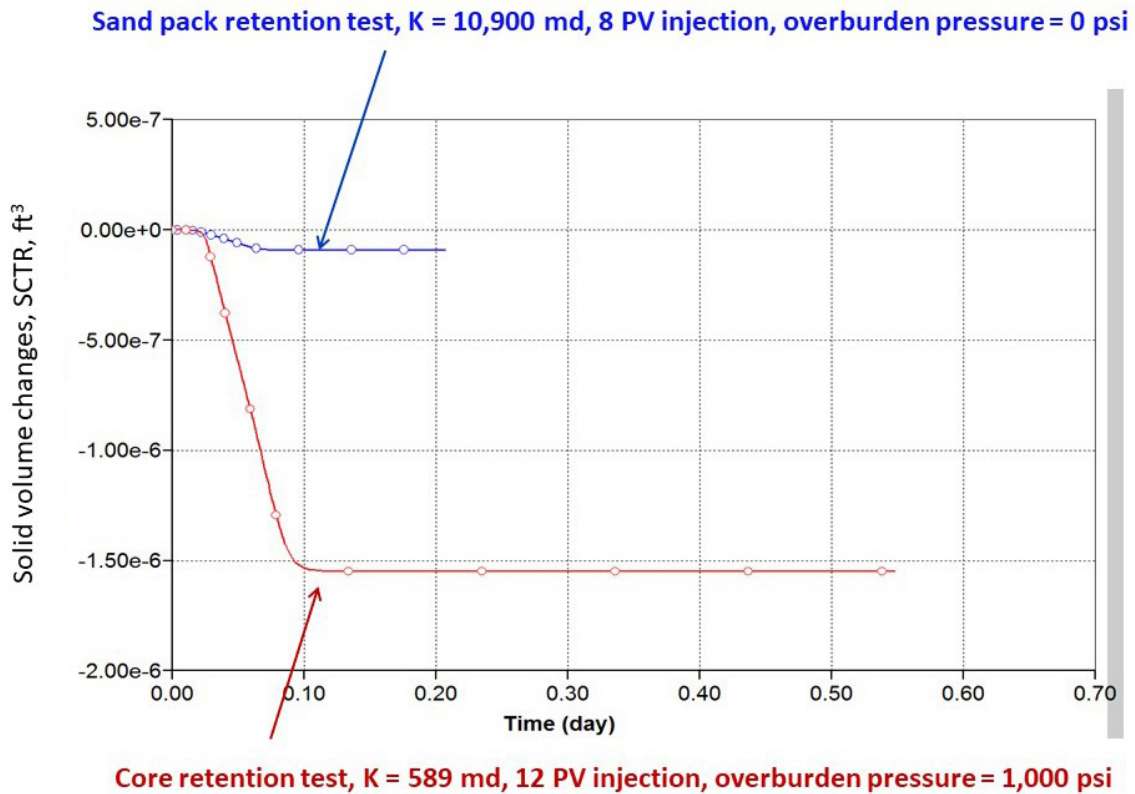
Figure 30: Solid volume changes for core flooding test and sandpack test on polymer retention.
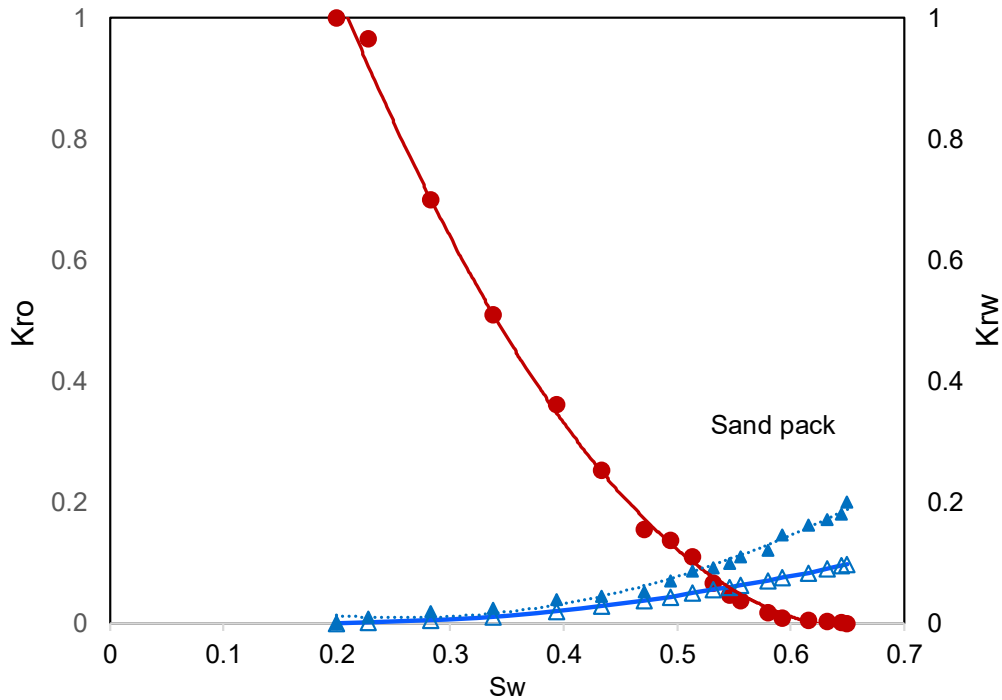
Figure 31: Relative permeability curves for lab-scale models on polymer retention.

History matching of field-scale model with incorporated experimental data
Two studies were conducted for the field-scale model: sub-region original oil in-place (STOOIP) estimation, production index history match, including tracer histories and oil recovery prediction using current polymer parameters.

STOOIP and sub-region pore volume (PV) estimation
For the STOOIP and reservoir pore volume estimations, the area was focused on the region which covers four polymer wells instead of the entire area of the field-scale model, as enclosed by red dashed lines in **Figure 32**. Equation 1 was used for the oil volume estimation, assuming under the condition of original oil saturation.

$$N = 7758 \frac{Ah\phi S_o}{B_o} \tag{1}$$

Where, N is the STOOIP; A is the reservoir area in acres; h is the thickness of the reservoir in ft; ϕ is the porosity of the reservoir in fraction; S_o is the saturation of oil in fraction; and B_o is the formation factor of oil in res. bbl/STB. All variables were sourced from the actual oil formation.
Based on the STOOIP estimation by the volumetric equation and the reservoir pore volume analytical calculation, good agreement was obtained with the current values from the simulation model– suggesting

no need for further revision in STOOIP or pore volume of the current field-scale model (**Table 7**).
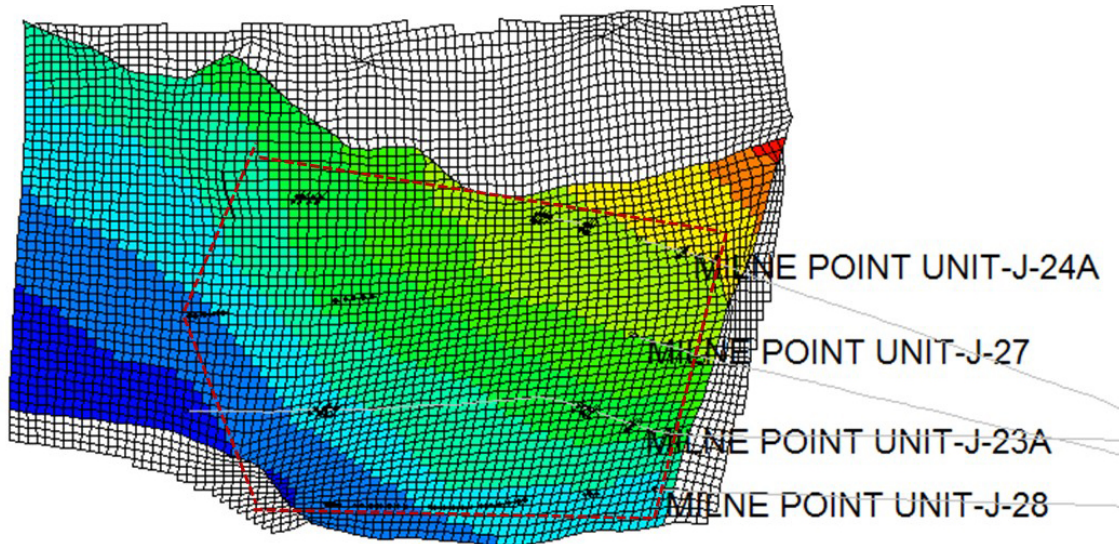

Figure 32: Area of STOOIP and PV estimation.

Table 7: Relative errors of comparison of STOOIP and PV in two methods.

Index	Equation basis	Field-scale model basis	Relative error, %
STOOIP, ft^3	8.034E+07	7.647E+07	4.8
Reservoir PV	1.032E+08	1.045E+08	1.2

Production index history match

Production index history match was conducted from the beginning of water injection to the end of March of 2019. Several methods were employed during the history match: using the functions of "transmissibility" plus "dispersion" to tune oil rates and water cuts of two production wells, and the modular "CMOST" of CMG plus transmissibility adjustments in high permeability regions to tune tracer production history. A transmissibility multiplier is a function which can be applied to both convective and dispersive flows. This function affects fluid flow by involving relative permeabilities and viscosities, and fluid-flow caused by dispersion. Transmissibility tuning can be varied with time. By tuning transmissibility during the period of injection and production to match production histories dynamically instead of adjusting permeability statically. As CMOST is explained by CMG: identify the best solution for your reservoir by combining advanced statistical analysis, machine learning, and non-biased data interpretation with your engineering expertise.

Figures 33 to **40** show the simulation results of history match in oil-rates, water cuts, and tracer productions of the two production wells. In all following figures, the actual production data are depicted by circles, and all simulation data are depicted by colored solid or dashed lines. Based on the figures, we conclude that when incorporated the function of transmissibility to tune the index of production history dynamically in the simulation model, production history match by simulation shows good agreement with the actual index in the period of production.
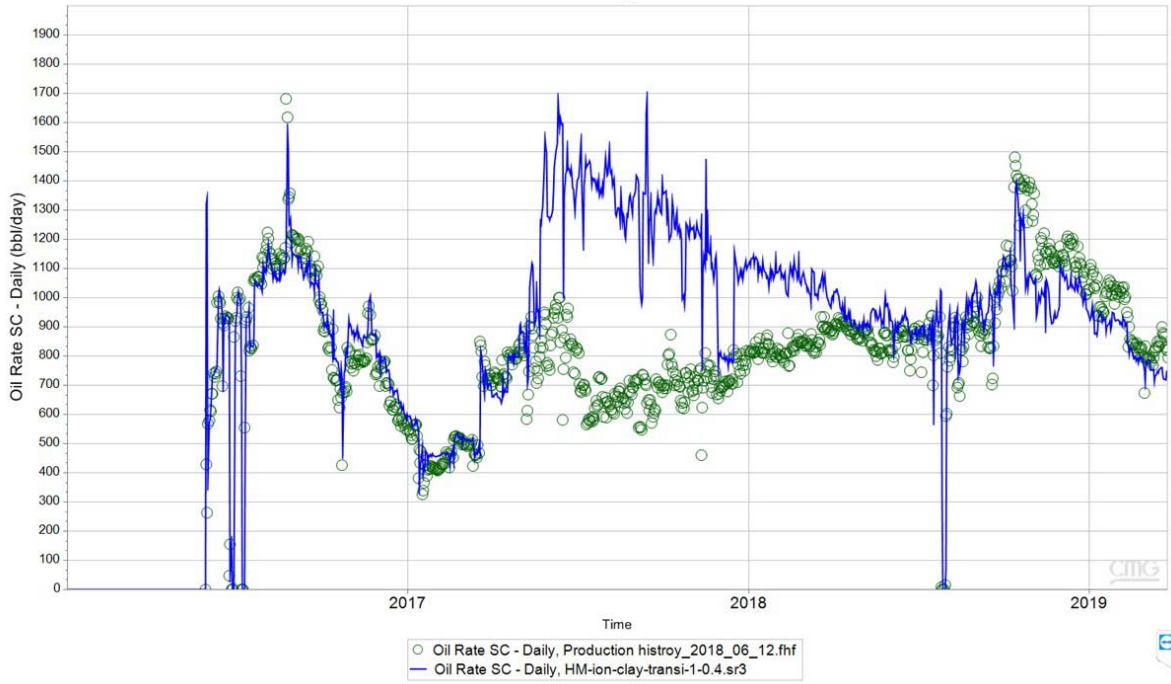

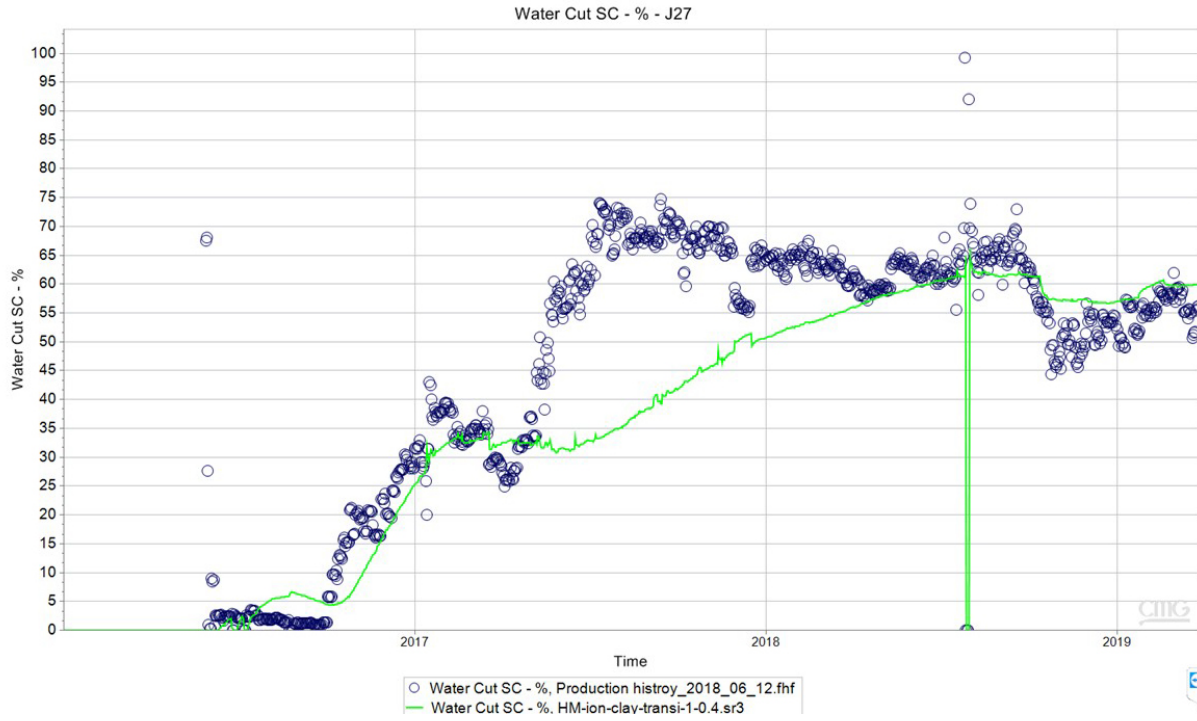**Figure 33: Oil rate history match of well J-27.**

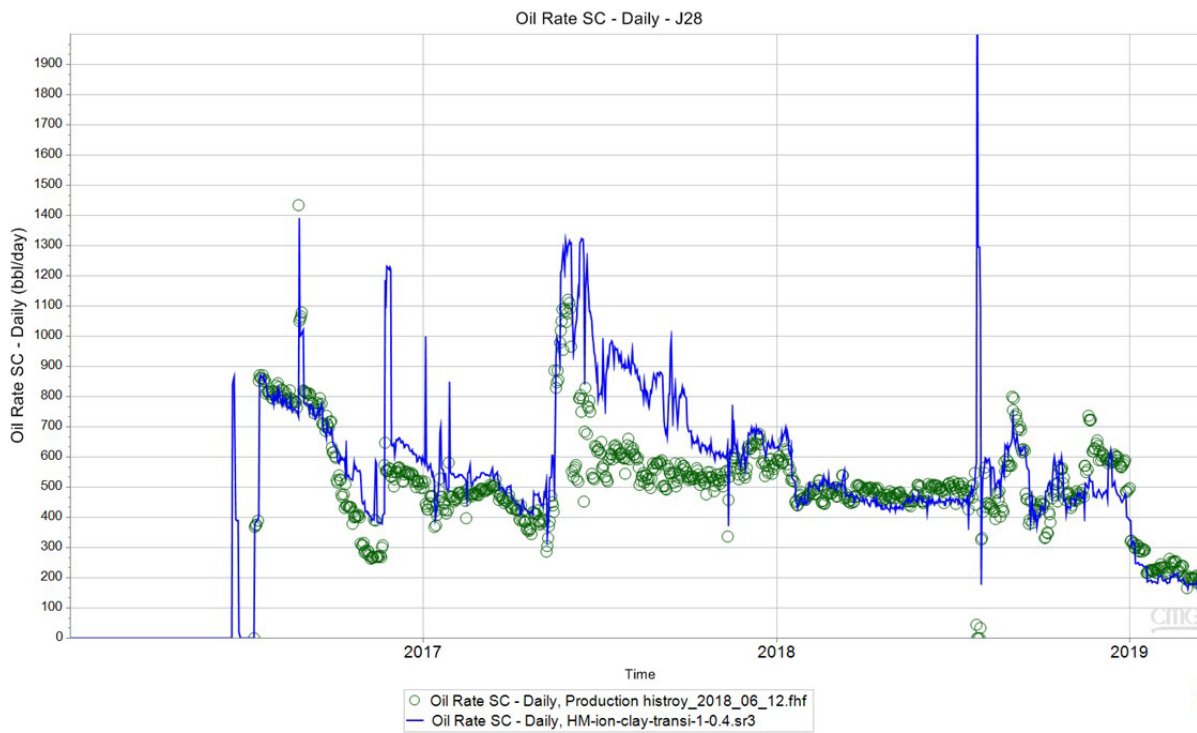**Figure 34: Water cut history match of well J-27.**

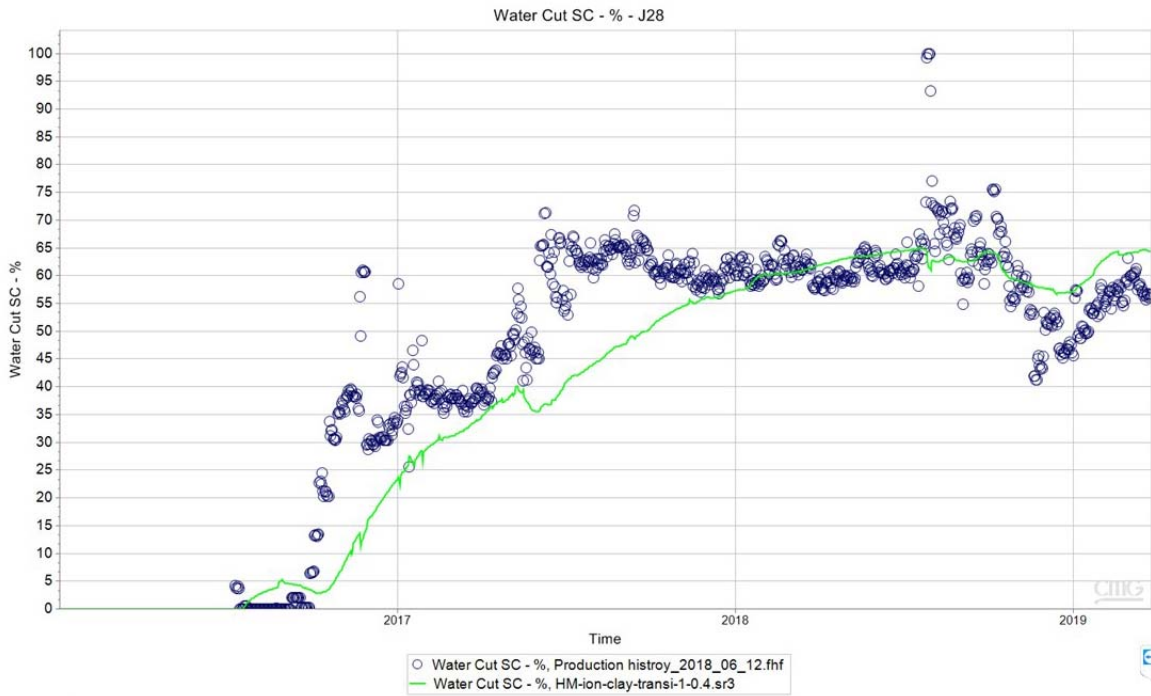**Figure 35: Oil rate history match of well J-28.**

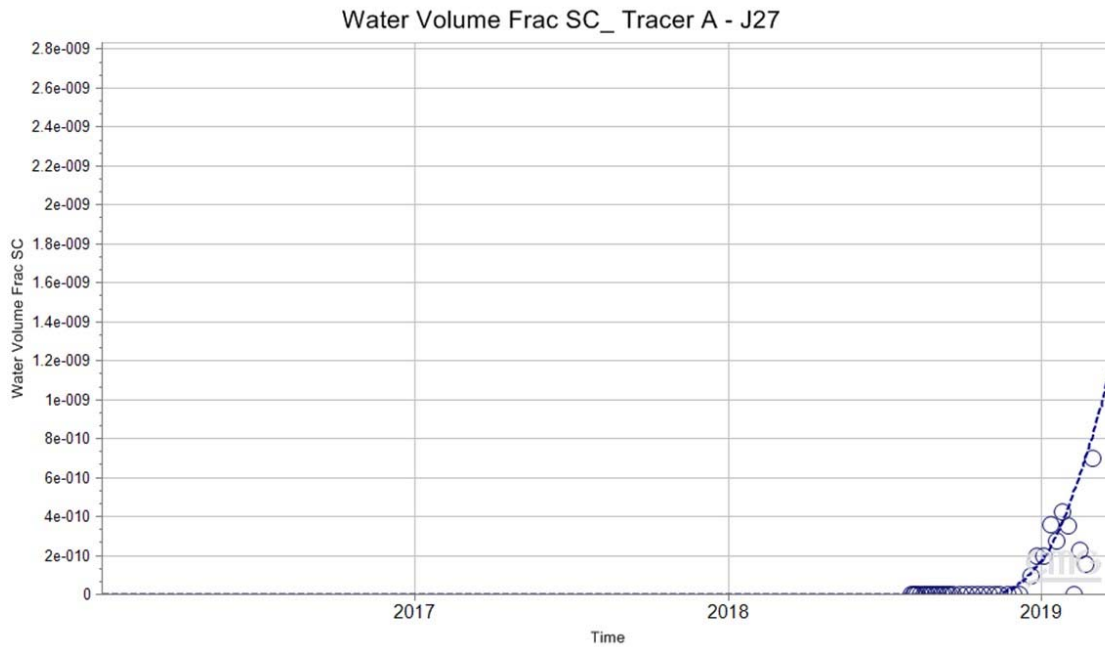**Figure 36: Water cut history match of well J-28.**

Figure 37: Tracer 140A history match of well J-27.

Figure 38: Tracer 140A history match of well J-28.

Figure 39: Tracer 140C history match of well J-27.

Figure 40: Tracer 140C history match of Well J-28.

Summary

(1) Polymer retention is affected by overburden pressure, permeability, and relative permeability;

(2) Using transmissibility function, the histories of tracer, oil rate, and water cut were matched well.

Next Plan

(1) Continue to simulate polymer retention behavior using core plug experimental conditions.

(2) Core flooding simulation in relative permeability effects on polymer rheology.

(3) Continue production history match using the field-scale model and predict and optimize polymer performance and polymer injection parameters.

UND activity is ongoing.

In this quarter, UAF's work focused on tracer data history matching and production forecast of waterflooding and polymer flooding, which is reported below.

Tracer test data for history matching

By collecting production data including tracer concentration from the tracer injection, the production history used to tune the reservoir simulation model was extended to March 25, 2019. The water injection rates and liquid production rates are set as well constraints in the reservoir simulation model, while oil production rates and tracer concentration measured in producers are to be history matched using CMOST.

Parameter setting of the reservoir simulation model

Tracer parameters. Tracer T-140A and T-140C, as two new components, are added to the simulation model. The properties of tracers (for example, molecular weight, critical pressure, and critical temperature) are assigned the same values as those of water. The propagation of injected tracers and chemicals employed in EOR processes are influenced by the tortuous flow and heterogeneities of the porous media in which they flow. Normally, this causes the tracer to disperse at different velocities in three directions in the reservoir simulation model. Because of this, the effective total dispersion coefficients of tracer T-140A and T-140C in the water phase for I, J and K directions inputted in the simulation are used to specify the flowability of tracers in the reservoir. Initially, the total dispersion coefficients of T-140A in I, J and K directions are assigned to be 1×10^{-8}, 1×10^{-4} and 1×10^{-8}, respectively, while the total dispersion coefficients of T-140C in I, J and K directions are assigned to be 1×10^{-4}, 1×10^{-2} and 1×10^{-4}, respectively. The mole fraction of tracer in the injection fluid is calculated by using the mass of the injected tracer and the injected water. In the simulation model, the mole fraction of T-140A in injector J-24A is 6×10^{-4}, and the mole fraction of T-140C in injector J-23A is 4×10^{-4}.

Permeability heterogeneity. Tracer test data shows that T-140C was first observed in J-27 on October 12, 70 days after injection, and the tracer concentration reached a peak at 155 days. It indicates there may exist strong communication between injector J-23A and producer J-27. Therefore, a block/strip permeability field is developed, as shown in **Figure 41,** to identify the potential high permeable channels between injector J-23A and producer J-27.
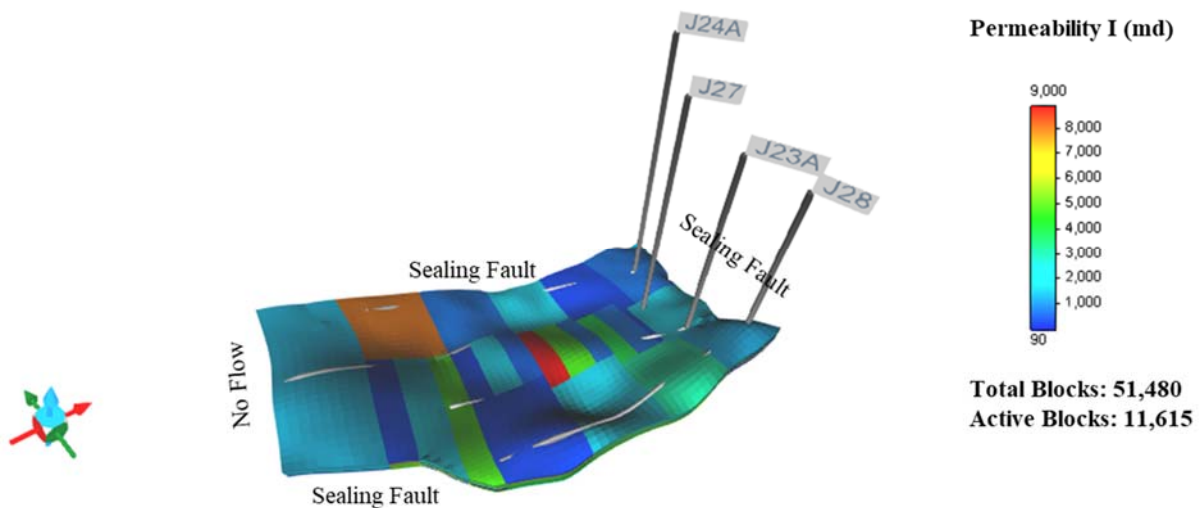
Figure 41: Permeability heterogeneity of block/strip type in the simulation model.

Twenty-six permeability blocks/stripes are assigned in each layer, resulting in 130 permeability blocks/stripes in the whole reservoir simulation model. The permeability of the blocks/strips in each layer are initially assigned with the average permeability of the layer (layer 1: 1806 mD, layer 2: 1598 mD, layer 3: 2269 mD, layer 4: 1801 mD and layer 5: 1029 mD) and then tuned between 100 and 7600 mD during the history matching process. In addition, the average porosity of each layer (layer 1: 0.3476, layer 2: 0.3474, layer 3: 0.3537, layer 4: 0.3497 and layer 5: 0.3417) and the estimated relative permeability

curves, as shown in **Figure 42,** from the previous history matching results are used in the simulation model.
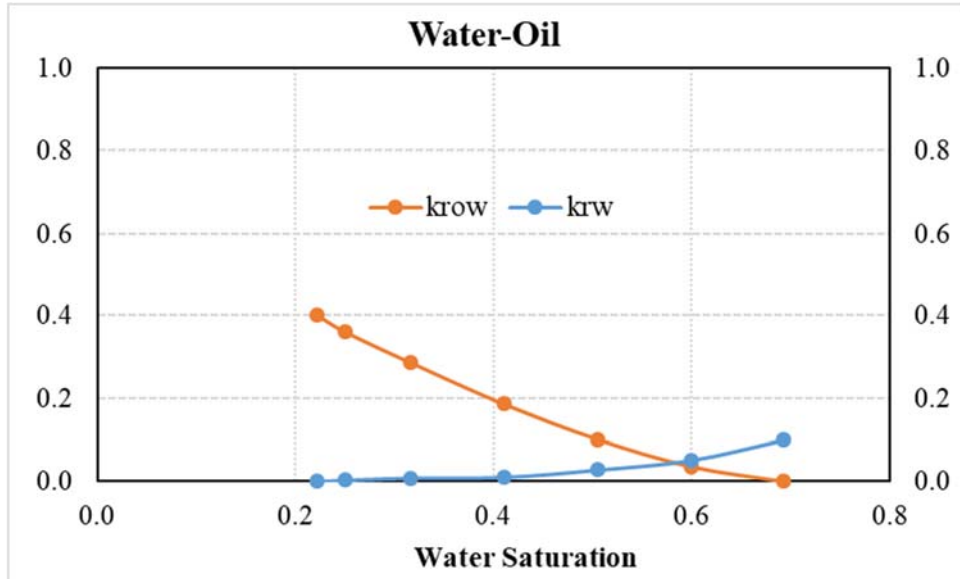
(a) Oil-water relative permeability
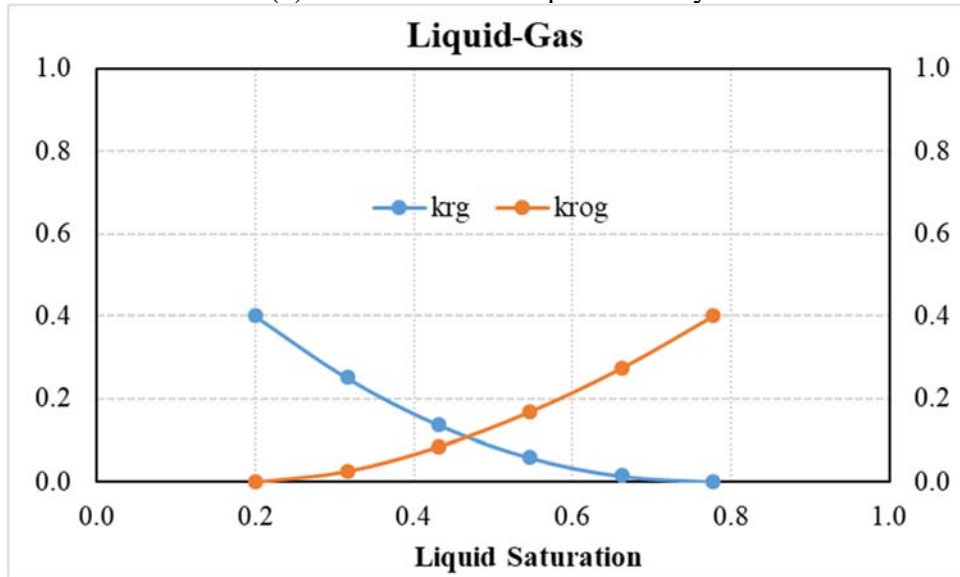
(b) Gas-oil relative permeability
Figure 42: Relative permeability curves of (a) oil-water and (b) gas-oil.

History matching results
During the history matching, we try to match not only the production profiles of waterflooding and polymer flooding but also the concentration profiles of tracer T-140A and T-140C in two producers. Tracer test data unit in part per billion (ppb) is converted to water mass fraction used in the simulation

model. The permeability of the blocks/strips in five layers and the total dispersion coefficients of tracer T-140A and T-140C are tuned together to try to match the water cut and water mass fraction of T-140A and T-140C in CMOST.

The optimal history matching results of the water cut and the oil production rate for the two producers are shown in **Figure 43**. It can be seen that the simulated production data are close to the observed ones for the polymer flooding period. As for the waterflooding period, the history matching results are not better than the previous work.

(a) Water cut of producer J-27

Oil Rate SC - J27

(b) Oil production rate of producer J-27

Water Cut SC - % - J28
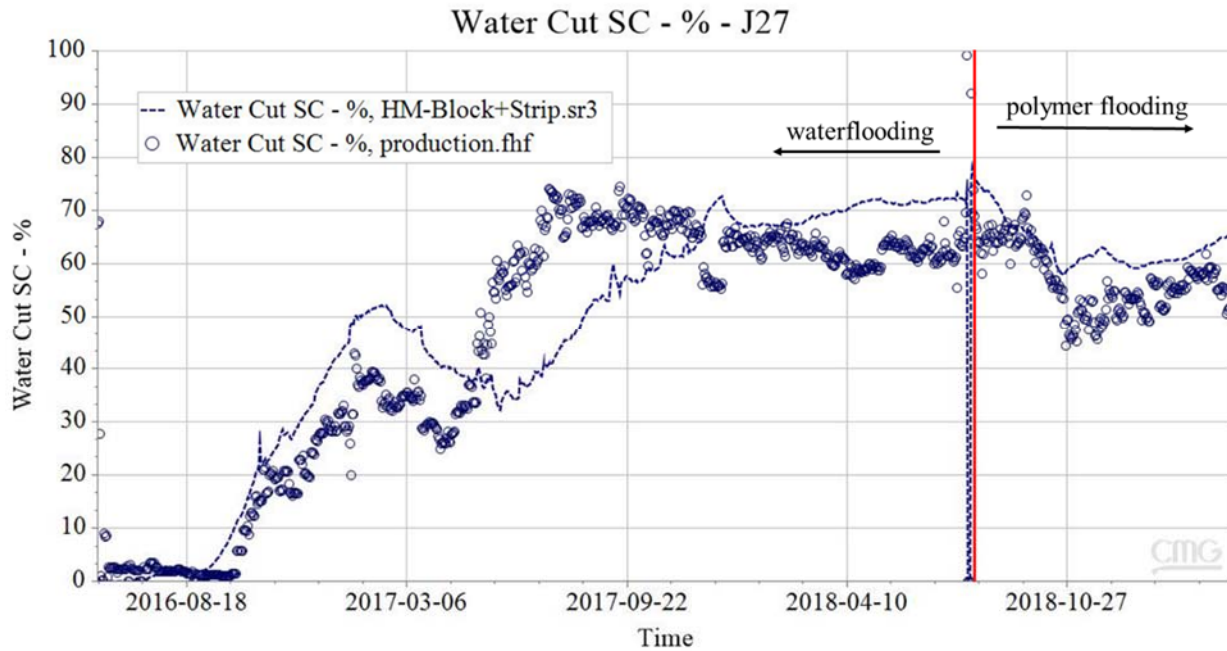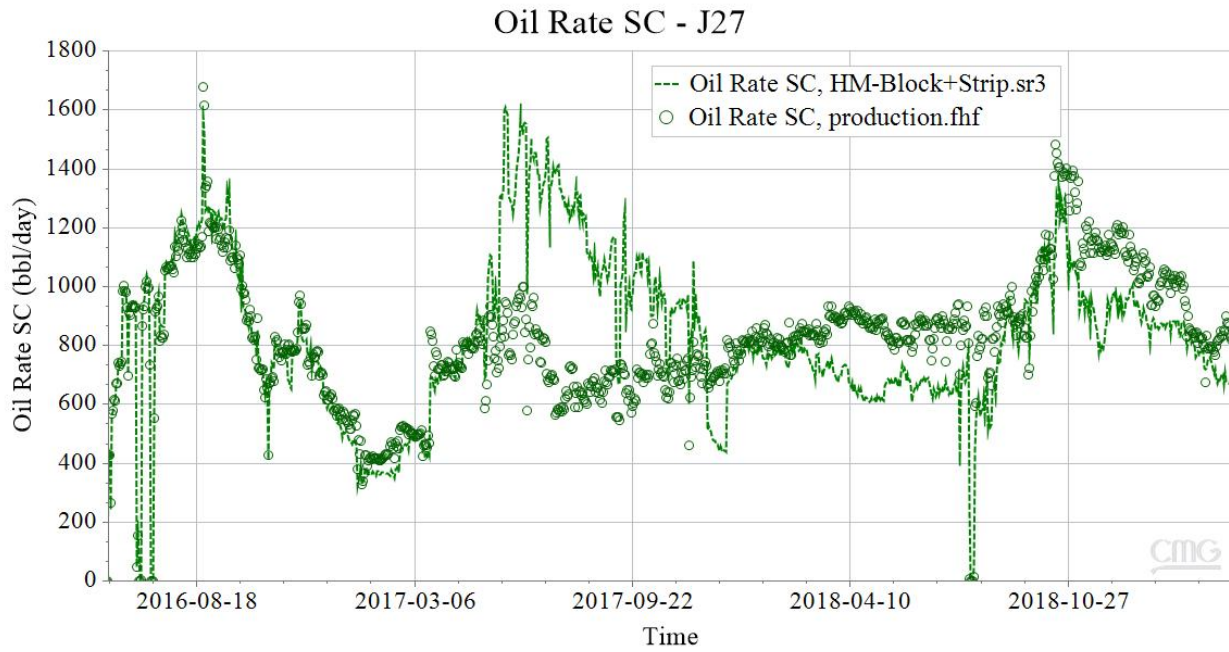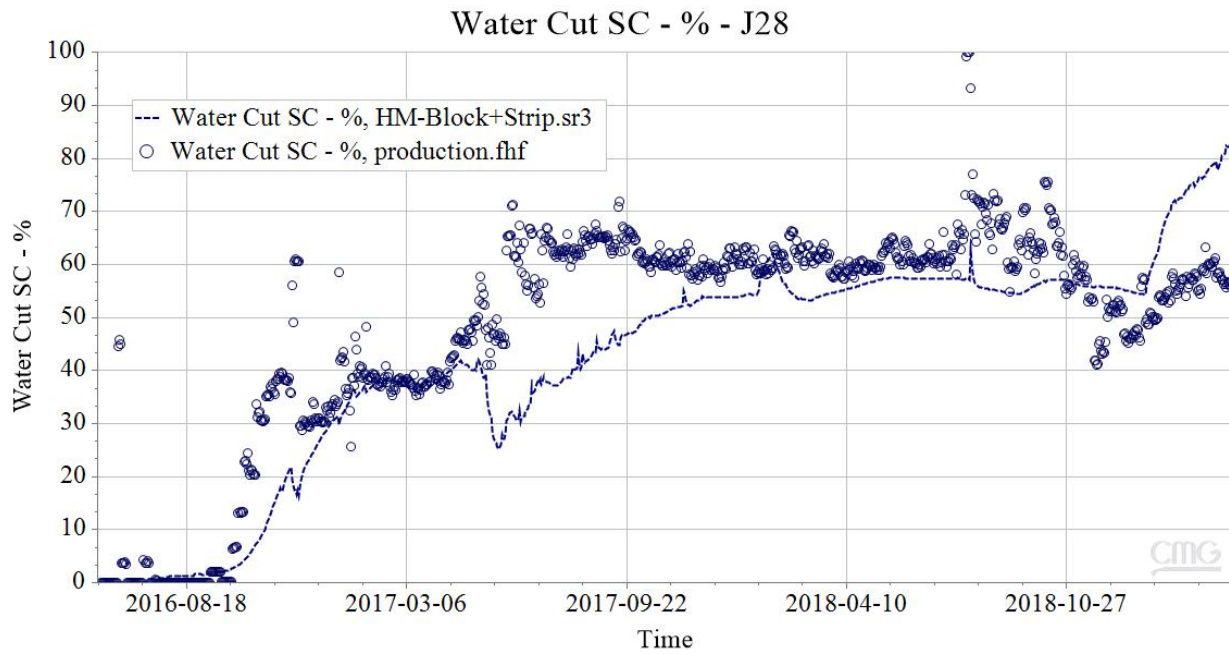
(c) Water cut of producer J-28
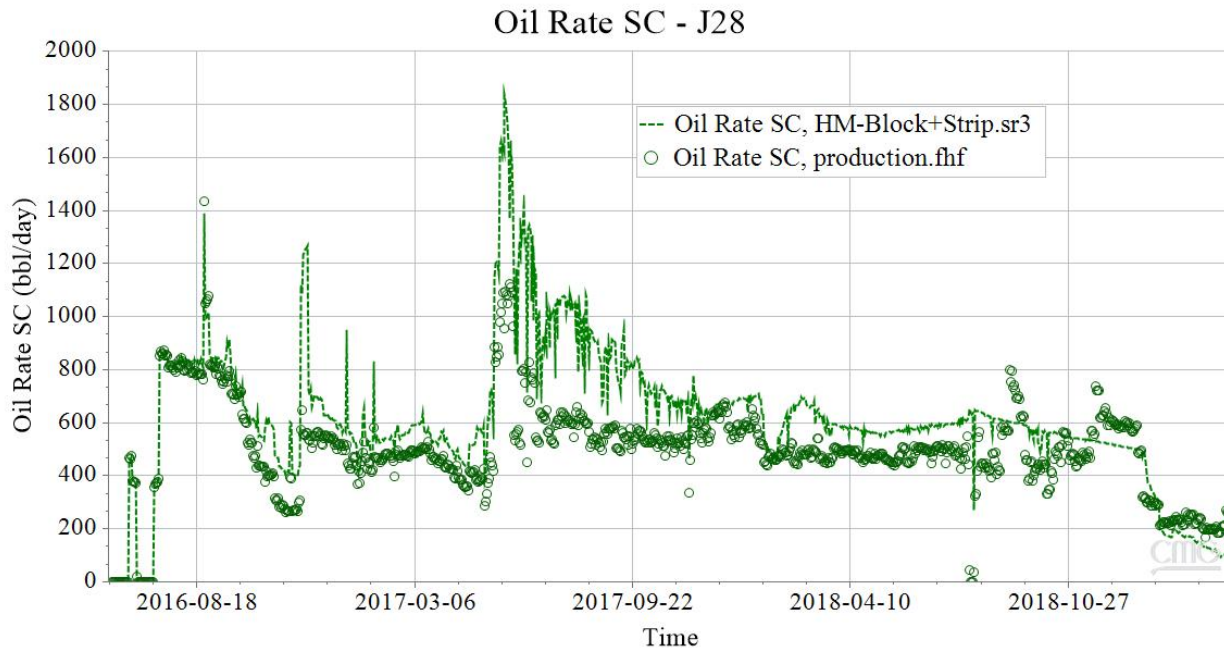
(d) Oil production rate of producer J-28

Figure 43: History matching results of (a) water cut (b) oil production rate for producer J-27 and (c) water cut (d) oil production rate for producer J-28.

The history matching results of tracer concentration in producer J-27 and J-28 is presented in **Figure 44**. It can be seen that there is an agreement between observed data and updated simulation result of T-140C concentration in producer J-28. Although tracer concentration profiles in producer J-27 obtained from the updated simulation model can reflect the increasing trends of concentration, there still exist significant disagreement between the simulated data and observed data.
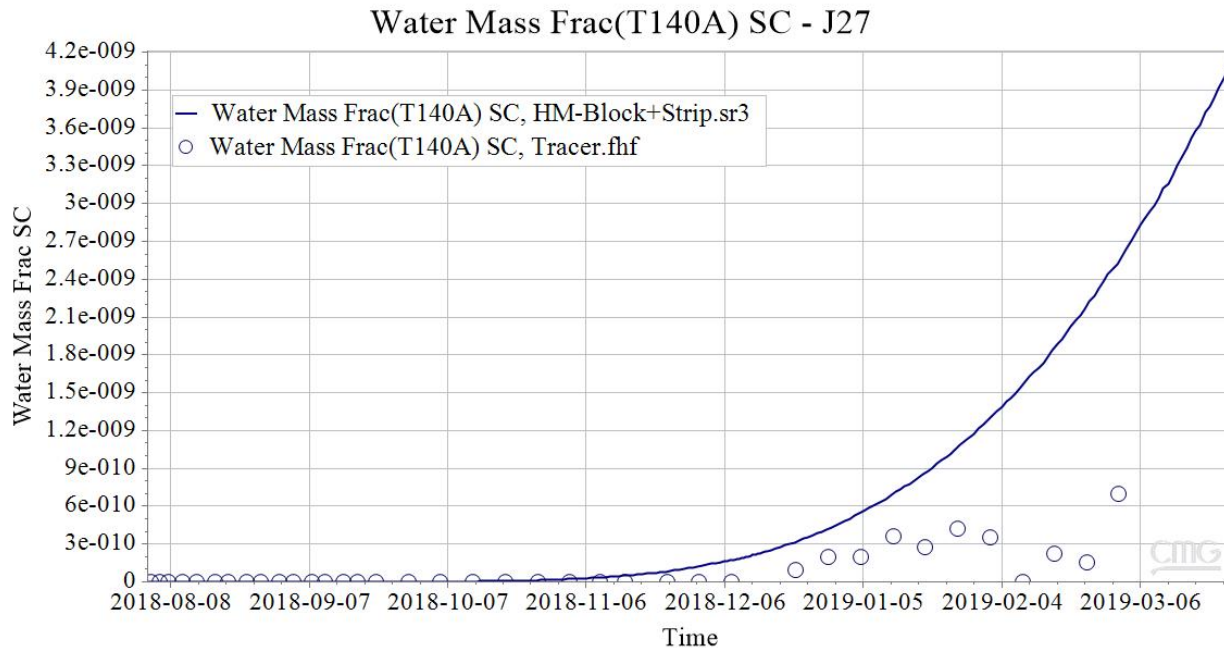
(a) History matching results of T-140A in producer J-27
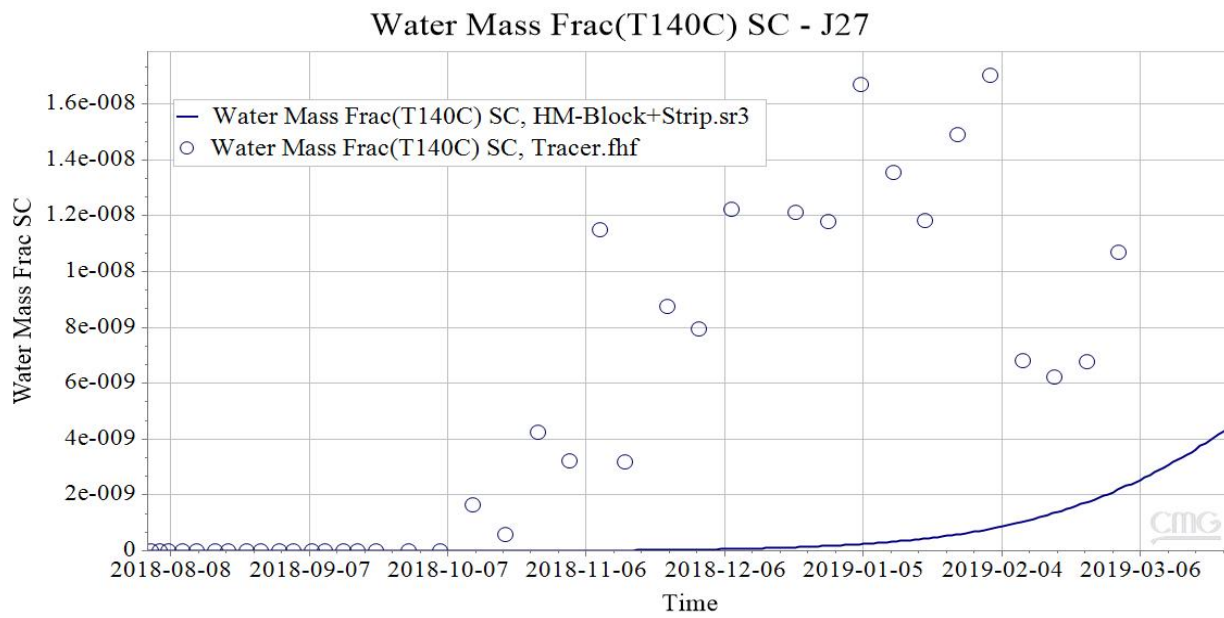
(b) History matching results of T-140C in producer J-27
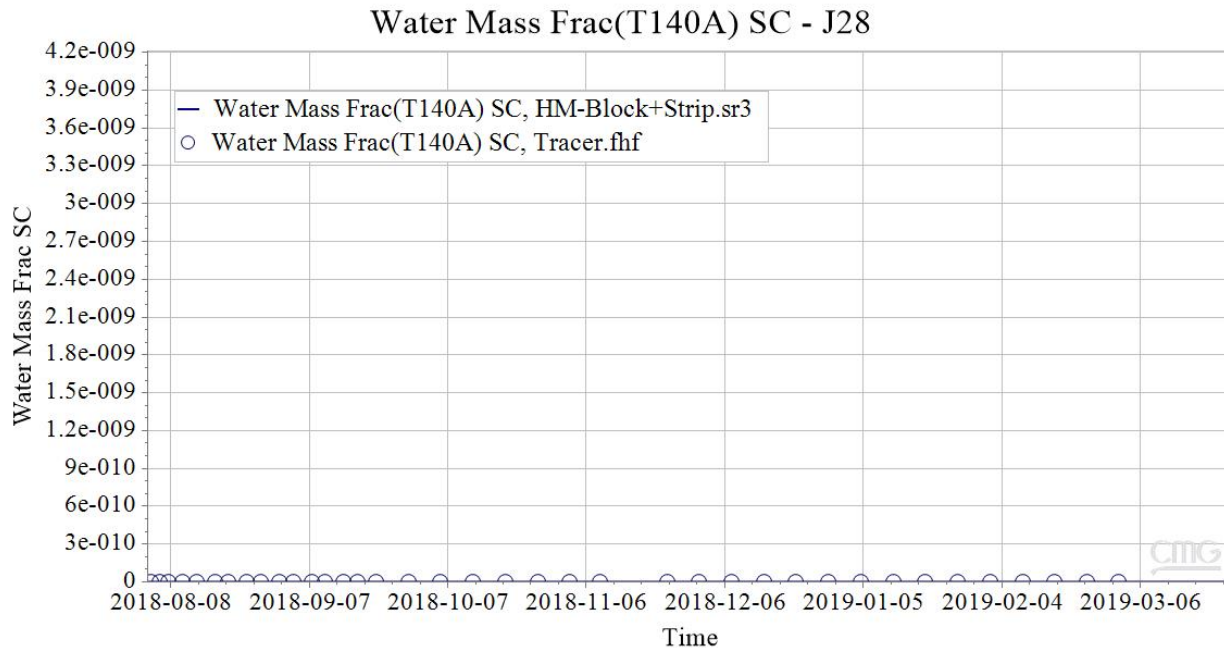
(c) History matching results of T-140A in producer J-28
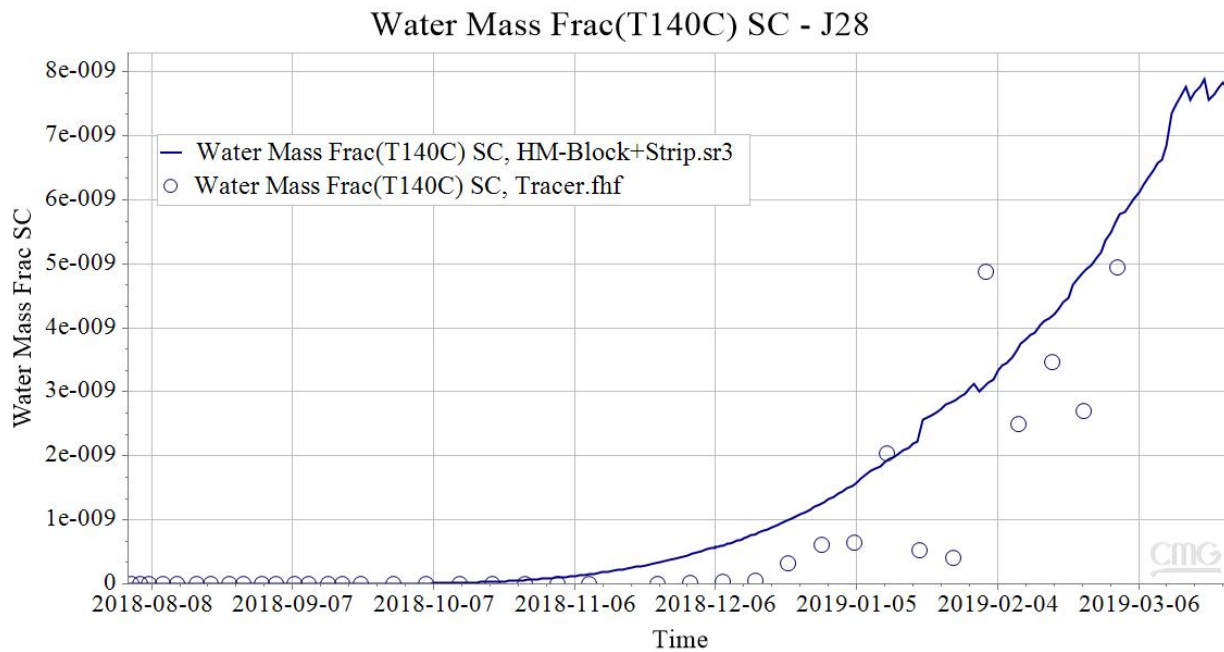
(d) History matching results of T-140C in producer J-28

Figure 44: History matching results of (a) T-140A concentration (b) T-140C concentration in producer J-27 and (c) T-140A concentration (d) T-140C concentration in producer J-28.

Updated reservoir simulation model

After history matching, the updated block/strip type permeability heterogeneity of the reservoir simulation model is presented in **Figure 45**. Meanwhile, the total dispersion coefficients of T-140A in I, J and K directions are 3.52×10^{-7}, 8.24×10^{-5} and 3.63×10^{-10}, respectively, and the total dispersion coefficients of T-140C in I, J and K directions are 9.51×10^{-9}, 2.70×10^{-4} and 1.82×10^{-5}, respectively.
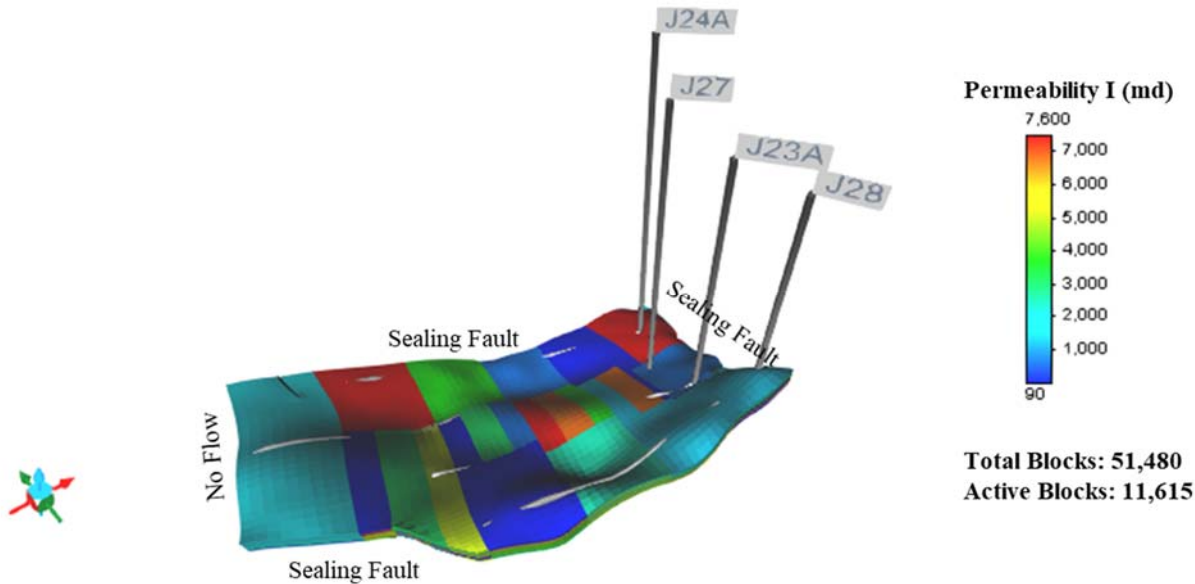
Figure 45: Updated permeability heterogeneity of the reservoir simulation model.

Reservoir EOR performance prediction

The updated simulation model, as shown in **Figure 45**, is used to forecast the production performance of the waterflooding and polymer flooding, respectively, for 10 years from March 25, 2019. During the prediction periods, the water injection rates of J-23A and J-24A are constrained to be 2400 bbl/day and 1200 bbl/day, respectively. Also, to conserve the material balance, the liquid production rates of J-27 and J-28 are constrained to be 2400 bbl/day and 1200 bbl/day, respectively. The following six case studies are conducted to investigate the reservoir EOR performance:

Case #1: inject water for 10 years
Case #2: inject polymer for 2 years followed by 8 years of waterflooding
Case #3: inject polymer for 4 years followed by 6 years of waterflooding
Case #4: inject polymer for 6 years followed by 4 years of waterflooding
Case #5: inject polymer for 8 years followed by 2 years of waterflooding
Case #6: inject polymer for 10 years

The predicted production profiles of the water cut and oil production rate for two produces are presented in **Figure 46**.
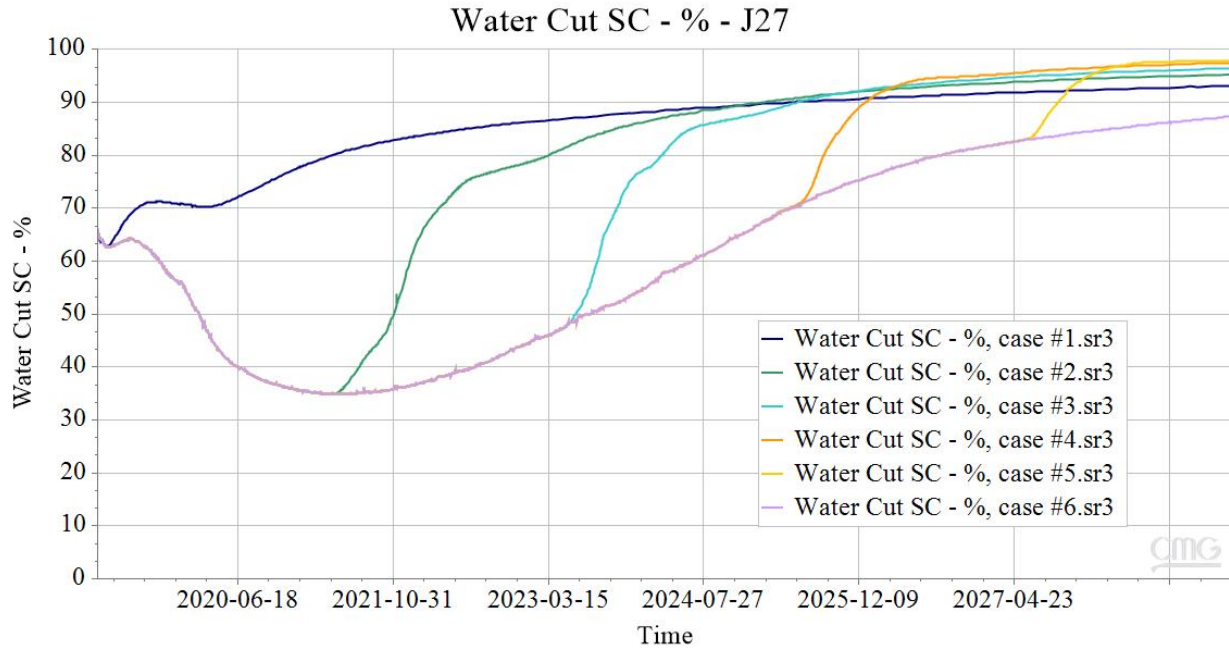
(a) Water cut of producer J-27
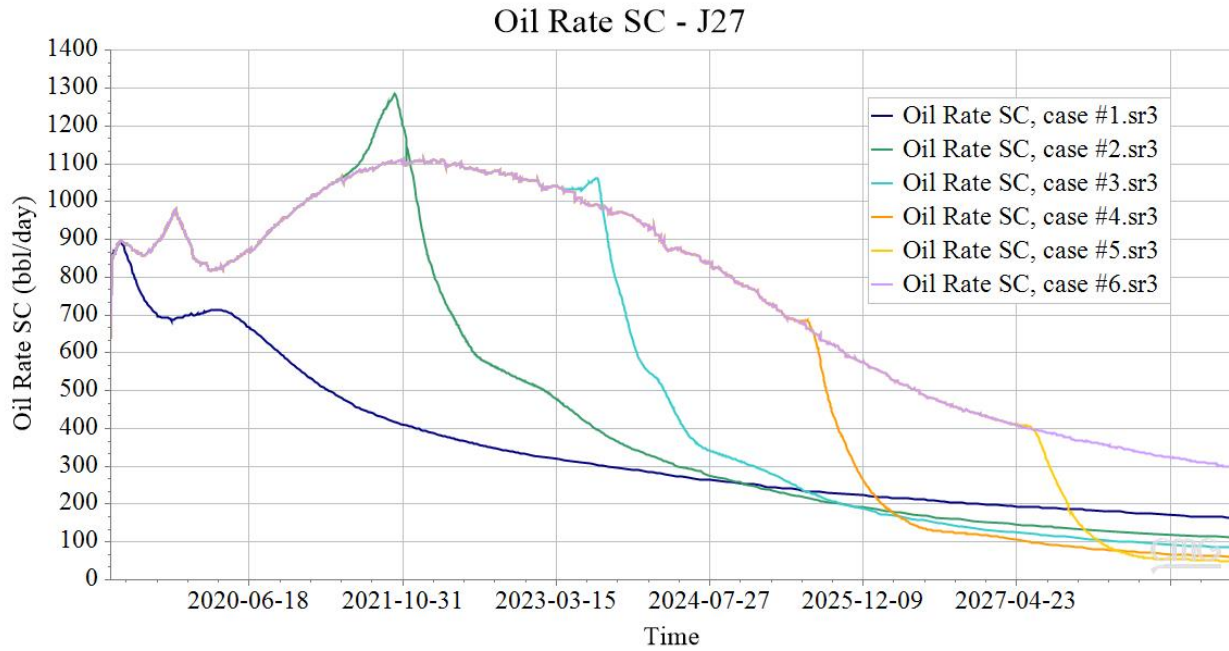
(b) Oil production rate of producer J-27

Water Cut SC - % - J28

(c) Water cut of producer J-28

Oil Rate SC - J28
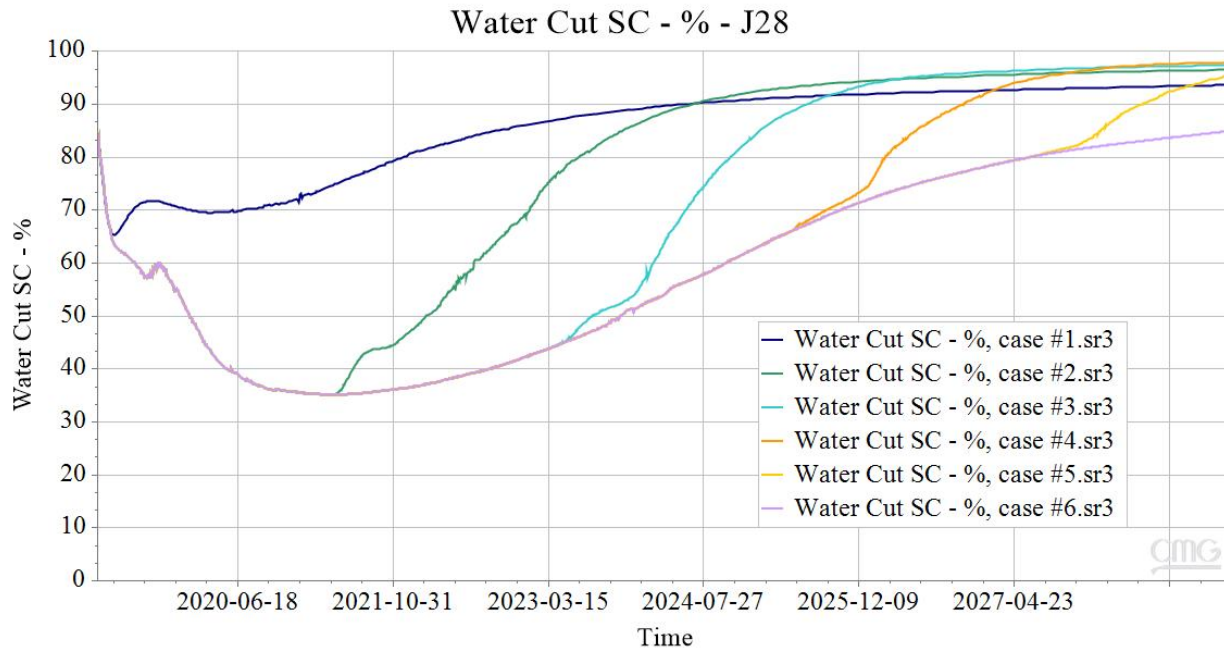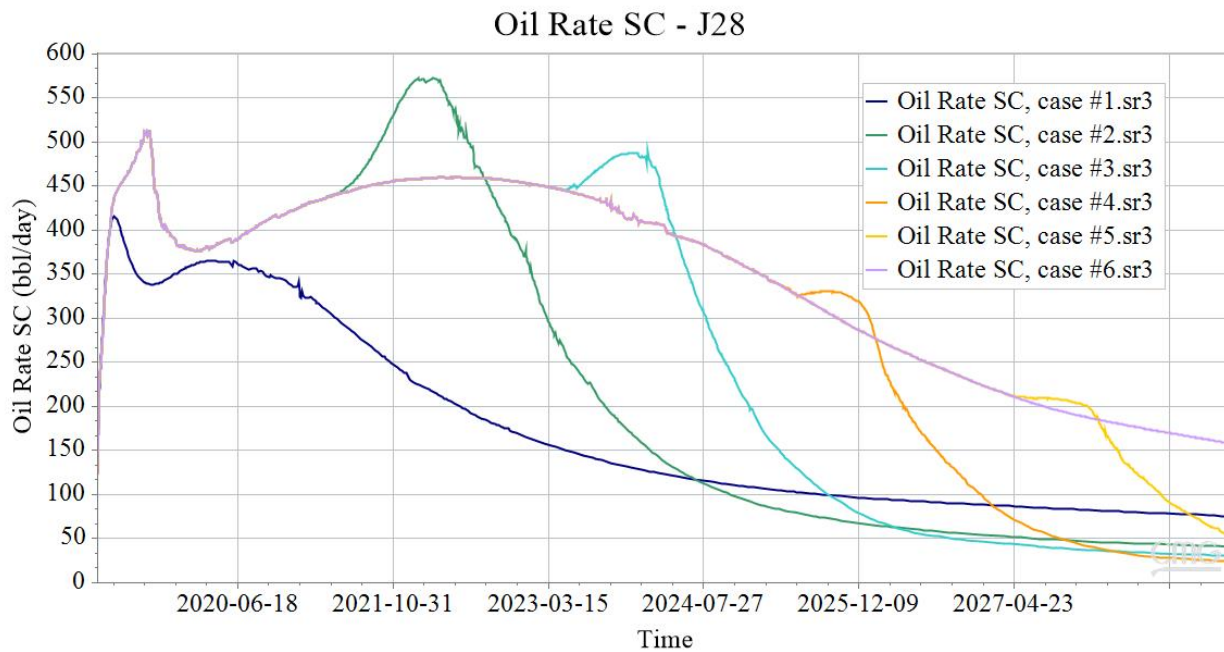
(d) Oil production rate of producer J-28

Figure 46: Predicted production profiles of (a) water cut (b) oil production rate in producer J-27 and (c) water cut (d) oil production rate in producer J-28.

As can be seen, the water cuts will decrease to a minimum in March 2021 and can be reduced by up to

40% using polymer flooding compared to waterflooding. After injecting polymer, the oil production rates will reach a peak and then drop to less than those of waterflooding in two years.

The oil recovery factor for each case during the prediction periods are shown in **Figure 47**. The oil recovery factor can merely reach 22% by the waterflooding in 10 years, but it will be promoted significantly by injecting polymer. More oil can be produced by increasing the amount of polymer injected, and the oil recovery factor will increase to 41% if the polymer is injected continuously for the next 10 years.
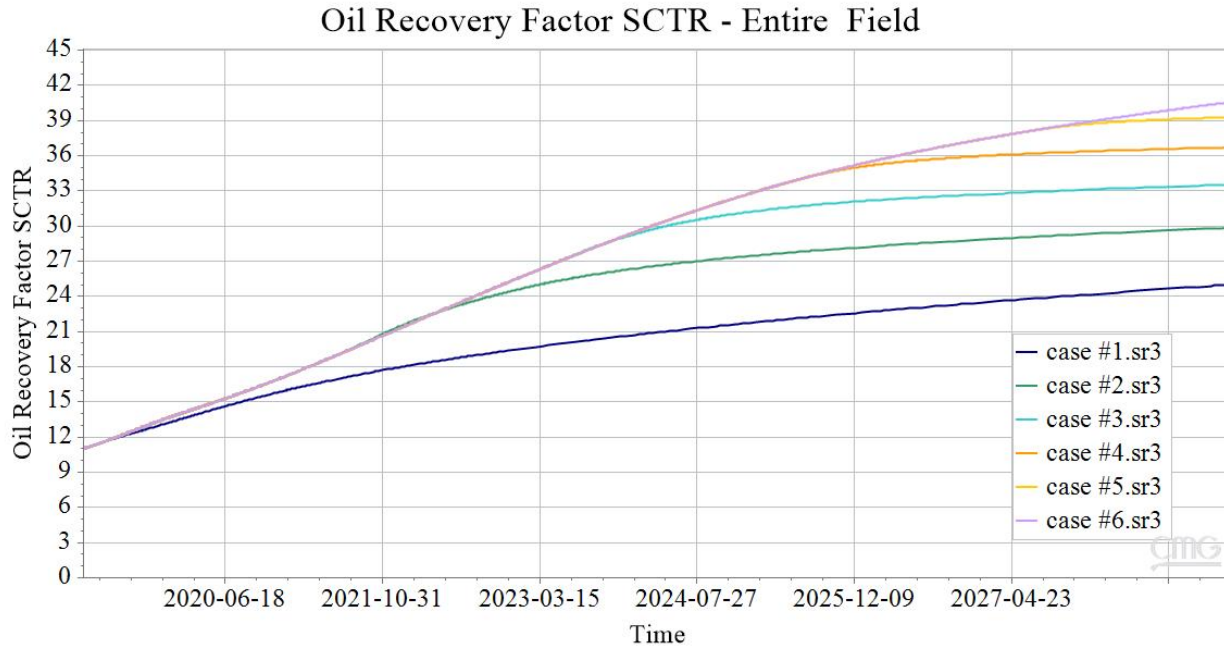
Figure 47: The profiles of oil recovery factor of the entire field by injecting different amounts of polymer in the next 10 years.

UAF's future work will focus on updating the reservoir model by matching cumulative oil production using tracer test data. And then the history matching results obtained from matching different production data will be compared.

UAF activity is ongoing.

● Task 5.0 - Implementation of Polymer Flood Field Pilot in Milne Point

Polymer has been injected continuously since startup on August 28th, 2018 except 2 shutdowns due to necessary equipment modifications and repairs in September and November 2018. Detailed pilot activities are summarized below:

Polymer Injection Status Timeline
- 8/23 polymer skid (PSU) online with water
- 8/28 polymer injection starts
- 9/25 PSU shutdown
  - More HC gas found in source water
  - Need to modify and reclassify PSU to Class I Div. II
- 10/15 Resume polymer injection
  - Ran downhole gauge
  - Performed post polymer step rate test
- 11/9 J-23A shut in for PFO while waiting for pump repair
- 11/16 J-24A shut in for PFO while repairing augur
- 12/3 Resume polymer injection
- 1/17/19 Attempted IPROF for J-23A, but tool covered by black goo
- 3/28/19 Pumped 8 kg Tracer T-801 into J-24A
- 3/29/19 Pumped 8 kg Tracer T-803 into J-23A
- 3/29/19 Coil tubing clean out J-23A, repeat IPROF.
  - Tool did not go all the way down, got partial results
  - ICD#1=5.6%, ICD#2=27.8%, ICD#3=40.7%
  - 74% polymer injecting into first segment (heel-2766')

Polymer Injection Performance

As of May 31, 2019, cumulative polymer injected was 266,000 lbs into J-23A and 120,000 lbs into J-24A. Polymer concentration was between 1200 to 2000 ppm to achieve a target viscosity of 45 cP as shown in **Figure 48**.
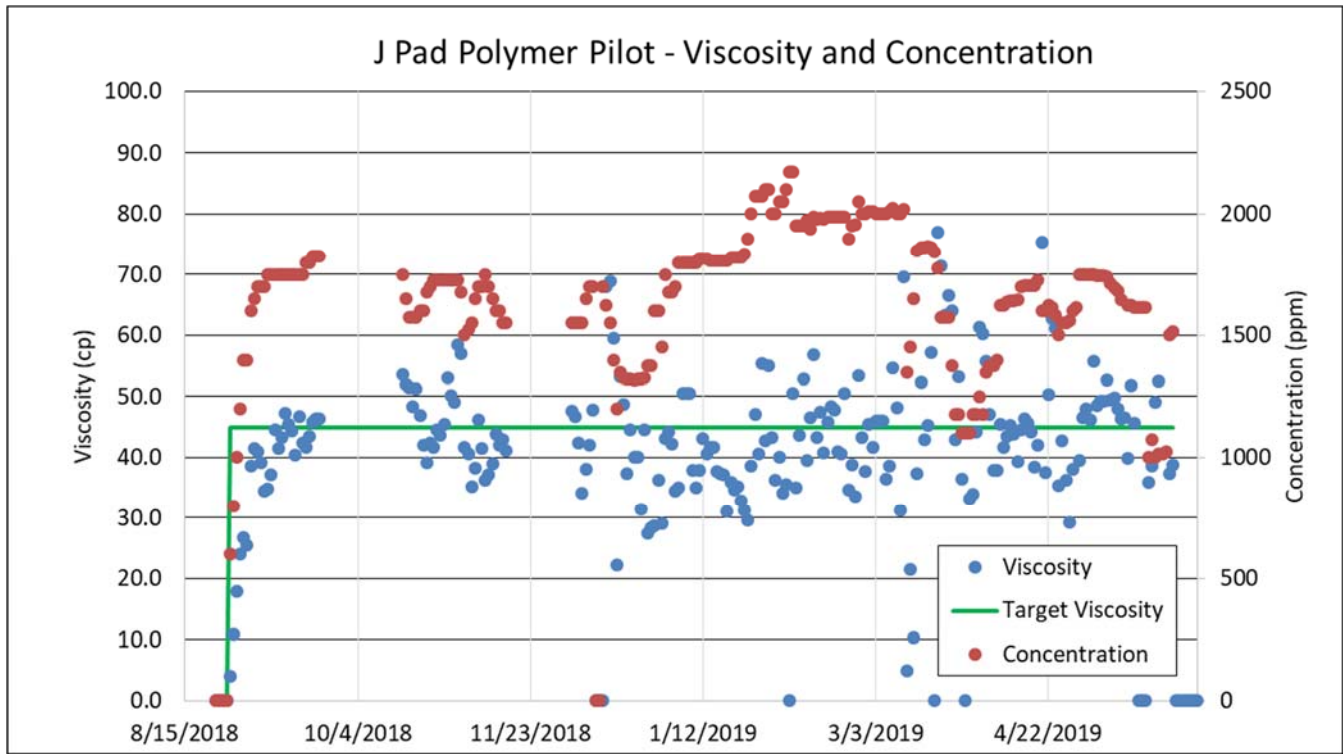
Figure 48: Polymer concentration and viscosity vs. time.

Figure 49 shows daily injection rate and pressure for J-23A. The injection rate was kept constant for about five months at approximately 2200 barrels per day (bpd) while the wellhead pressure stayed at or below 500 psi for the most part, which then started to creep up, indicating that the injectivity is decreasing as the reservoir is filled with polymer. Current injection pressure is approximately 850 psi and the injection rate is 1700 bpd, respectively.
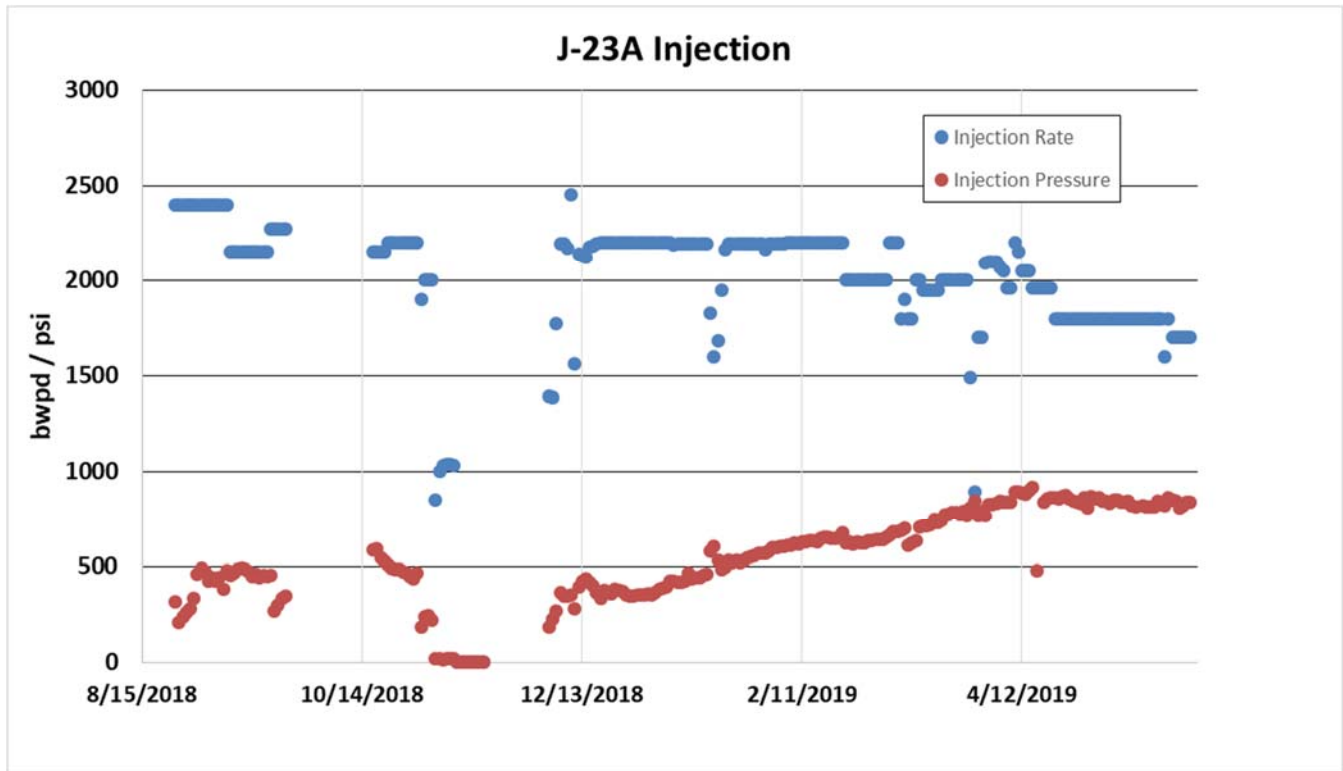
Figure 49: J-23A injection rate and pressure.

Figure 50 show daily injection rate and pressure for J-24A. The polymer injection rate had to be reduced from 1200 bpd to 600 bpd to keep the injection pressure below the target pressure of 700 psi, which translates to a pressure gradient of 0.63 psi/ft, to avoid fracturing the formation. This was the case until the beginning of March 2019. However, since it is not practical to keep reducing the injection rate, we increased the target pressure to ~850 psi to catch up with the reservoir voidage, with corresponds to a steady rate of 800 bpd.
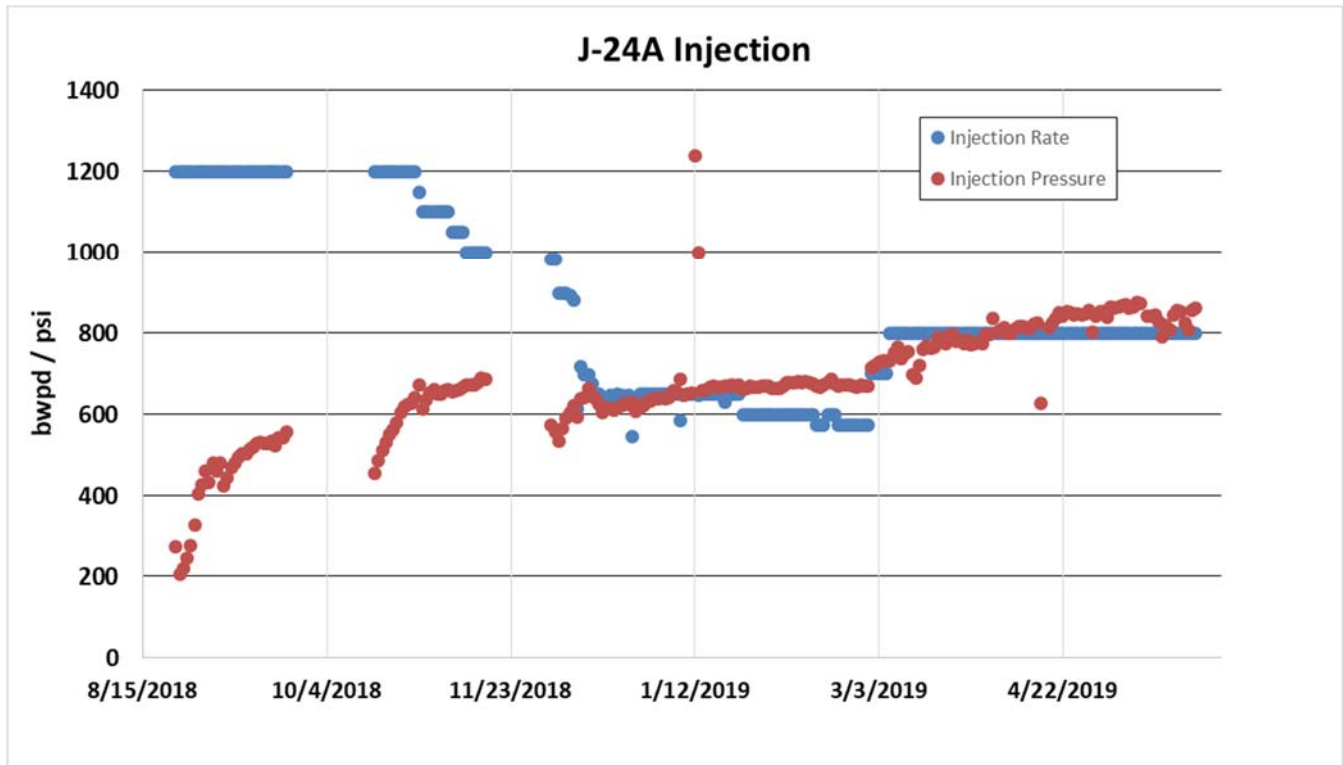
Figure 50: J-24A injection rate and pressure.

Figure 51 is a Hall Plot for both J-23A and J-24A, which plots the integration of the differential pressure between the injector and the reservoir versus cumulative water injection. The data would form a straight line if the injectivity stays constant over time, curve up if the injectivity decreases and vice versa. After a decrease in the injectivity of both J-23A and J-24A, which were reported in the last quarterly report, current Hall plot diagnostic indicates that J-23A injectivity is stabilizing, whereas J-24A injectivity has stabilized.
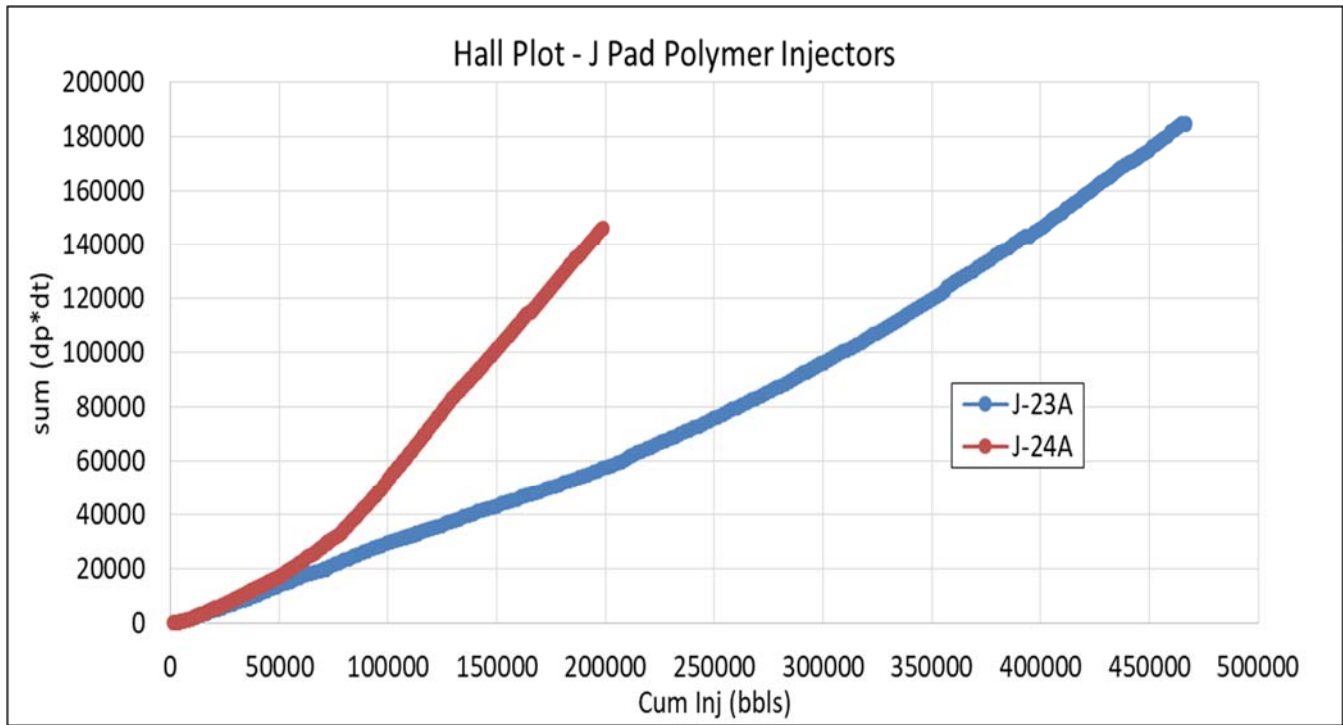
Figure 51: Hall plot for J-23A and J-24A.

Production Performance

Figure 52 depicts the production performance of producer J-27 which is supported by both injectors, J-23A from the south side and J-24A from the North, whereas the performance of J-28, supported by only J-23A is shown in **Figure 53**. In the reporting quarter, the water cut (light green) in both producers has varied only between 50 – 60%, averaging at about 55%. Although, the oil rate (sharp green) as well as the total fluid rate (light blue) in J-28 stabilized much earlier, and has remained steady since the middle of January 2019, J-27 also is showing similar trend for the last month. Overall, this may be indicative of approaching steady-state with VRR closer to one. However, it is still too early to quantify the amount of incremental oil production due to polymer injection since the total polymer solution injected into the reservoir is only about 4% of the total pore volume (TPV) in the flood patterns.
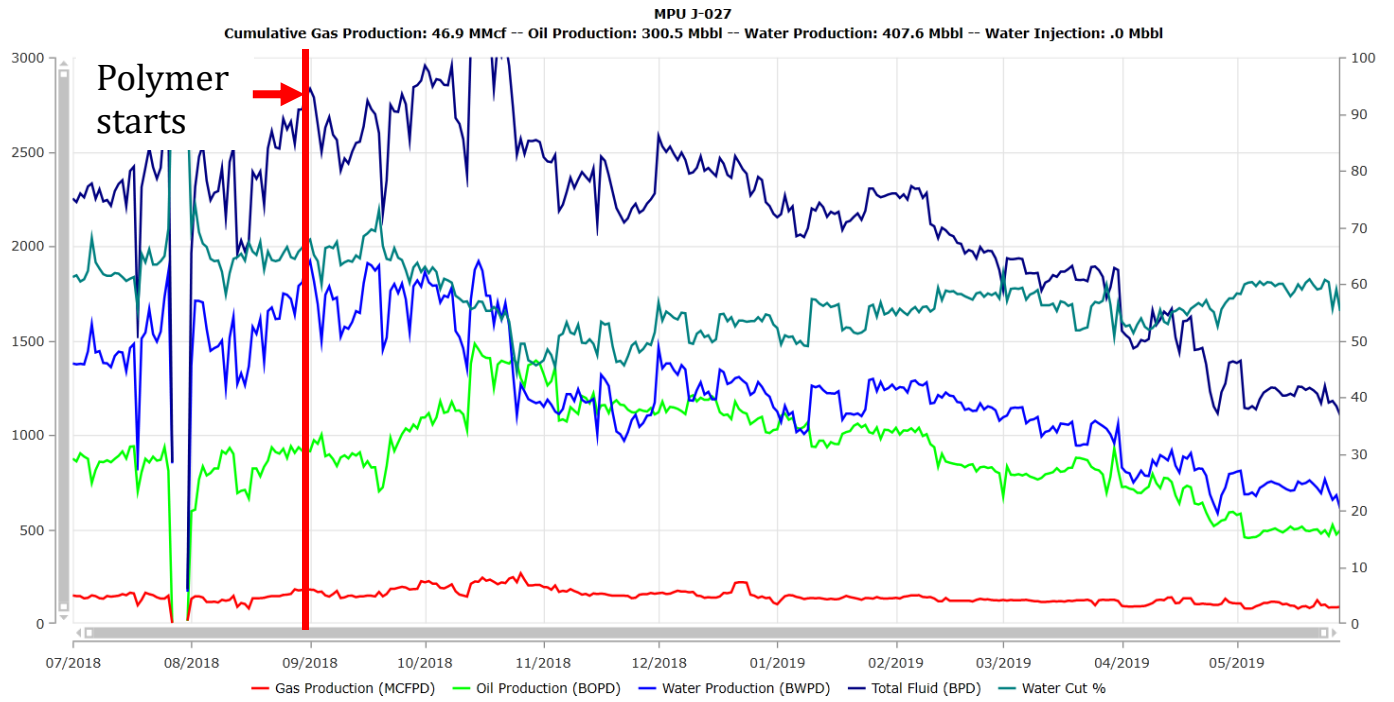
Figure 52: J-27 production performance.
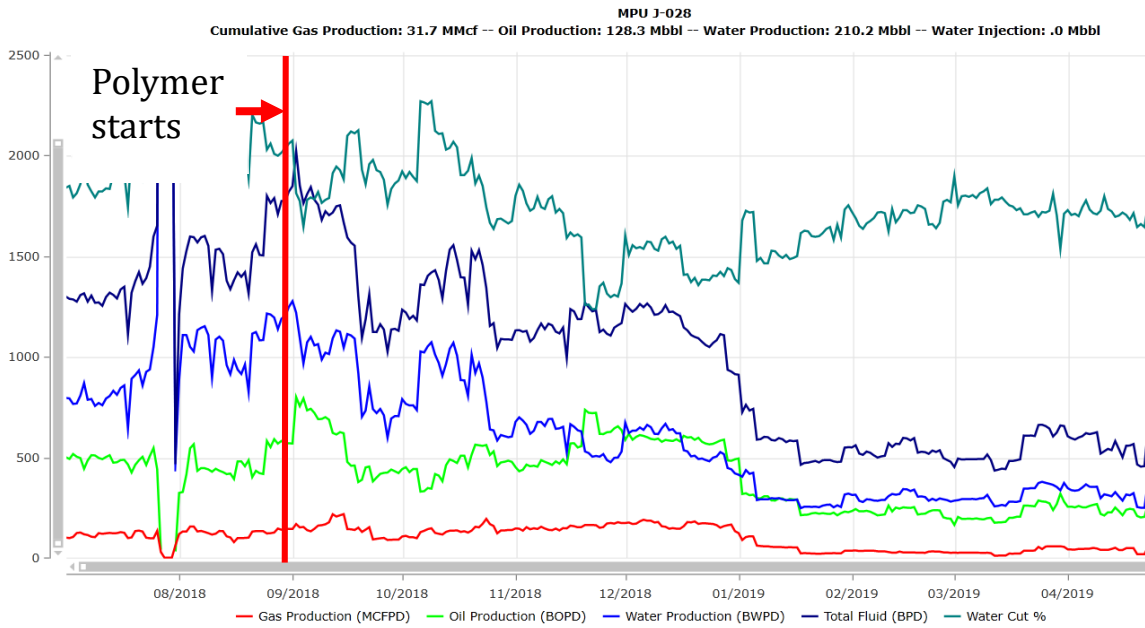
Figure 53: J-28 production performance.

59

Pre-Polymer Tracer Test

Two different tracers named T-140C and T-140A were pumped into injectors J-23A and J-24A respectively on August 3, 2018. Produced water samples are taken weekly from producers J-27 and J-28 and analyzed to detect tracer concentration. The latest tracer concentration plot to establish the injector – producer communication is shown in **Figure 54**. Time of appearance and magnitude of the tracer concentration in the two producers is an indicator of this communication. Accordingly, communication between injector J-23A and producer J-27 is strong (T-140C first seen 70 days); however, the J-23A to J-28 (T-140C first seen 140 days) and J-24A to J-27 (T-140A first seen 140 days) indicate poor communication between these well pairs.
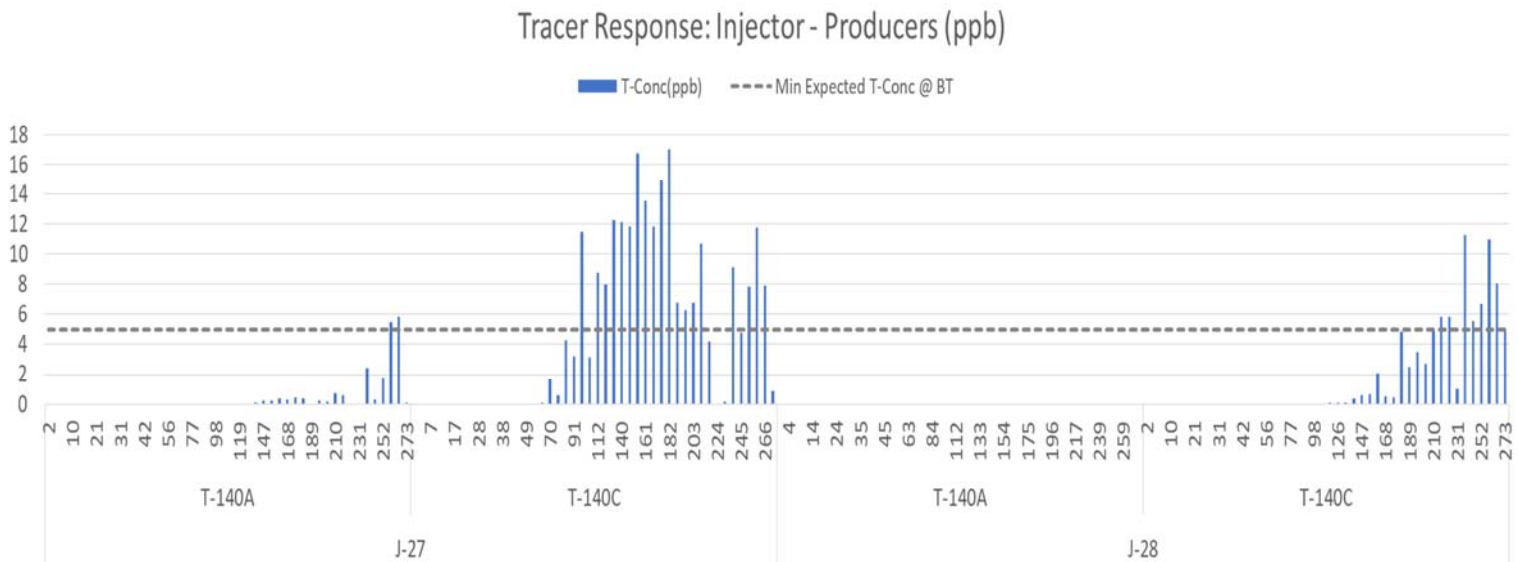

Figure 54: Tracer concentration in produced water.

Monitoring Polymer Breakthrough

Since the start of polymer injection, produced water samples have been collected weekly and analyzed onsite using the clay flocculation test, as well as in the laboratory via nitrogen-fluorescence water composition analyses to detect the presence of produced polymer in the production stream. As of the end of May 2019, 9 months after the start of polymer injection, no polymer has been observed in the production stream.

Activity is ongoing.

● Task 6.0 -Analysis of Effective Ways to Treat Produced Water that Contains Polymer

Experimental details

In the reporting quarter, oil water separation studies have continued using various emulsion breakers or demulsifiers E12085A, E18276A, N1691 and R01319, which have been employed as received without further processing. The water soluble demulsifier N1691 and other oil soluble demulsifiers were dissolved

into methanol (0.5 g/50 mL) and xylene (0.5 g/50 mL) respectively to prepare 10000 mg/L original solution. The amount of solution added into the crude oil emulsion is determined by the total volume of the emulsion

Polymer solutions have been prepared as follows, 1g polymer solution mixed overnight with 1 Liter produced water by the magnetic stirrer to prepare 1000 ppm polymer solution. The prepared polymer solution was sheared at 15000rpm for 3mins to mimic the shearing environment in the oilfield. The shearing condition was finally determined at the point where the viscosity of polymer solution after shearing is reduced by around 50% of the original polymer solution. The viscosity of polymer solution before and after shearing is shown in **Figure 55**.
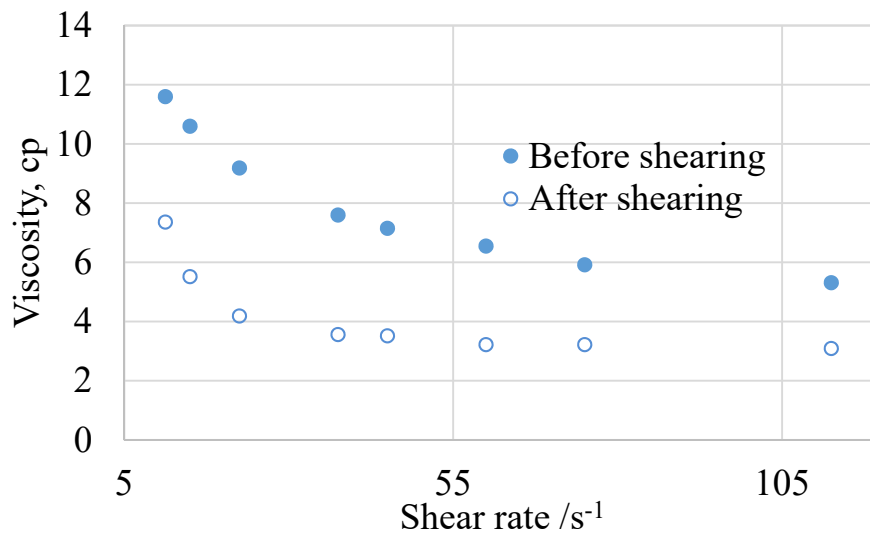
Figure 55: The viscosity comparison of polymer solution before and after shearing.

The sheared polymer solution was diluted with produced water in different ratio to prepare the polymer solutions at different concentrations. The polymer concentration of 50ppm, 150ppm, 300ppm and 500ppm was prepared and stored in the glassware for use in experiments. The viscosity of polymer solutions at all four concentrations were also measured.

Treated crude oil was preheated to 130ºF to promote viscosity reduction. Produced water or polymer solution was heated to 130ºF to facilitate its incorporation into the oil phase. Aqueous solution was slowly added into the crude oil at lower rotating speed and continued to mix for 3mins at 5000 rpm to produce emulsions representing water/oil ratio of 20:80, 50:50 and 80:20.

Microscope imaging of the emulsion and bottle test procedures have been described in previous reports, thus they are not repeated here. Refined oil content measurements following the bottle tests are as follows. After settling for 24hrs, 15 mL water was sampled from the bottle of the colorimetric tube by 4 in long pipette and collected in a 45 mL plastic tube. The water sample was poured into 150 mL separation funnel followed by the addition of 1.5 mL HCl. 10 mL unleaded gasoline was then added into the separation

funnel. The separation funnel was capped and then shaken upside down for 2mins by hand. When the water layer became clear, the upper gasoline layer and bottom water layer were collected in two graduated cylinder and the volume was recorded as Vg and Vw respectively. The upper gasoline was transferred into the sample vial of UV/Vis spectrophotometer to measure the oil content of separated water at the wavelength of 600 nm. The oil concentration (C_o) was calculated using the standard curve. The oil content in the water sample (T_o) can be calculated from the following equation:

$$T_o = \frac{C_o \times V_g}{V_w} \qquad (2)$$

Results and Discussion

The effect of adding sequence of emulsion breaker. In the oilfield, the emulsion breaker is added downhole and mixed continuously during the anticipated formation of emulsion. To mimic this process, a modification of the previous method was made. The emulsion breaker was added to the emulsion while blending rather than after the emulsion preparation in the modified method. The best two emulsion breakers were selected based on the prior experiments. The performance of emulsion breaker was compared between these two methods. **Figure 56** and **57** shows the water separation rate and the quality of separated water for the previous method and modified method respectively for the two tested EB's for a water cut of 20%. Although the separation efficiency is good in the previous method, the oil content in the separated water after 24 hours is significantly higher (**Figure 56**). However, in the case of the modified method, exact opposite is observed, i.e., the separation efficiency is low but the separated water quality is much improved with significantly low oil content, and relatively cleaner water (**Figure 57**). **Figure 58** and **59** demonstrate the same trend for a water cut of 50%.
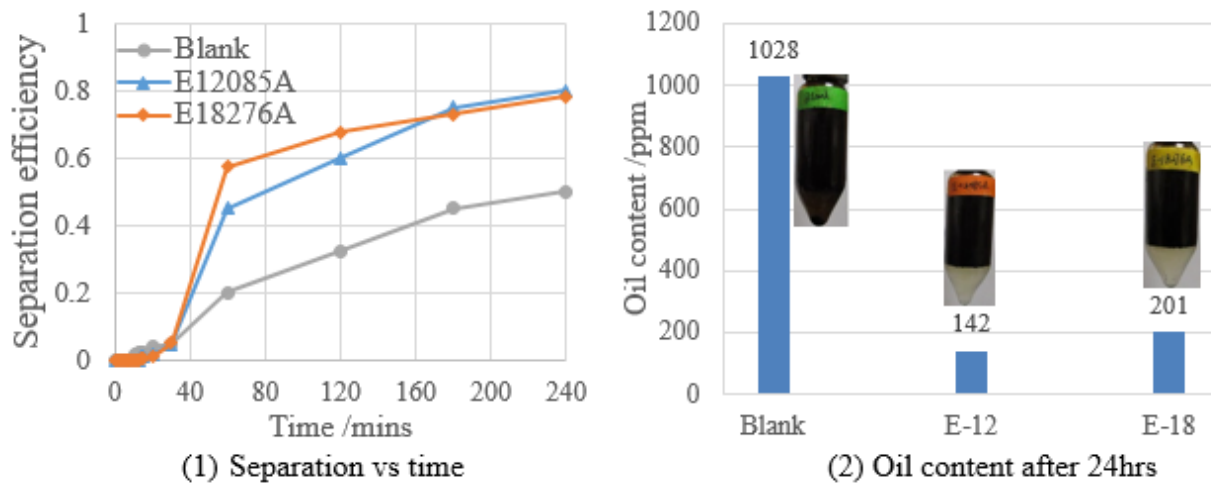
Figure 56: The performance of tested EB in the previous method at water cut of 20%.
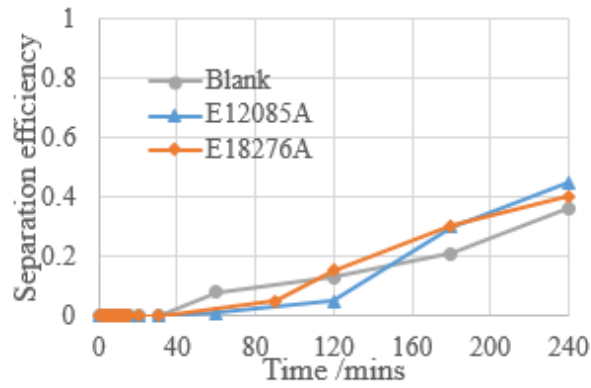
(1) Separation vs time
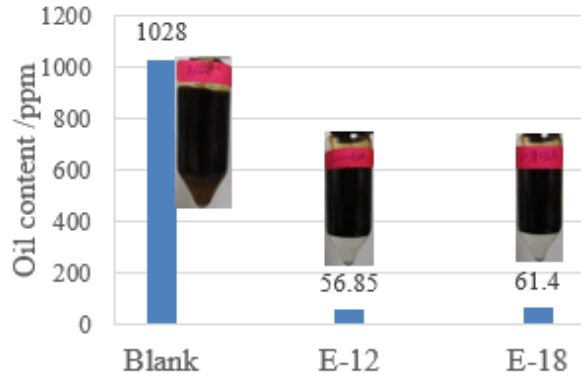
(2) Oil content after 24hrs

Figure 57: The performance of tested EB in the modified method at water cut of 20%.
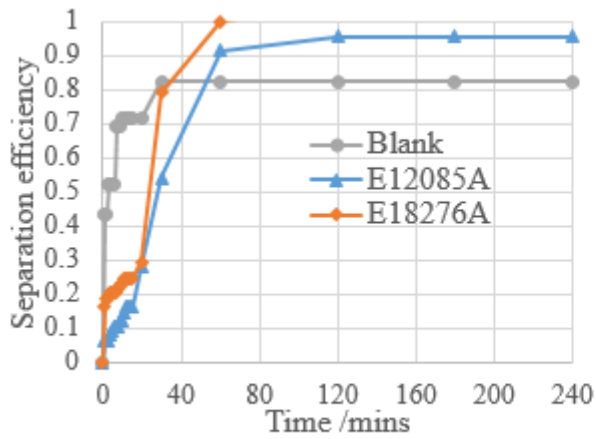
(1) Separation vs time
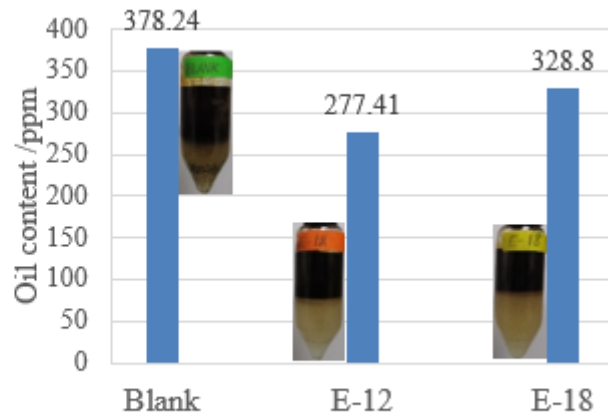
(2) Oil content after 24hrs

Figure 58: The performance of tested EB in the previous method at water cut of 50%
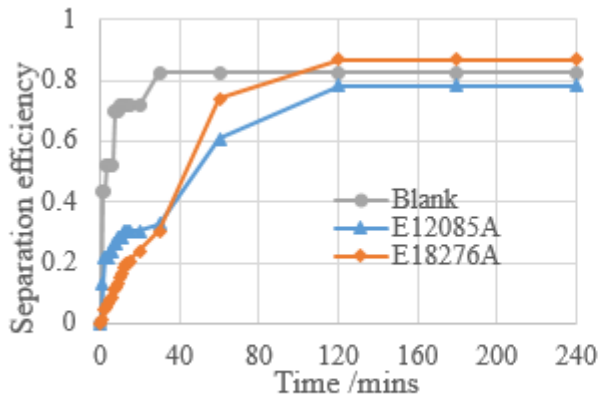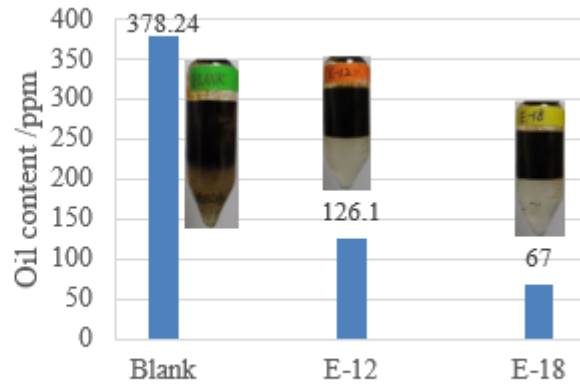
(1) Separation vs time   (2) Oil content after 24hrs

Figure 59: The performance of tested EB in the modified method at water cut of 50%

The effect of polymer concentration. The water cut of 20% and 50% were selected to study the effect of polymer concentration, which represents the typical w/o and o/w emulsion respectively. As indicated by **Figure 60**, w/o emulsion was detected at all polymer concentrations when the water cut is 20%. The dispersed water drop size becomes larger and the number of small drops declines as the polymer concentration increases. Similarly, at 50% water cut, which forms o/w emulsion at all polymer concentration, the oil droplet size tends to increase and the number of small droplets declines as shown in **Figure 61**.
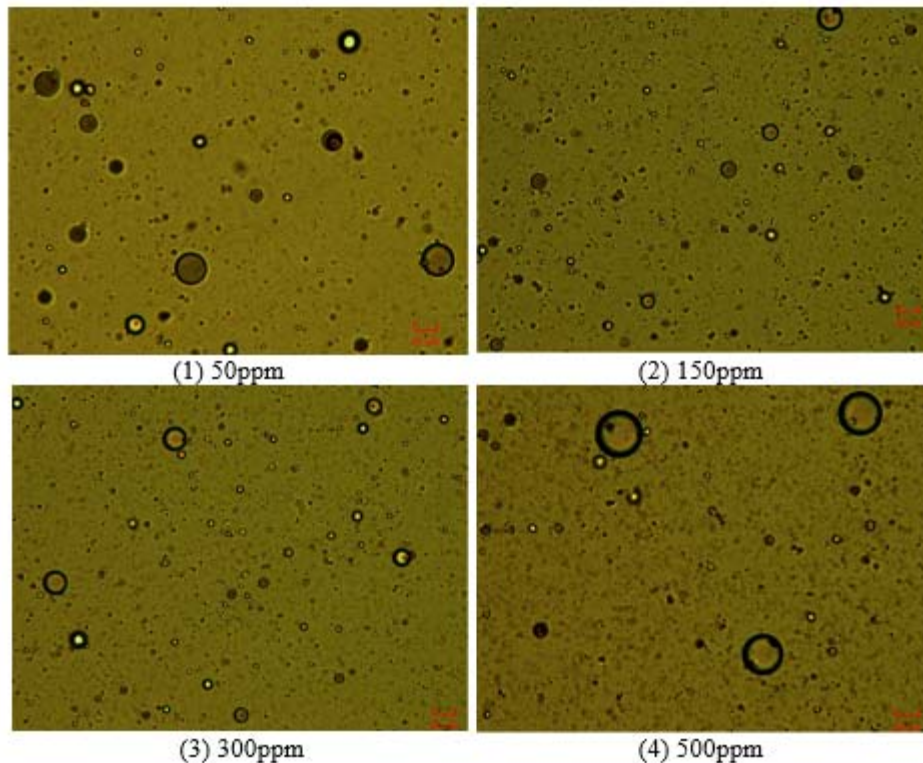
Figure 60: Micromorphology of emulsions with different polymer concentration at 20% water cut.
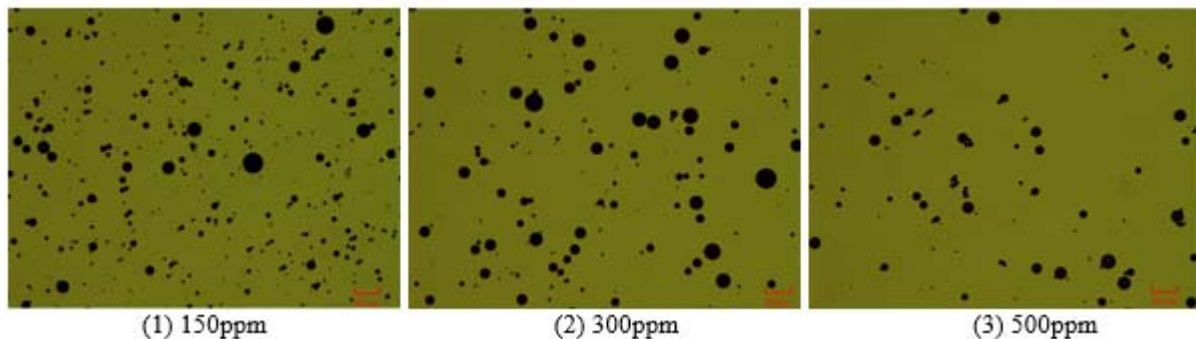
Figure 61: Micromorphology of emulsions with different polymer concentration at 50% water cut

Bottle test. The results for the 20% water cut case is shown in **Figure 62**, which indicates that the separation efficiency increases at higher polymer concentration of 300 and 500ppm. However, the emulsion at polymer concentration of 150ppm, which appears to be an outlier, is slightly more stable than the emulsion formed by the blank (0 ppm polymer). Currently, there is no reasonable explanation for this anomaly. And the stability effect of polymer on the emulsion which is frequently reported in the literature was not seen in this experiment. More efforts need to be devoted to the study of interaction mechanism between the polymer and the crude oil. Even though, the separation efficiency in the case of 300 and

500ppm polymer concentrations is high, the quality of the separated water worsens, as evidenced by the turbidity in the bottle images (**Figure 62**).

(1) Separation efficiency vs time   (2) Bottle test at 4 hours interval
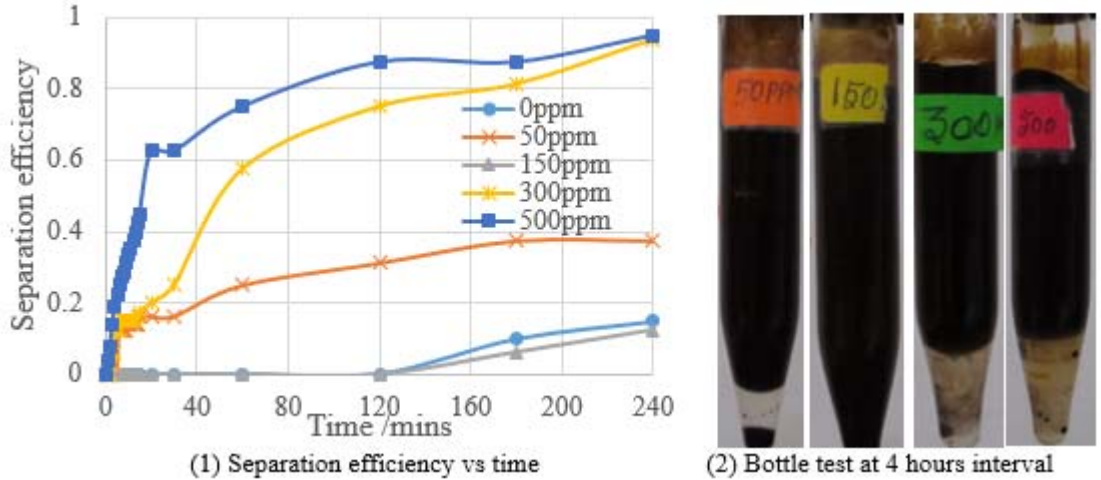
Figure 62: The effect of polymer concentration on emulsion stability at 20% water cut.

In the case of 50% water cut measurement of separation efficiency becomes difficult due to nearly immediate phase separation. Meanwhile, as seen in **Figure 63**, the separated water becomes oilier with increasing polymer concentration. To further probe into this effect, the viscosity of polymer solution at the same concentrations were measured as shown in **Figure 64**. Obviously, the viscosity gradually increases with increasing polymer concentration. The increasing viscosity of polymer solution slows down the upward motion of the oil droplets, thus impeding the separation and leading to the turbid water phase (Yang et. al., 2015). We plan to further investigate this hypothesis.
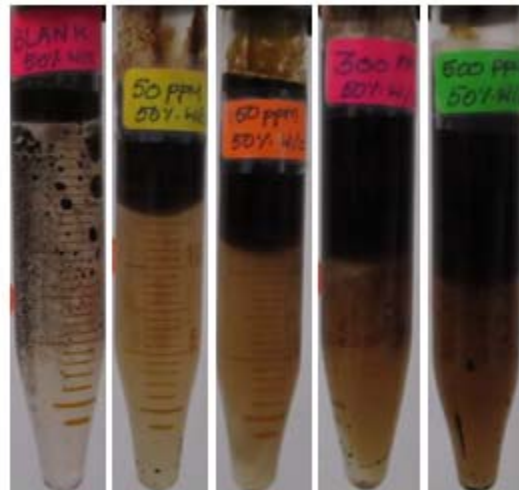
Figure 63: Bottle test for various polymer concentration at 50% water cut.
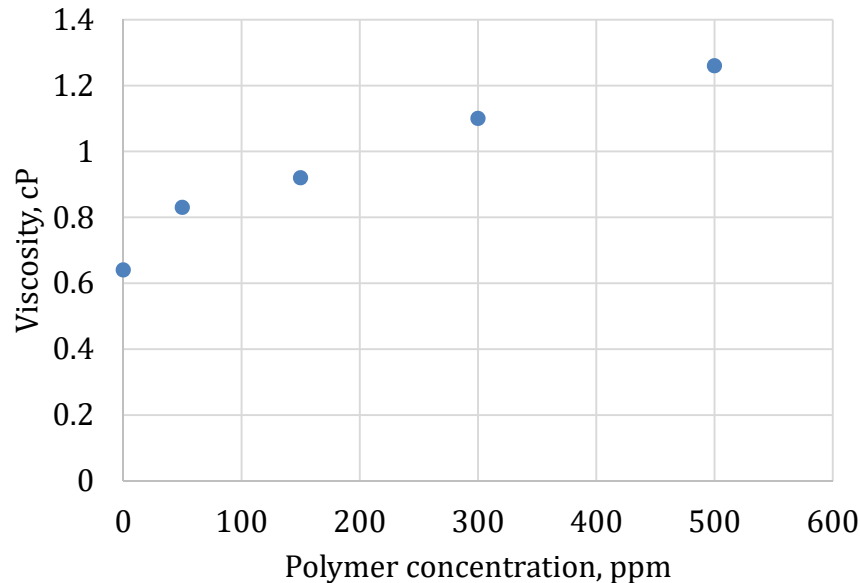
Figure 64: Viscosity of polymer solution as a function of concentration.

Future Work

This will focus on studying the emulsification behavior of emulsions in the presence of polymer at the current water cut, as well as the evaluation of performance of emulsion breakers. The separation behavior of emulsions will be investigated in the graduated cylinder to avoid transfers.

● Task 6.0 –Polymer Fouling of Heater Tubes

Prior to embarking on the experimental work, an extensive literature review was carried out to study other reported cases of polymer fouling. This revealed that very limited work has been done to study the scaling and fouling in heat exchangers in presence of polymers. Some of the findings from the literature review are briefly summarized:

1. Wang et. al. (2018) reported that with the presence of EOR chemicals (Partially hydrolyzed polyacrylamide-based polymer and surfactant) deteriorated the performance of $CaCO_3$ inhibitors thereby requiring a new inhibition solution. Interaction was observed between EOR chemicals and $CaCO_3$.
2. Mittal et. al. (2018) also reported fouling problems when HPAM flood was used in Mangala Field by Cairn Oil & Gas, Vedanta Limited at an average polymer concentration of ~2500 ppm.
3. Jonathan et. al. (2010) reported that the problem of scaling increases drastically at elevated temperatures due to which the fire tubes have to be changed frequently resulting in economic losses.

Proposed plan

Based on the limited literature, discussions with Hilcorp and UAF's own assessments, the following key

parameters have been identified as those affecting the fouling in the exchanger, the effects of which will be studied at UAF:

- Skin temperature of tubes
- Velocity of process fluids
- Residence time of process fluids
- Polymer concentration

Accordingly, UAF has planned 3 different types of tests for the first phase of expanded Task 6.0.

- Static bottle test followed by chemical composition analysis
- Deposit analysis test on hot copper tubes
- Dynamic scale loop test

Description of proposed experimental procedure and current status

The parameters of the heat exchanger (reported by Hilcorp to UAF) at Milne are as follows:

- Velocity of process fluid - 1.56 m/s
- Residence time of process fluid - 2.092 minutes
- Skin temperature of tubes – 165ºF
- Inlet temperature of process fluids – 85ºF
- Outlet temperature of process fluids – 106ºF
- Variable polymer concentration such as the one used in the oil-water separation studies.

UAF will mimic these parameters in the lab using the same composition of produced water as that at Milne Point, and in order to be consistent, the same as the one used in the oil-water separation studies. These 3 experimental tests will give a complete picture of the scaling and fouling when polymers are present in the produced water.

Static Bottle Test – This is also a commonly used industry standard test where the solution to be tested (produced water with and without polymer) is heated and stirred in bottles for a long time ranging between 2-24 hours and the deposit which forms is analyzed for chemical composition and morphology. The change in composition helps study the scaling potential and UAF will study how the polymer behaves at high temperatures in presence of salts in the produced water. These tests are currently in progress and we expect to report results on them in the next quarterly report.

Deposit Analysis Test on Hot Copper Tubes – This is a new experimental setup UAF has designed. This will involve circulating hot oil inside copper tubes to heat the surface of the tubes to the desired testing temperatures and then immersing the hot tubes in produced water and produced water containing polymer. The time taken to heat the produced water from inlet temperature of process fluids at Milne to outlet temperature of process fluids at Milne will be recorded. Also, the increase in weight of tubes due to scaling and fouling will be recorded. Multiple runs will be made with the same tubes with another batch of produced water (with and without polymer in different sets of experiment) and the increase in time to heat the water will give change in heating efficiency of the tubes. These tests are in the process of commencing in due course and we expect to report results on them in the next quarterly report.

Dynamic Scale Loop – In principle the schematic of this set-up is the same as shown in the application for the expanded scope of Task 6.0. The experimental set-up will be able to mimic the parameters mentioned before and the rise in differential pressure across the scaling loop will be recorded with time as the produced water flows through it and analysis of how much time it takes to block the loop will be done. Comparison of times between solutions with and without Polymer will be made. Currently, some parts are awaited and as soon as they are received the loop set-up will be completed and we expect to report on the actual images of the set-up and perhaps a trial run to test the loop, in the next quarterly report.

Activity is ongoing.

- Task 7.0 - Feasibility of Commercial Application of the Proposed Advanced Polymer Flooding in ANS Heavy Oil Reservoirs

Activity has not yet started.

c.   Opportunities for Training and Professional Development
All the graduate students working on the project are obvious recipients of training and professional development in petroleum engineering.

d.   Dissemination of Results to Communities of Interest
Engineers from ConocoPhillips and Hilcorp continue to communicate about the project on a regular basis.

e.   Plan for Next Quarter
Building on the current progress achieved by the research team, work planned for the next quarter will include steadily progressing toward the planned completion dates outlined in **Table 8** below.

Table 8: Summary of milestone status.

Milestones	Task No.	Planned Completion Date	Actual Completion Date	Verification Method	Comments
Project Management Plan	1a	o 9/30/2022	o Ongoing (latest revision 4/30/2019)	Report	None
Data Management Plan	1b	o 8/31/2018	o 7/20/2018 (latest revision 4/30/2019)	Report	None

● Quantify polymer retention	2	o 3/31/2019	o Some tests completed but is ongoing	Report	None
● Effect of water salinity on S_{or} ● Screening of gel products for conformance control	3	o 4/30/2019 o 6/30/2019	o Some tests completed but is ongoing o Initiated	Report	None
● Pilot area model waterflooding history match ● Coreflooding model history match ● Updated area model for polymer flood prediction ● Reservoir modeling report	4	o 12/312018 o 4/30/2019 o 5/31/2019 o 5/31/2019	o 2/1/2019 o Some completed but is ongoing o Completed but is also ongoing refinement o Extensively reported in Quarterlies, but a formal report will be completed by the middle of July 2019 as special status report	Report	None
● Injection profile with polymer inj. ● PFO (post-polymer) ● Tracer tests (post-polymer)	5	o 12/31/2018 o 12/31/2018 o 12/31/2018	o Ongoing o Ongoing o Ongoing *Note – all have been completed, but also ongoing*	Report	None
● Initial treatment plan recommendation based upon literature survey ● Finalization of the fouling flow loop design	6	o 12/31/2018 o 06/30/2019	o Ongoing (challenges with spent polymer present) o Ongoing	Report	None

University of Alaska Fairbanks

2. PRODUCTS

Following is the citation of the URTeC abstract that will be presented in July 2019. This paper will soon appear on the conference website and on www.onepetro.org.

Samson Ning, John Barnes, Reid Edwards, Kyler Dunford, Abhijit Dandekar, Yin Zhang, Dave Cercone, Jared Ciferno: First Ever Polymer Flood Field Pilot to Enhance the Recovery of Heavy Oils on Alaska North Slope – Polymer Injection Performance. Selected for presentation at the Unconventional Resources Technology Conference Denver, CO July 22-24, 2019. URTeC 643.

A.Y. Dandekar, University of Alaska - Fairbanks; B. Bai, Missouri University of Science & Tech; J.A. Barnes, Hilcorp Alaska LLC; D.P. Cercone, J. Ciferno, National Energy Technology Laboratory; S.X. Ning, Reservoir Experts LLC; R.S. Seright, New Mexico Inst-Mining & Tech; B. Sheets, University of Alaska Fairbanks; D. Wang, University of North Dakota; Y. Zhang, University of Alaska – Fairbanks: "First Ever Polymer Flood Field Pilot - A Game Changer to Enhance the Recovery of Heavy Oils on Alaska's North Slope". SPE-195257-MS.

3. PARTICIPANTS & OTHER COLLABORATING ORGANIZATIONS

Hilcorp hired two operators dedicated to the project operations. Two reservoir engineers are in charge of the test design and analysis; one facilities engineer is in charge of polymer skid design and installation; and one operations engineer is in charge of downhole well work.

All the listed project personnel identified on the second page, the post-doc, and graduate students working on different tasks formally contribute 2 hours every other Friday in a project working meeting. Additionally, sub-group working meetings, typically lasting for 2-4 hours in a month are also held to discuss specific tasks such as reservoir simulation. For the post-doc and graduate students, the typical formal working hours per week are 40 and 20 respectively, whereas the latter is typical of personnel identified in the aforementioned table to supervise the students. Besides these, additional hours are typical in preparing reports, presentations for meetings, and potential publications.

4. IMPACT

The project continues to be an outreach tool since it is actually showcased (relevant parts of it) in the petroleum engineering curriculum. On May 30th an Arctic Open House event was organized at the University of Alaska Fairbanks, in which a poster on the project was presented for the visiting public in the Fairbanks area.

5. CHANGES/PROBLEMS

a) Recent polymer retention experiments conducted on the NB sandpacks under overburden conditions have again resulted in very high polymer retention values, which will next be compared with OA sandpacks. If these values also are very high then that constitutes a major challenge for the project.
b) Variability in the characteristics of the oil samples (some already containing water) received from the field continues to pose challenges in produced water treatment experiments.

6. **SPECIAL REPORTING REQUIREMENTS**
    Nothing to Report.

7. **BUDGETARY INFORMATION**
    A summary of the budgetary information for the first budget period of the project is provided in **Table 9**. This table shows the planned costs, reported costs, and the variance between the two. Reported costs is the sum of UAF's incurred expenses and the sum of the invoices received from our project partners.

Table 9: Budgetary information for Budget Period 1, Q4.

Baseline Reporting Quarter	Budget Period 1	
	March 1 2019 – May 31 2019	
	Q4	Cumulative Total
Baseline Cost Plan		
Federal Share	309,556	2,240,146
Non-Federal Share	39,347	757,765
Total Planned	**348,903**	**2,997,911**
Actual Incurred Cost		
Federal Share	98,887	1,136,520
Non-Federal Share	150,908	1,110,783
Total Incurred Cost	**249,795**	**2,247,303**
Variance		
Federal Share	-210,670	-1,103,626
Non-Federal Share	111,561	353,019
Total Variance	**-99,109**	**-750,607**

Please note that the PMP also has a spending plan that is based on calendar quarters.

8. PROJECT OUTCOMES

Nothing to Report.

9. REFERENCES

Jonathan J. Wylde, Jeff McMahon, Steve Mayner. Scale Inhibitor Application in Northern Alberta: A Case History of an Ultra High Temperature Scale Inhibition Solution in Fire Tube Heater Treaters, 2010. SPE 130307.

Johnson, E.F., Bossler, D.P., and Naumann, V.O., Calculation of relative permeability from displacement experiments, Transactions of the AIME, 216, 370–372, 1959.

Mittal, S., Anand, S., Venkat, P. S., Mathur, V., Zagitov, R., Subramanian, J., Hammonds, P. Influence of EOR Polymers on Fouling in Production Wells and Facilities,2018. SPE 192943-MS.

Qiwei Wang, Feng Liang, Waleed Al-Nasser, Faez Al-Dawood, Tawfiq Al-Shafai, Hameed Al-Badairy, Shouwen Shen, Hassan Al-Ajwad. Laboratory study on efficiency of three calcium carbonate scale inhibitors in the presence of EOR chemicals. Petroleum, 4(4) (2018) 375-384.

Yang, L., Zhihua, W., Xianglong, Z and Shanzhe, W. Study on emulsification behavior and optimized separation technology of high concentration polymer flooding produced liquid in Daqing Oilfield. SPE Middle East Oil & Gas Show and Conference. Society of Petroleum Engineers, 2015.